

**The Expedition ARKTIS-XV/2
of "Polarstern" in 1999**

**Edited by Wilfried Jokat
with contributions of the participants**

**Ber. Polarforsch. 368 (2000)
ISSN 0176 - 5027**

Contents

ARK XV/2 Tromsøe - Tromsøe

21 July - 08 September 1999

	Summary	2
1	Meteorological conditions.....	5
2	Marine Geophysics	8
3	Marine Geology	27
3.1	Subbottom profiling using PARASOUND.....	29
3.2	Geological sampling	40
3.3	Sediment characteristics.....	43
3.4	Smear-slide analyses	46
3.5	Watersampling for Ra-226 analysis.....	47
3.6	Summary	47
3.7	Physical Properties of the Sediments	48
4	Petrology.....	59
5	Hydrosweep DS2 Bathymetry.....	71
5.1	Hydrographic Survey Equipment on RV POLARSTERN.....	71
5.2	Surveys	72
5.3	Data processing.....	72
5.4	Plotting bathymetric charts.....	75
5.5	Final results and future work.....	76
6	Planktonic foraminifera.....	77
7	The ice edge and its influence on the smallest benthic biota	89
8	The GEUS/AWI programs during POLARSTERN cruise ARK-XV/2.....	94
	References.....	101
	Appendix 1 - Geophysical tables for magnetic surveys -.....	102
	Appendix 2 - Core descriptions -	107
	Appendix 3 - Geological Tables -	119
	Participating Institutions	125
	Cruise Participants.....	127
	Ship's Crew.....	128

ARK XV/2 Tromsøe - Tromsøe

(21 July - 08 September 1999)

Summary

The expedition ARK XV/2 of RV POLARSTERN started at the 21st of July 1999 in Tromsøe and terminated again in Tromsøe at the 8th of September. The main purpose of the expedition was to perform geoscientific research (geophysics, geology, petrology and bathymetry) off the North-East Greenland coast, the Fram Strait and Northern/Western Svalbard. This programme was supplemented by biological and glaciological research activities.

One reason for the early start of the expedition in July was to have the possibility for reaching the Morris Jessup Rise north of Greenland. Ice observations of the past 2 years indicated that large polynyas were present around North Greenland mostly till end of July. In comparison with these observations this season was unusual. Throughout the whole July 1999 no open water formed at the North Greenland coast facing the Arctic Ocean. Continuous pressed ice conditions prevented any research north of 81°N. Even in the Fram Strait we hit extremely difficult ice conditions. It therefore was necessary to modify our scientific programme (Fig. 1).

On the transit to the research area on the North Greenland Shelf biological investigations were performed in the Fram Strait at 80°N. Afterwards we seismically investigated the North Greenland shelf to supplement the seismic network acquired in 1997. The data were acquired without any damage of the equipment but only in a small strip parallel to the coast. The new gravity and seismic data clearly show the presence of salt domes up to 80°N on the shelf. Although the deeper parts of the profiles are masked by water bottom multiples the sonobuoys deployed will provide constraints on the thickness of the sediments. In parallel, glaciological investigations were performed onshore using the helicopters. The main tasks were to visit the new islands and to recover automatic climate stations from the 79Fjord-glacier. Of the total of 7 stations 6 were recovered. 4 of these were still in more or less working conditions. The activities on the North Greenland shelf lasted from the 28th of July till 2nd of August 1999.

The second part of the research programme was concentrated in the Fram Strait. Seismic investigations were not possible due to the ice conditions. After reaching the Lena Trough the shipboard programme concentrated on dredging the shoulders of the Lena Trough. The petrological sampling needed three days. The dredge samples were a big surprise. In total 600 kg of hardrocks were gathered with 5 dredge hauls. Nearly all major and minor lithologies found on the ocean floor are represented in the dredge hauls, ranging from serpentized upper mantle rocks, fresh pillow basalt to hydrothermal sulfide deposits.

Following these activities the western margin of the Yermak Plateau was investigated for retrieving geological and biological samples. The topic of the geological programme was to gather high resolution Holocene sediments to better describe fast fluctuation in the past climate. The biological sampling was concentrated on the benthic environment. The Fram Strait can be understood as an boundary area to the central Arctic Ocean. Here, the benthic environment is influenced by various biotic and abiotic factors on a geographic small scale. The sampling was designed to supplement other data in this region to estimate the variability of the benthic environment depending on the ice cover. Results are not available at the moment.

The difficult ice conditions in the Fram Strait highly influenced the geophysical and bathymetric programme in the next weeks. Both disciplines concentrated their research north of Svalbard. Here, an exceptional wide polynya up to 82°N was present and allowed systematic bathymetric and seismic investigations. The bathymetric and seismic surveys lasted from the 9th till the 20th of August 1999. The combined data sets indicate a sediment starved margin with deeply increased canyons and slumping activity.

From August, 20th onwards a deep seismic sounding experiment started to investigate the crustal structure of Northern and Western Svalbard. In total three profiles with 15 oceanbottom seismometers/hydrophones and up to 10 landbased recording stations for each line were acquired till the end of the cruise. Two large airguns with a total of 90 l were used from POLARSTERN to generate seismic energy. Dynamite shots were fired with charges up to 50 kg from the Polish ship EL TANIN. Along the last profile only few shots could be fired due to the bad weather conditions and the tied time schedule. The signal range varies between well over 100 km for the landstations to 30 - 50 km for the oceanbottom stations. Currently no detailed results are available.

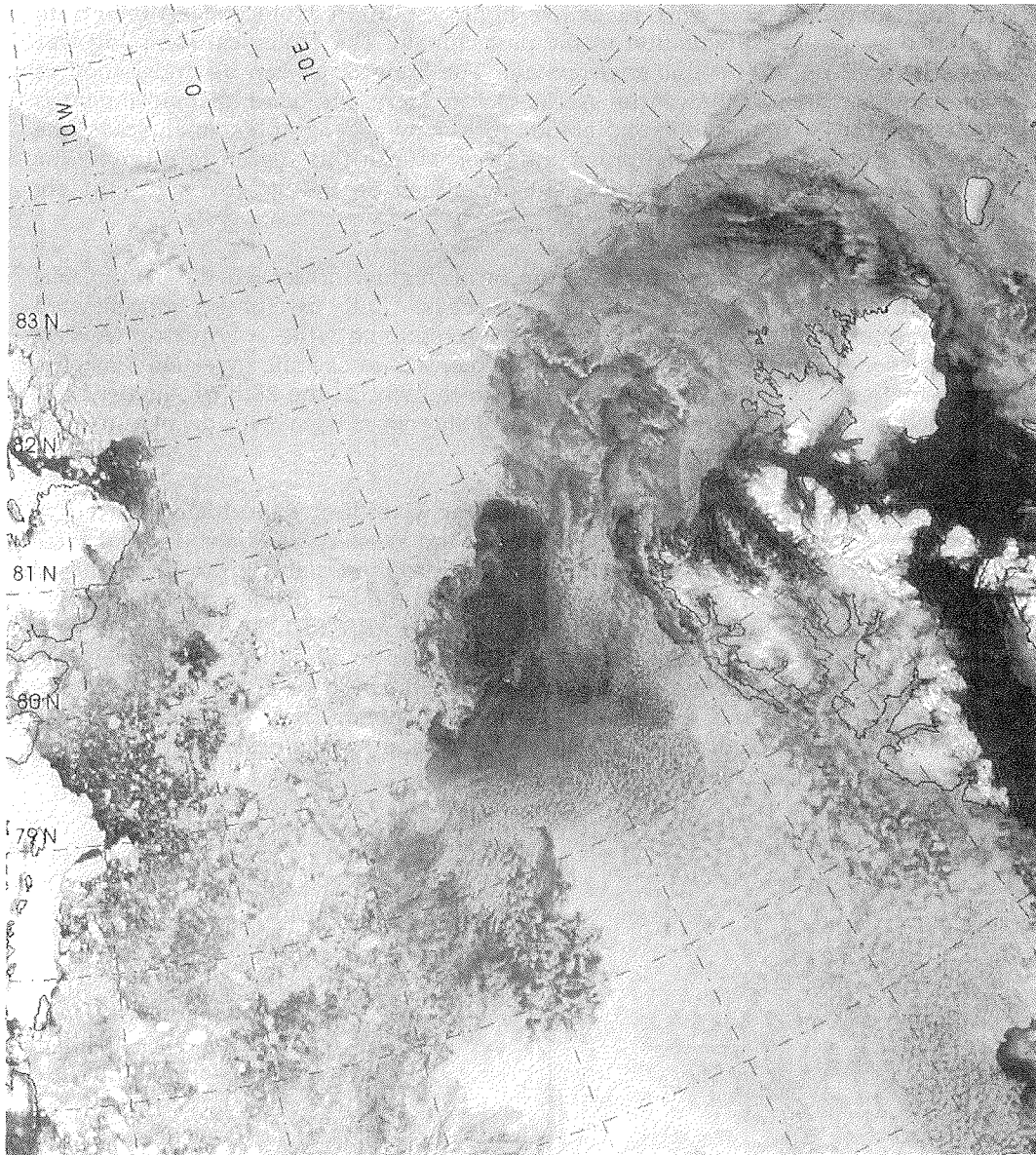


Fig. 1: Typical ice conditions in the area of the Fram Strait/East Greenland and Northern Svalbard during ARK-XV/2

1 Meteorological Conditions during Cruise ARK XV/2 (R. Brauner)

POLARSTERN left Tromsø on the 21st of July at 23:00 hours with light south-easterly winds and a temperature of about 20°C. During the first three weeks the weather in the working area of POLARSTERN was dominated by a stationary low pressure system west of Svalbard and a stationary high over Greenland. Between these systems a light to moderate and rather strong breeze from northerly directions (Figure 2 and 3) was observed with air temperatures between plus 1°C and minus 6°C. The horizontal visibilities varied between 4 to 20 km accompanied with low stratus layer clouds with a ceiling frequently below 500 feet (Figure 4). Sometimes the visibility become worse because of the ceiling descending to the surface with shallow fog patches. Southward moving troughs with light to moderate snowfall produced heavy icing conditions for the bord helicopters. In most cases the sea was subdued by closed fast ice. From the fourth week until the end of the cruise the weather was dominated by low pressure systems moving from south-eastern part of Greenland across Svalbard to northern part of Russia in periods of 3 to 5 days when POLARSTERN was operating near Svalbard. On the front side of the low pressure systems relative warm air with temperatures about +4°C and a high humidity streamed in from south-easterly directions mostly accompanied by a broken to overcast cloudiness and moderate rainfall. The visibilities were generally misty and sometimes fog developed due to the high dewpoints in relation to the cold water. Moderate to strong winds from westerly to northerly directions with dry air and good visibilities were experienced at the rear of the low-pressure systems. The daily temperatures varied between +2°C and -6°C. The sky was partly cloudy with moderate to heavy snow- and rain-showers. In some cases granulated snow was observed on POLARSTERN. The sea was relatively calm due to the short fetch in the vicinity of the fast ice edge or Svalbard. Only in the last week of the cruise an intensive gale centre developed on the front side and also on the rear side wind forces up to 9 Beaufort with waves up to 5 meter.

On the 5th of September, POLARSTERN left for Tromsø. The cruise ARK XV/2 ended in the morning of the 8th of September 1999 in Tromsø.

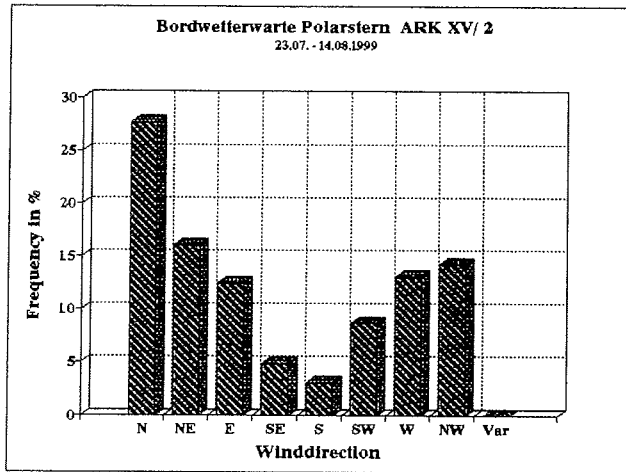


Fig. 2: Frequency of wind direction from 23.07. until 14.08.99

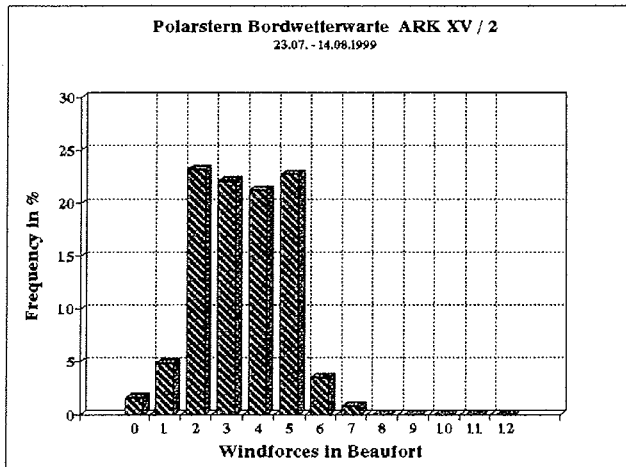


Fig. 3: Frequency of wind forces from 23.07. until 14.08.99

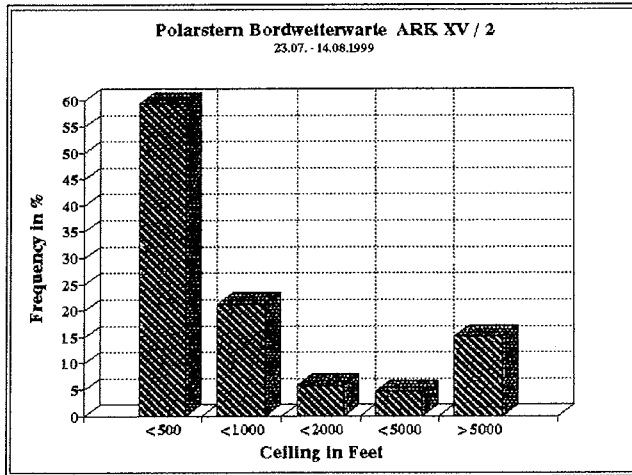


Fig. 4: Frequency of ceiling from 23.07. until 14.08.99

2 Marine Geophysics

(Jokat, W., Czuba, W., Dzewas, J., Ehrhardt, A., Gierlich, A., Kühn, D., Martens, H., Lensch, N., Nicolaus, M., Nishimura, Y., Ritzmann, O., Schmidt-Aursch, M., Sroda, P., Wildeboer-Schut, E.)

Introduction

The current geographical position of Svalbard relative to the Greenlandic Island is the consequence of a continuous strike slip and/or oblique rifting between the Greenland and Eurasian plates. Current plate tectonic reconstructions locate the Svalbard archipelago north of the North Greenland coast some 60 - 70 Ma. While the Eurasian Basin began to open approximately 60 Ma, relative movements between Svalbard and Greenland also started. Evidence for such large strike slip movements can be found along the western coast of Svalbard. Here, the Tertiary fold belt of Svalbard is exposed with altitudes up to 1000 m. This coast parallel fold belt, however, has no such prominent expression at the onshore geology of North Greenland. Although tectonic lineaments with NW-SE striking trends exist, it is not known how the North Greenland shelf was affected by this tectonic event.

As a result of this continuous rifting some time between 3 and 15 Ma the Fram Strait opened. Today the Fram Strait is the only deep-water gateway of the Arctic Ocean to the world oceans. It is believed that the formation of such a deep-water passage had a profound influence on Earth's climate. Cold deep-water masses from the Arctic can now freely exchange with the North Atlantic. Most likely this event caused a change in ocean circulation in the Atlantic to the system which we know at present. The propagation of the mid-ocean ridge system towards the north placed the active mid-ocean Knipovich Ridge close to the continental margin of western Svalbard. This world-wide quite rare geodynamic situation rises questions how the modern crustal structure is affected by this thermal rifting event. Further north, the tectonic situation is less obvious. North of 80°N, the Lena Trough is the morphological connection to the well-known mid-Arctic spreading centre, the Gakkel Ridge. Does the Lena Trough consists out of a series of transforms or is it also an active spreading centre? These scientific problems are still not resolved.

A first successful experiment to provide constraints on the geodynamic evolution of the area was conducted in 1997 using the research icebreaker POLARSTERN. First seismic profiles could be acquired at 81°N, 80°30'N and 80°N across the entire Fram Strait. The new data show complex geological structures across the Greenland continental margin and in the Lena Trough north of 80°30'N. The swath bathymetry data indicate that the trough is a continuous bathymetric feature from 80°N to 81°N. Here, the strike of the eastern flank slightly turns to the NW. The central part of the Lena Trough has a water depth of 4400 m and has a first order transform at 81°N. A typical feature indicating a change in spreading directions. In strong contrast to the North Greenland continental margin, the conjugate Yermak Plateau Margin shows no evidence for recent tectonics. The sediments are up to 2 km thick. These units are most likely contourites deposited

by currents along the West Svalbard margin transporting an enormous amount of sediments northwards.

For a more detailed investigation of the tectonic features on both margins a major geophysical experiment was conducted in summer 1999. The seismic data were supplemented by gravity and magnetic data acquired in parallel with the acquisition of the seismic data.

Experimental Set-up

Multichannel seismic data (MCS) on the East Greenland Shelf/Wandel Sea were acquired with a 1600 m streamer and a 2400 m long streamer north of Spitsbergen. The seismic source was a tuned airgun cluster with a total volume of 24 l along most of the lines. In the Wandel Sea a large volume airgun PS100 (60 l) was occasionally added to the seismic array to gain deeper penetration for the seismic signals. For details see table 1. Seismic data processing was performed on board of POLARSTERN according to table 2.

Across the Lena Trough we flew several east-west trending magnetic profiles with the Scintrex Helimag system attached to the POLARSTERN helicopters. In total 5800 km of magnetic data were acquired in such a way.

During the entire cruise a Bodenseewerke gravimeter KSS31 collected continuously gravity data. The data were stored every 10 s on hard disc. Harbour measurements were made twice in Tromsø at the old Police Station. There was no failure of the KSS31 instrument during the expedition.

For the seismic refraction experiment recording stations onshore and on the sea bottom were used. Offshore we deployed a mixture of OBS stations from the Universities of Hokkaido and Bergen as well as OBH stations of the Alfred Wegener Institute. Onshore up to 12 Reftek recorders were installed on outcropping basement patches. Most of the instruments worked without failure during the three profiles we acquired across the western Spitsbergen continental margin.

As seismic source we used large volume airguns as well as dynamite. Due to the loss of one PS100 airgun just at the beginning of profile 99200, we used a BOLT and a PS100 airgun with a total volume of 90 l onboard POLARSTERN only. The dynamite shots were fired from the Polish ship EL TANIN. The charges varied between 25 and 50 kg. As EL TANIN could only carry 1.6 t TNT of in total 2.5 t TNT needed for all three profiles the ship had to pick up the rest of the dynamite between the 27th August and the 1st September at the Polish Hornsund base.

Shot statistics and profiles ARK XV/2

Profile Number	Start		End		Source	Streamer		Sonobuoys Number	Number of Shots	Length (km)	Start		End	
	Date	Time	Date	Time		Act. Len. (m)	Offset (m)				Lat	Lon	Lat	Lon
North / East Greenland														
99001	28.07.99	11:55	28.07.99	14:33	8 VLF / 1 PS100	1600	173		615	27.3	79.9595	-10.7692	80.077	-11.9777
99002	28.07.99	14:33	28.07.99	18:55	8 VLF / 1 PS100	1600	173		884	40.4	80.0773	-11.9791	80.0804	-14.021
99005	28.07.99	18:21	28.07.99	18:44	8 VLF / 1 PS100	1600	173		91	4.1	80.0871	-14.0569	80.1233	-14.0498
99006	28.07.99	18:44	28.07.99	21:40	8 VLF / 1 PS100	1600	173		701	32.4	80.1236	-14.0485	80.2723	-12.6054
99010	28.07.99	21:44	28.07.99	23:48	8 VLF / 1 PS100	1600	173		493	24.5	80.2786	-12.6036	80.349	-13.7768
99015	28.07.99	23:48	29.07.99	00:16	8 VLF *	1600	173		112	5.6	80.3491	-13.7795	80.3881	-13.7281
99016	29.07.99	00:16	29.07.99	01:12	8 VLF	1600	173		223	11.2	80.3883	-13.7257	80.4019	-13.1749
99017	29.07.99	01:12	29.07.99	02:33	8 VLF	1600	173		322	16.5	80.4022	-13.1731	80.5258	-12.9286
99018	29.07.99	02:33	29.07.99	03:39	8 VLF	1600	173		263	12.8	80.5263	-12.9291	80.6309	-13.2111
99019	29.07.99	03:39	29.07.99	04:40	8 VLF	1600	173		243	11.9	80.6314	-13.2116	80.7188	-12.8441
99020	29.07.99	04:40	29.07.99	08:16	8 VLF	1600	173		859	39.8	80.7192	-12.8431	81.0699	-12.5179
99021	29.07.99	08:26	29.07.99	11:03	8 VLF *	1600	173		625	29.5	81.0791	-12.4441	81.0826	-10.7561
99025	29.07.99	11:17	29.07.99	12:11	8 VLF / 1 PS100	1600	173		215	10	81.0689	-10.6883	81.0049	-11.0825
99026	29.07.99	12:22	29.07.99	13:00	8 VLF / 1 PS100	1600	173		151	7.8	80.9999	-11.1984	81.051	-11.4756
99027	29.07.99	13:00	29.07.99	15:38	8 VLF / 1 PS100	1600	173		629	28.4	81.0513	-11.478	80.9113	-12.765
99028	29.07.99	15:38	29.07.99	16:08	8 VLF / 1 PS100	1600	173		119	6.5	80.9108	-12.7649	80.854	-12.697
99030	29.07.99	16:08	29.07.99	18:20	8 VLF / 1 PS100	1600	173	9901	525	28.3	80.8535	-12.6969	80.6402	-13.4992
99035	29.07.99	18:20	29.07.99	20:18	8 VLF / 1 PS100	1600	173		470	23.5	80.6398	-13.498	80.4945	-12.5829
99036	29.07.99	20:18	30.07.99	01:12	8 VLF / 1 PS100 **	1600	173	9902	1170	55.6	80.494	-12.582	80.0167	-11.9851
99037	30.07.99	01:12	30.07.99	03:52	8 VLF / 1 PS100	1600	173		637	28.3	80.0164	-11.9854	79.7715	-12.2496
99040	30.07.99	04:01	30.07.99	07:53	8 VLF / 1 PS100	1600	173	9903	923	43.9	79.7629	-12.3032	79.8026	-14.4629
99045	30.07.99	08:05	30.07.99	09:00	8 VLF / 1 PS100	1600	173		219	10.5	79.7871	-14.5397	79.6936	-14.5369
99046	30.07.99	09:05	30.07.99	09:22	8 VLF / 1 PS100	1600	173		68	2.9	79.6902	-14.4959	79.7062	-14.3865
99047	30.07.99	09:22	30.07.99	10:02	8 VLF / 1 PS100	1600	173		159	7.2	79.7062	-14.3843	79.6587	-14.1515
99050	30.07.99	10:02	30.07.99	12:16	7 VLF / 1 PS100 *	1600	173		531	24.9	79.6586	-14.1495	79.6763	-12.9492
99055	30.07.99	12:16	30.07.99	13:56	7 VLF / 1 PS100	1600	173		398	18	79.6761	-12.9474	79.517	-12.9206
99060	30.07.99	14:05	30.07.99	16:11	7 VLF / 1 PS100	1600	173		502	25	79.5098	-12.8717	79.5072	-11.6502
99061	30.07.99	16:11	30.07.99	16:59	7 VLF / 1 PS100	1600	173	9904	191	9.5	79.5072	-11.6478	79.5383	-11.2285
99062	30.07.99	16:59	30.07.99	17:58	7 VLF *	1600	173		235	11.6	79.5383	-11.2259	79.4852	-10.7578
99063	30.07.99	17:58	30.07.99	18:35	7 VLF	1600	173		147	7.1	79.4851	-10.7553	79.4808	-10.4103
99065	30.07.99	18:40	30.07.99	20:32	7 VLF	1600	173		446	21.8	79.4754	-10.379	79.2936	-10.4017
99066	30.07.99	20:40	31.07.99	02:18	7 VLF / 1 PS100 **	1600	173	9905	1346	61.1	79.2837	-10.4498	79.2629	-13.2017
99067	31.07.99	02:18	31.07.99	03:08	7 VLF	1600	173		199	9.9	79.2631	-13.2035	79.3266	-13.5082
99075	31.07.99	03:14	31.07.99	03:47	7 VLF	1600	173		131	6.2	79.3233	-13.542	79.2915	-13.3027
99076	31.07.99	03:47	31.07.99	04:12	7 VLF	1600	173		99	4.7	79.2912	-13.3018	79.249	-13.2997
99077	31.07.99	04:12	31.07.99	07:03	7 VLF ==> 5 VLF	1600	173		681	31.5	79.2486	-13.2992	79.0168	-12.6729
99080	31.07.99	09:40	31.07.99	14:18	7 VLF	1600	173	9906	1095	48.4	78.9901	-12.4828	79.0065	-10.2712
99081	31.07.99	14:18	31.07.99	16:00	7 VLF	1600	173		406	19.4	79.0082	-10.2442	79.1649	-10.0179
99085	31.07.99	16:00	31.07.99	19:02	7 VLF	1600	173	9907	724	33	79.1652	-10.0192	79.3208	-11.2834
99086	31.07.99	19:02	31.07.99	20:45	7 VLF	1600	173		410	17.5	79.3211	-11.2844	79.4663	-11.1364

Tab. 1: Profile and shot statistics of all seismic reflection profiles during ARK-XV/2

Tab. 1 (continuation)

Profile Number	Start		End		Source	Streamer		Sonobuoys Number	Number of Shots	Length (km)	Start		End	
	Date	Time	Date	Time		Act. Len. (m)	Offset (m)				Lat	Lon	Lat	Lon
99087	31.07.99	20:45	31.07.99	23:07	6 VLF *	1600	173	9908	565	25.3	79.4666	-11.1363	79.6359	-11.6686
99090	31.07.99	23:07	01.08.99	01:35	6 VLF	1600	173		587	26.5	79.6363	-11.6684	79.6563	-12.9422
99095	01.08.99	01:44	01.08.99	06:10	6 VLF	1600	173	9909	1059	49.9	79.6676	-12.9847	79.8798	-10.9606
99100	01.08.99	06:10	01.08.99	08:00	6 VLF	1600	173	9910	438	20.7	79.8798	-10.9585	79.886	-9.9358
99105	01.08.99	08:15	01.08.99	11:10	6 VLF	1600	173		696	30.1	79.8951	-9.8753	79.8959	-11.2756
99106	01.08.99	11:10	01.08.99	12:13	6 VLF	1600	173		251	11.2	79.8957	-11.2775	79.8342	-11.5632
99107	01.08.99	12:13	01.08.99	17:00	6 VLF	1600	173	9911	1142	54.3	79.8342	-11.5658	80.0035	-14.0773
99110	01.08.99	17:15	01.08.99	20:51	6 VLF	1600	173	9912	860	40.7	80.0172	-14.0656	80.117	-12.0864
99115	02.08.99	03:02	02.08.99	04:15	8 VLF	1600	173	9913	291	13.3	80.1182	-11.759	80.2037	-11.7695
99116	02.08.99	04:15	02.08.99	06:06	8 VLF	1600	173		441	20.7	80.2045	-11.7679	80.2805	-10.9154
99117	02.08.99	06:06	02.08.99	07:00	8 VLF	1600	173		214	10.1	80.2807	-10.9103	80.2621	-10.4155
99118	02.08.99	07:00	02.08.99	07:16	8 VLF	1600	173		63	2.9	80.2618	-10.414	80.2384	-10.3618
99119	02.08.99	07:16	02.08.99	08:08	8 VLF	1600	173		207	9.3	80.238	-10.3607	80.248	-9.9392
99120	02.08.99	08:08	02.08.99	08:50	8 VLF	1600	173	9914	168	5.3	80.2484	-9.9394	80.2738	-10.1138
North / West Svalbard														
99125	13.08.99	14:53	13.08.99	16:13	8 VLF	2400	173		318	14.5	81.9342	19.0591	81.9243	19.9552
99130	13.08.99	16:20	14.08.99	05:16	8 VLF	2400	173	9915-18	3083	131.6	81.9177	20.001	80.7467	19.9506
99135	14.08.99	07:00	14.08.99	11:30	8 VLF	2400	173	9919	1073	52.7	80.7512	19.9988	81.122	18.3138
99136	14.08.99	12:31	14.08.99	17:49	8 VLF	2400	173	9920	1263	59.6	81.1811	18.3115	81.5409	16.3514
99137	14.08.99	18:07	14.08.99	22:17	8 VLF	2400	173	9921-22	992	48.3	81.5538	16.3946	81.8503	14.2353
99140	14.08.99	22:25	15.08.99	04:59	8 VLF	2400	173	9923	1565	66.8	81.8464	14.1863	81.2543	14.3302
99145	15.08.99	05:06	15.08.99	09:26	8 VLF	2400	173		1032	46.3	81.2487	14.285	81.3467	11.6364
99150	15.08.99	09:26	15.08.99	13:25	8 VLF	2400	173		949	39.8	81.3463	11.6326	81.0072	12.02
99155	15.08.99	13:29	16.08.99	02:10	8 VLF	2400	173	9924-26	3020	139.2	81.0013	12.0122	80.2092	6.2058
99156	16.08.99	02:16	16.08.99	09:59	8 VLF	2400	173		1839	75.2	80.2034	6.2154	80.0021	9.9338
99157	16.08.99	10:05	16.08.99	14:15	8 VLF	2400	173		992	40.3	80.0029	9.9817	80.1002	11.982
99160	16.08.99	14:20	16.08.99	21:22	7 VLF *	2400	173		1676	77.3	80.1044	12.0146	80.5832	14.9592
99161	16.08.99	21:27	17.08.99	04:40	7 VLF	2400	173	9927	1720	74.4	80.5902	14.974	81.2435	14.2766
99165	17.08.99	04:46	17.08.99	20:17	7 VLF	2400	173	9928-29	3697	161	81.2519	14.2955	82.0472	22.2106
99166	17.08.99	20:17	18.08.99	01:41	7 VLF	2400	173	9930-31	1287	59.5	82.0472	22.2138	81.9315	25.7762
99170	18.08.99	01:50	18.08.99	16:00	7 VLF	2400	173	9932-35	3375	151.5	81.9214	25.8223	80.5741	25.8029
99175	18.08.99	17:31	18.08.99	23:16	7 VLF	2400	173	9936	1375	62.9	80.5576	25.9134	80.5096	29.3063
99176	18.08.99	23:24	19.08.99	14:34	7 VLF	2400	173	9937	3615	167.5	80.5176	29.3591	82.003	29.2235

* Changing configuration of airguns during the profile. The dominating configuration is listed here.

** Temporary failure of PS100

Tab. 2: Processing statistics for the onboard processing. As hardware platform a SGI Origin 200 with 2 CPU's were used.

Seismic processing ARK XV/2

Profile	Lead-in (m)	Offset to 1st Hydrophone (m)	Chan	Group (m)	RL (s)	SR (ms)	SI (s)	Field-Cartridge No.	Demultiplexing File	Demultiplexing Date	Cartridge No.	File	Sorting Date	Cartridge No.
99001	10	173	64	25	12	2	15	F03300-F03307	001DEMUX	01.08.1999	C16550-C16554	001CDPSORT	22.08.1999	
99002	10	173	64	25	12	2	15	F03307-F03311	005DEMUX	01.08.1999	C16555-C16557	002CDPSORT	22.08.1999	
99005	10	173	64	25	12	2	15	F03311-F03314	010DEMUX	01.08.1999	C16558-C16560	006CDPSORT	22.08.1999	
99010	10	173	64	25	12	2	15	F03314-F03319	015DEMUX	01.08.1999	C16561-C16567	010CDPSORT	22.08.1999	
99015	10	173	64	25	12	2	15					016CDPSORT	22.08.1999	
99016												017CDPSORT	22.08.1999	
99017												018CDPSORT	22.08.1999	
99018												019CDPSORT	22.08.1999	
99019												020CDPSORT	22.08.1999	
99020	10	173	64	25	12	2	15	F03320-F03327	020DEMUX	01.08.1999	C16561-C16567*	021CDPSORT	22.08.1999	
99021											C16568-C16570*	025CDPSORT	22.08.1999	
99025	10	173	64	25	12	2	15	F03327-F03336	025DEMUX	01.08.1999	C16571-C16576	026CDPSORT	22.08.1999	
99026												027CDPSORT	22.08.1999	
99027												028CDPSORT	22.08.1999	
99028												029CDPSORT	22.08.1999	
99030												030CDPSORT	22.08.1999	
99035	10	173	64	25	12	2	15	F03336-F03347	035DEMUX	01.08.1999	C16577-C16584	035CDPSORT	22.08.1999	
99036												036CDPSORT	22.08.1999	
99037												037CDPSORT	22.08.1999	
99040	10	173	64	25	12	2	15	F03347-F03351	040DEMUX	04.08.1999	C16585-C16587	040CDPSORT	22.08.1999	
99045	10	173	64	25	12	2	15	F03352-F03358	045DEMUX	04.08.1999	C16588-C16591	045CDPSORT	22.08.1999	
99046												046CDPSORT	22.08.1999	
99047												047CDPSORT	22.08.1999	
99050												050CDPSORT	22.08.1999	
99055	10	173	64	25	12	2	15	F03358-F03365	055DEMUX	04.08.1999	C16592-C16593	055CDPSORT	22.08.1999	
99060	10	173	64	25	12	2	15	F03365-F03367	060DEMUX	04.08.1999	C16594-C16597	060CDPSORT	22.08.1999	
99061												061CDPSORT	22.08.1999	
99062												062CDPSORT	22.08.1999	
99063												063CDPSORT	22.08.1999	
99065	10	173	64	25	12	2	15	F03368-F03367	065DEMUX	04.08.1999	C16598-C16599	065CDPSORT	22.08.1999	
99066												066CDPSORT	22.08.1999	
99067												067CDPSORT	22.08.1999	
99075	10	173	64	25	12	2	15	F03376-F03380	075DEMUX	04.08.1999	C16605-C16607	075CDPSORT	22.08.1999	
99076												076CDPSORT	22.08.1999	
99077												077CDPSORT	22.08.1999	
99080	10	173	64	25	12	2	15	F03381-F03388	080DEMUX	10.08.1999	C16608-C16612	080CDPSORT	22.08.1999	
99081												081CDPSORT	22.08.1999	
99085	10	173	64	25	12	2	15	F03388-F03397	085DEMUX	10.08.1999	C16613-C16618	085CDPSORT	22.08.1999	
99086												086CDPSORT	22.08.1999	
99087												087CDPSORT	22.08.1999	
99090	10	173	64	25	12	2	15	F03397-F03399	090DEMUX	10.08.1999	C16619-C16620	090CDPSORT	22.08.1999	
99095	10	173	64	25	12	2	15	F03400-F03405	095DEMUX	10.08.1999	C16621-C16624	095CDPSORT	22.08.1999	
99100	10	173	64	25	12	2	15	F03405-F03407	100DEMUX	10.08.1999	C16625-C16626	100CDPSORT	22.08.1999	

Tab. 2 (continuation):

99105	10	173	64	25	12	2	15	F03406-F03418	105DEMUX	10.08.1999	C16627-C16633	105CDPSORT	22.08.1999
99106												106CDPSORT	22.08.1999
99107												107CDPSORT	22.08.1999
99110	10	173	64	25	12	2	15	F03418-F03422	110DEMUX	12.08.1999	C16634-C16636	110CDPSORT	22.08.1999
99115	10	173	64	25	12	2	15	F03423-F03429	115DEMUX	12.08.1999	C16637-C16641	115CDPSORT	22.08.1999
99116												116CDPSORT	22.08.1999
99117												117CDPSORT	22.08.1999
99118												118CDPSORT	22.08.1999
99119												119CDPSORT	22.08.1999
99120	10	173	64	25	12	2	15	F03429-F03430	120DEMUX	12.08.1999	C16642	120CDPSORT	24.08.1999
99125	10	173	94	25	12	2	15	F03431-F03433	125DEMUX	13.08.1999	C16643-C16644	125CDPSORT	24.08.1999
99130	10	173	94	25	12	2	15	F03433-F03455	130DEMUX	14.08.1999	C16645-C16658	130CDPSORT	24.08.1999
99135	10	173	94	25	12	2	15	F03456-F03483	135DEMUX	15.08.1999	C16659-C16676	135CDPSORT	24.08.1999
99136												136CDPSORT	24.08.1999
99137												137CDPSORT	24.08.1999
99140	10	173	94	25	12	2	15	F03483-F03494	140DEMUX	16.08.1999	C16677-C16684	140CDPSORT	24.08.1999
99145	10	173	94	25	12	2	15	F03494-F03501	145DEMUX	16.08.1999	C16685-C16689	145CDPSORT	24.08.1999
99150	10	173	94	25	12	2	15	F03502-F03508	150DEMUX	16.08.1999	C16690-C16694	150CDPSORT	24.08.1999
99155	10	173	94	25	12	2	15	F03508-F03530	155DEMUX	16.08.1999	C16695-C16708	155CDPSORT	24.08.1999
99156	10	173	94	25	12	2	15	F03530-F03543	156DEMUX	17.08.1999	C16709-C16717	156CDPSORT	24.08.1999
99157	10	173	94	25	12	2	15	F03543-F03551	157DEMUX	17.08.1999	C16718-C16723	157CDPSORT	24.08.1999
99130	10	173	94	25	12	2	15	F03551-F03563	160DEMUX	17.08.1999	C16724-C16731	160CDPSORT	24.08.1999
99161	10	173	94	25	12	2	15	F03563-F03575	161DEMUX	17.08.1999	C16732-C16739	161CDPSORT	24.08.1999
99165	10	173	94	25	12	2	15	F03575-F03602	165DEMUX	18.08.1999	C16740-C16757	165CDPSORT	24.08.1999
99166	10	173	94	25	12	2	15	F03602-F03611	166DEMUX	18.08.1999	C16758-C16764	166CDPSORT	24.08.1999
99170	10	173	94	25	12	2	15	F03611-F03635	170DEMUX	18.08.1999	C16765-C16779	170CDPSORT	24.08.1999
99175	10	173	94	25	12	2	15	F03636-F03645	175DEMUX	18.08.1999	C16780-C16786	175CDPSORT	24.08.1999
99176	10	173	94	25	12	2	15	F03646-F03671	176DEMUX	19.08.1999	C16878-C16802	176CDPSORT	24.08.1999
99200	none	F03672											
99300	none	F03673											
99400	??	??	??	25	12	2	15	F03674-F03680					24.08.1999

* After demultiplexing profile 99020 renames to profile 99021 and 99020 becomes a part of the original 99015

Results

East Greenland/Wandel Sea

This season intermediate ice conditions were present on the East Greenland shelf. While the North Greenland Shelf was fully covered by heavy pack ice, reasonable ice conditions were found in the inner shelf area. This year the shelf edge could not be reached with towed seismic systems. In total 1183 km of MCS data were acquired with a 1600 m streamer and a tuned airgun array of 24 l (Fig.5, for details see tab. 1). They were partly processed onboard of POLARSTERN (tab. 2).

The seismic lines are dominated by strong water bottom multiples caused by an overcompacted sea floor. However, the experimental set-up will allow to remove the multiple noise and resolve also deeper strata (Fig. 6). At some locations outcropping sediment sequences can be observed on the EPC recordings. Such areas are connected with pronounced gravity lows as already mapped by satellite altimeter data. Gravity and seismic data strongly suggest that these bodies represent salt domes, which rose up from deeper levels. Such a salt province is also indicated in the most recent tectonic map for East Greenland based on seismic and gravity interpretations. More detailed interpretations will be possible after careful data processing. Parallel to the MCS data acquisition we deployed in total 14 sonobuoys to gain additional wide-angle velocity information for the depth conversion of the MCS data. Most of the sonobuoys recorded seismic signals up to 40 km offset. This allowed determining the thickness of the sediments. At most of the recordings typical upper crustal velocities of 6.0 km/s can be observed in the far offsets.

Lena Trough

No new seismic data across the Lena Trough and the western margin of the Yermak Plateau were acquired due to the heavy ice conditions. Also the planned magnetic helicopter survey was strongly hindered by bad weather conditions, especially fog. Finally, only the southern part of the research area between 81°N and 80°N could be covered with magnetic profiles. The data show a very smooth magnetic field, with almost no evidence for spreading anomalies. A final processing of the data was not possible on board POLARSTERN, as the daily variations from the permanent stations onshore Spitsbergen and Greenland were not available. So, the interpretation can only be preliminary. Later, the helicopter data will be merged with a similar magnetic data acquired in this season by the Dornier aircraft POLAR 2 in the same area.

Northern Spitsbergen/Nansen Basin

One of the alternate research areas was the margin off Northern Spitsbergen and if possible to penetrate the Nansen Basin. These measurements were favoured by an extreme large polynia both in northern and eastern directions along the northern Barents Shelf continental margin. First systematic MCS data could be acquired between 15°E and 30°E describing the structural fabric of the southernmost margin of the Eurasian Basin. The northernmost profile was collected up 82°N. In total 1470 km of MCS data were acquired. In combination

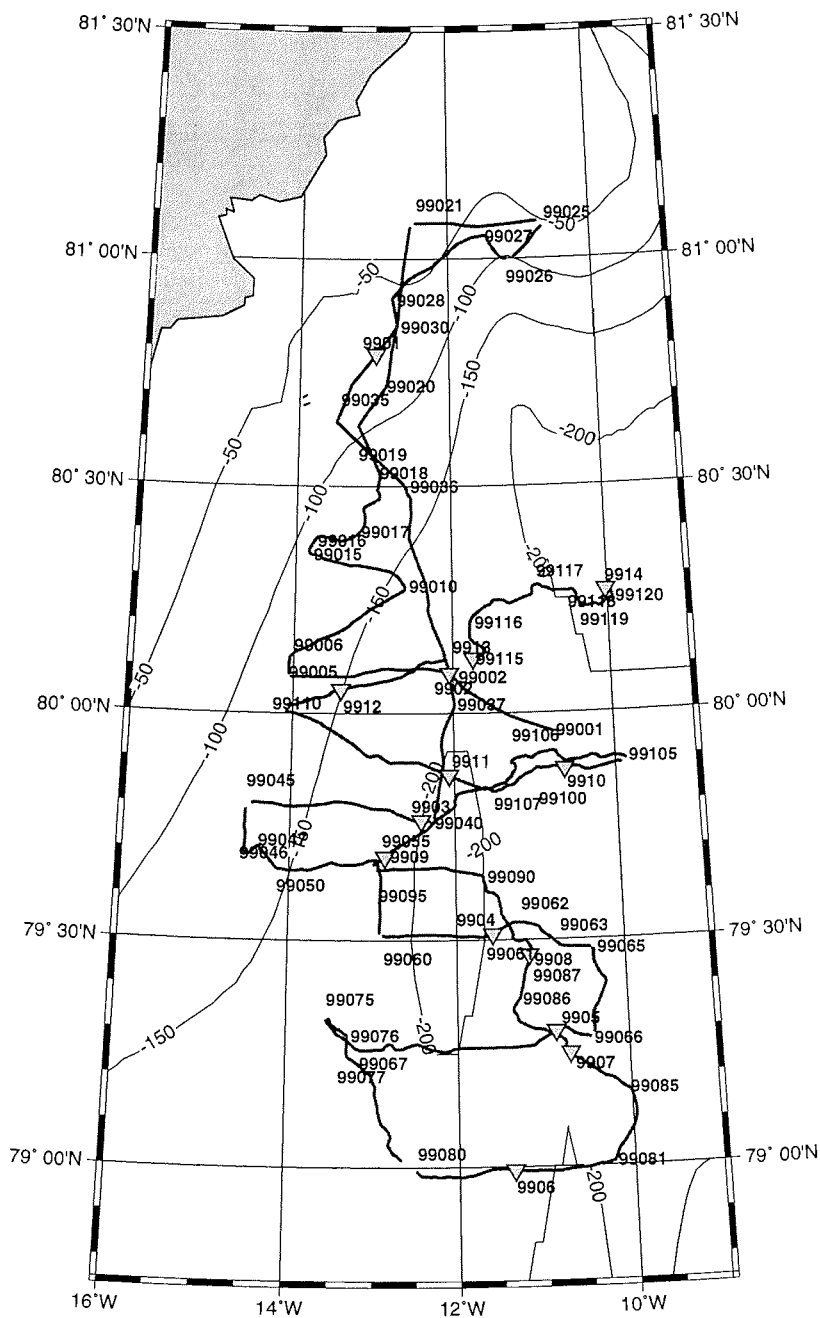


Fig. 5: Seismic reflection network acquired during the summer 1999 off North-East Greenland removal with standard processing techniques.

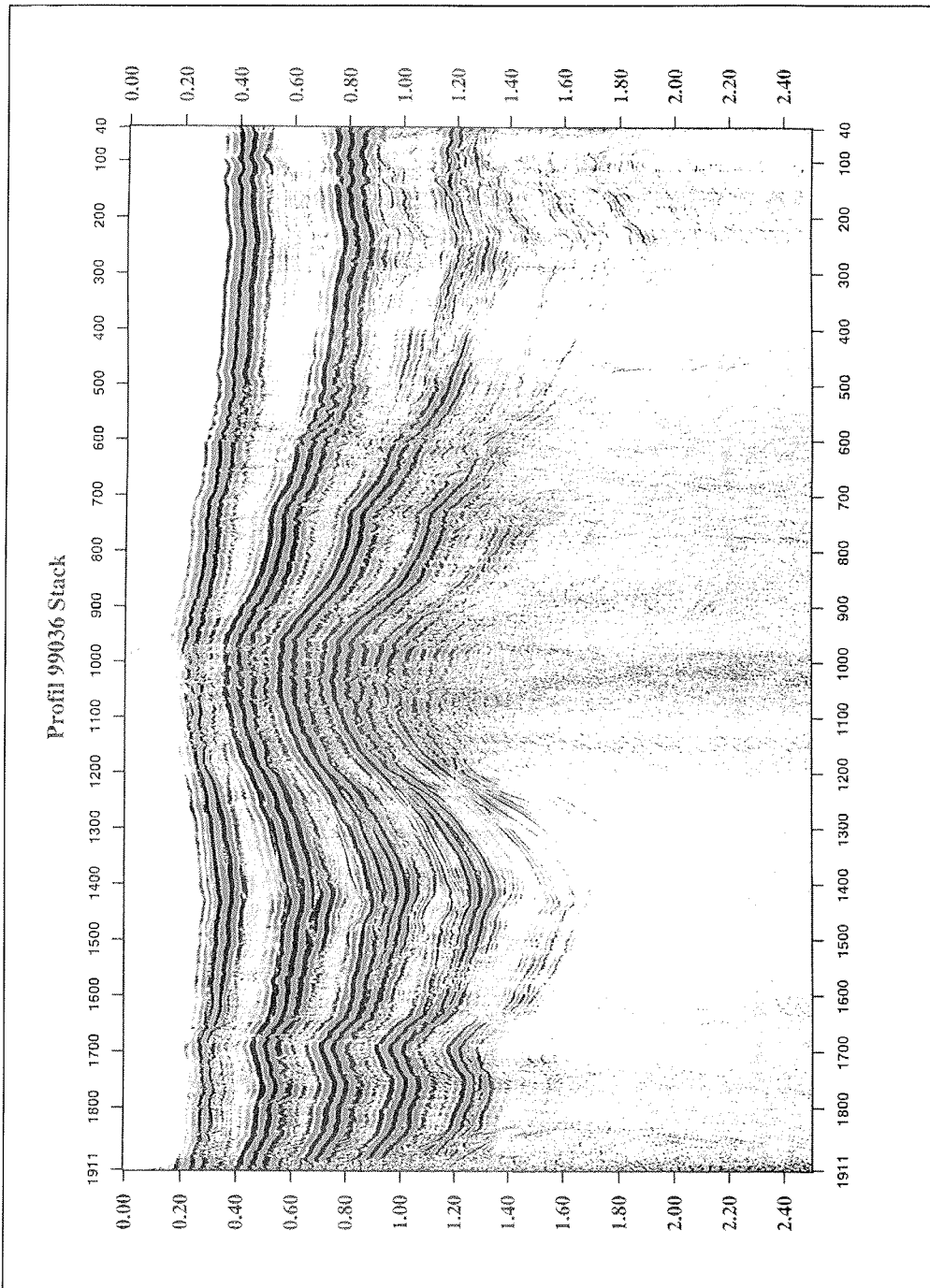


Fig. 6: Seismic profile across a proposed salt dome. Please note the complete failure of multiple removal with standard processing techniques.

with the new swath bathymetry (see chapter 5) the data give the most complete view available on the structural elements of this margin. Furthermore, 23 sonobuoys were deployed along the seismic lines for additional wide-angle seismic velocity information (Fig. 7).

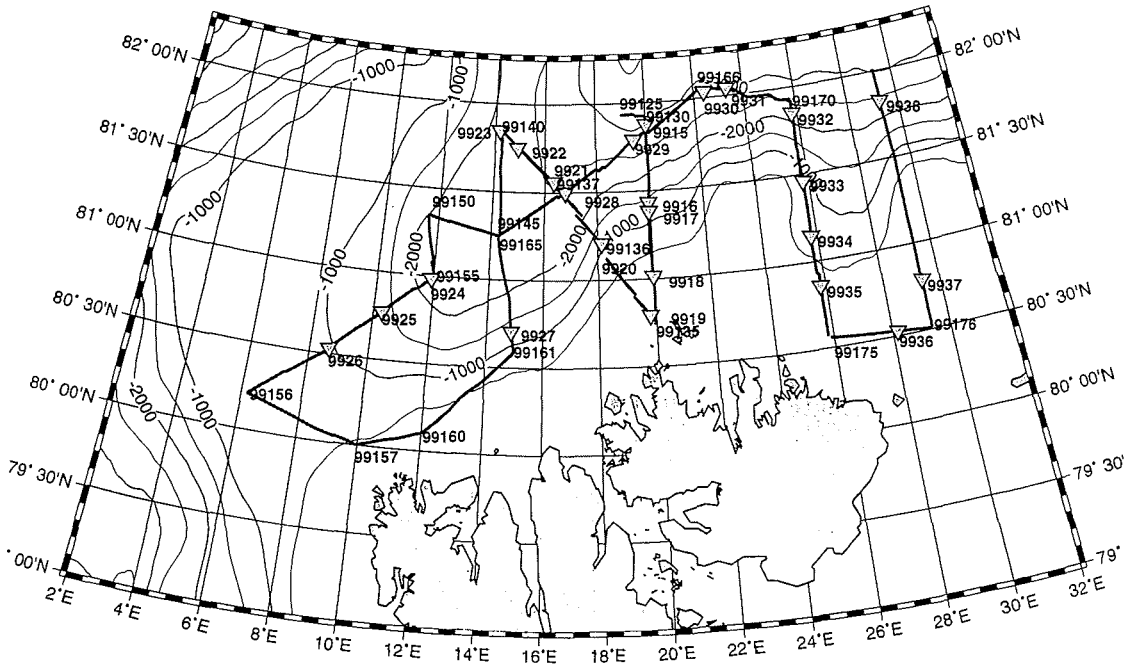


Fig.7: Seismic reflection network acquired during the summer 1999 off Northern Svalbard

At 25°E the continental slope is dominated by rough topography and steep escarpments. Strong currents/turbidites must have formed this topography. Even in the deep sea the seismic data indicate the presence of coarse material at water depths greater than 3000 m. The continental slope is becoming more gentle at 30°E. Almost no canyons can be observed on the continental slope. Basement reflectors are not observed on the analog recordings available during the measurements. Future data processing of the seismic reflection and refraction data will allow to calculate some reliable depths.

Based on information from the swath bathymetric mapping, which shows two topographic highs at the southern margin of the Yermak Plateau, the structures

were investigated. The MCS data clearly show only the presence of a thin sedimentary cover. Steep escarpments with dips up to 10° at the southern flanks consist of basement rocks of unknown origin. Dredging as described in chapter 4 was not successful at the western most location (Mosby Peak). A second trial at 15°E recovered some gneisses from the basement. On the first view, this type of rocks is similar to those found along the northern coast of Spitsbergen. Here, the gneisses belong to the Hekla Hoek formation. This supports models, which interpret the region between the northern Spitsbergen margin and the Yermak Plateau not to consist of oceanic crust but a mixture of both, continental and oceanic. This is also a hypothesis, which has been suggested based on the very quiet magnetic field in this area. No sea floor spreading anomalies are visible between 10°E and 20°E , which might support the presence of stretched continental crust.

Results - Magnetic data -

Parallel to the seismic lines across the North Svalbard Margin magnetic data were collected with the helicopter system Helimag (Fig. 8). The survey tried to fill a gap in the available magnetic data set for the Arctic. The spacing of the flight lines was 7 km (App. 1). Between 10°E and 20°E the magnetic field is very smooth. Only in the north strong positive anomalies across the Yermak Plateau can be observed. Continuous bad weather conditions prevented the acquisition of additional data more to the east. In the east only one line at 30°E exists. The magnetic data show low frequent anomalies, which can be interpreted to be the result of sea floor spreading. The processing of the data was not completed onboard of POLARSTERN as the daily variation from the magnetic base stations were not available.

Results - Seismic refraction data -

Off the northern and western coast of Spitsbergen in total three deep seismic profiles were acquired during summer 1999 (Fig. 9). Both, land and ocean bottom stations were used to record the seismic signals generated by large volume airguns on POLARSTERN and dynamite shots from the Polish ship EL TANIN. Seven ocean bottom hydrophones (OBH) from AWI and eight ocean bottom seismometers (OBS) from the Universities of Hokkaido and Bergen were used throughout the experiment (Tab. 3 - 7).

In general, the Reftek land stations have an excellent data quality with offsets well over 100 km. On most of the stations clear PmP and Pn arrivals from the Moho discontinuity and the earth's mantle are recorded (Fig. 10).

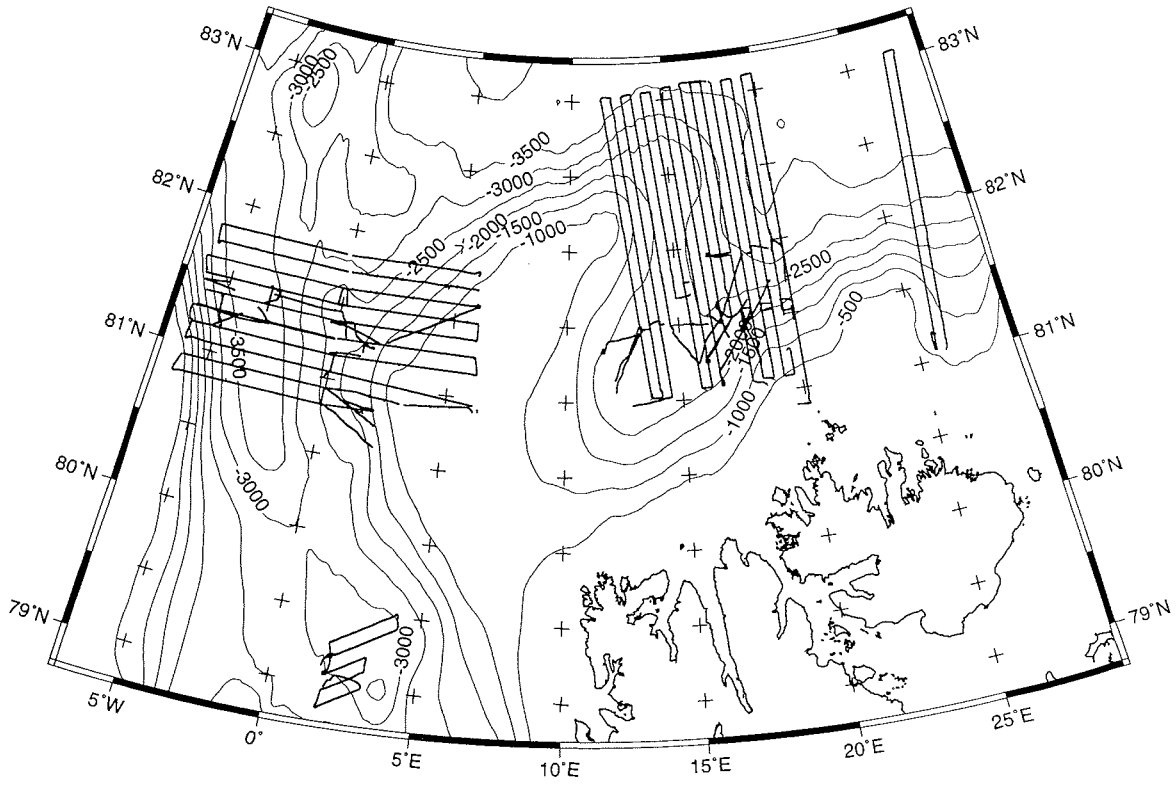


Fig. 8: Magnetic flight lines with the Helicopter borne HELIMAG system off Svalbard

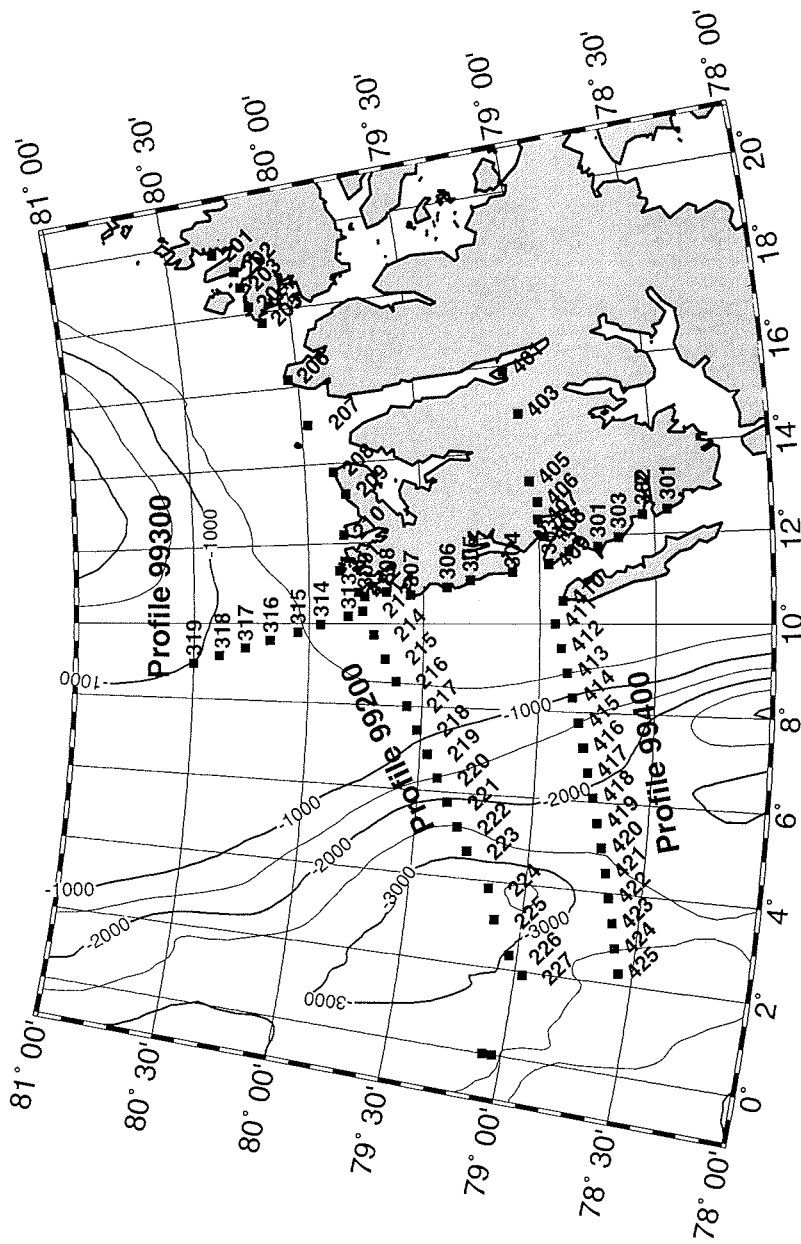


Fig. 9: Deep seismic sounding lines acquired off Svalbard. Only the locations of the REFTEK landstations and the OBS/OBH systems are shown.

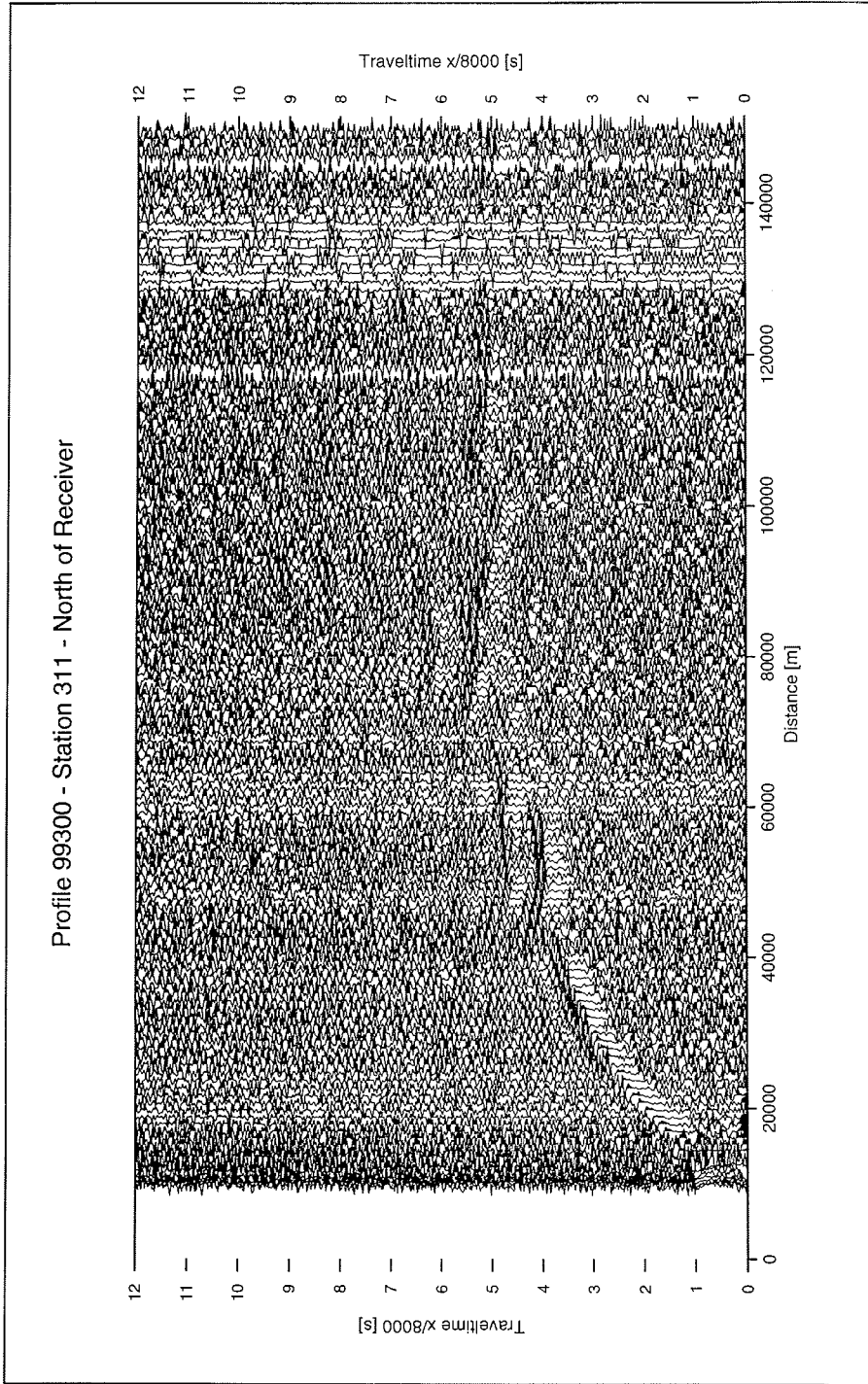


Fig. 10: Example for a deep seismic sounding recording along line 99300. The data of a landbased station is shown.

Refraction profiles: ocean bottom- and land stations

Profile Nr.	Station Nr.	Device Name	Chan. Nr.	Deployment		Retrieval		Altitude m	Start		Stop		Tape Nr.	Signalrange in km
				Lat. (N)	Long. (E)	Lat. (N)	Long. (E)		Date	Time	Date	Time		
99200	201	AWI 01	3	80°17.94	19°48.62	80°17.94	19°48.62	15	20.08.99	09:33	23.08.99	11:10	9	
99200	202	AWI 03	3	80°17.30	19°04.97	80°17.30	19°04.97	20	20.08.99	08:20	23.08.99	10:36	1	
99200	203	AWI 04	3	80°10.29	18°43.83	80°10.29	18°43.83	23	20.08.99	12:07	23.08.99	11:47	2	
99200	204	AWI 05	3	80°09.32	17°58.37	80°09.32	17°58.37	15	20.08.99	13:17	23.08.99	12:30	5	
99200	205	AWI 06	3	80°08.12	17°46.26	80°08.12	17°46.26	5	20.08.99	13:01	23.08.99	12:32	4	
99200	206	AWI 12	3	80°00.46	16°17.12	80°00.46	16°17.12	40	20.08.99	11:20	23.08.99	12:47	6	
99200	207	OBH 1	4	79°57.30	15°00.10	79°57.25	14°56.54	-140	20.08.99	15:11	23.08.99	22:24		
99200	208	AWI 08	3	79°50.38	13°47.99	79°50.38	13°47.99	40	20.08.99	17:16	23.08.99	14:46	11	
99200	209	AWI 13	3	79°48.96	13°15.39	79°48.96	13°15.39	23	20.08.99	16:18	23.08.99	15:46	3	
99200	210	AWI 15	3	79°49.63	12°22.60	79°49.63	12°22.60	15	20.08.99	14:57	23.08.99	17:47	7	
99200	211	AWI 16	3	79°53.08	11°28.76	79°53.08	11°28.76	10	20.08.99	17:37	23.08.99	18:47	8	
99200	212	AWI 17	3	79°46.26	10°44.34	79°46.26	10°44.34	20	20.08.99	18:46	23.08.99	19:42	10	
99200	213	OBS A	3	79°46.20	10°19.10	79°46.40	19°19.00	-140						
99200	214	OBH 2	4	79°43.04	09°43.20	79°43.10	09°43.50	-360	20.08.99	23:39	24.08.99	00:45		
99200	215	OBS B	3	79°40.06	09°08.57	79°40.10	09°08.50	-380						
99200	216	OBH 3	4	79°37.10	08°35.10	79°37.13	08°35.85	-460	21.08.99	01:02	24.08.99	03:39		
99200	217	OBS C	3	79°34.09	08°01.00	79°34.20	08°00.40	-700						
99200	218	OBH 4	4	79°31.13	07°27.20	79°31.20	07°27.00	-900	21.08.99	02:10	24.08.99	05:34		
99200	219	OBS D	3	79°28.00	06°52.80	79°28.10	06°52.30	-1230						
99200	220	OBH 5	4	79°25.03	06°18.48	79°51.00	06°18.40	-1630	21.08.99	03:00	24.08.99	09:05		
99200	221	OBS E	3	79°22.00	05°46.00	79°21.80	05°46.40	-1910						
99200	222	OBH 6	4	79°19.02	05°11.80	79°18.90	05°11.91	-2050	21.08.99	03:43	25.08.99	13:26		
99200	223	OBS F	3	79°16.00	04°38.60	79°16.00	04°38.10	-2290						
99200	224	OBH 7	4	79°09.66	03°50.02	79°09.45	03°47.41	-2370	21.08.99	04:38	24.08.99	22:34		
99200	225	OBS G	3	79°07.00	03°07.80	79°06.90	03°07.90	-5450						
99200	226	OBS H	3	79°02.00	02°20.90	79°02.20	02°20.30	-2700						
99200	227								not deployed					

Tab. 3: Locations of all OBS/OBH and landstations deployed along profile 99200

Tab. 4: Location of dynamite shots fired from the EL TANIN along profile 99200

Shotlist of Eltanin

Profile 99200

Shotnumber	Long. (N)	Lat. (E)	Depth (m)	TNT (kg)	Status
2001	79°44.611	10°00.66	340	25	ok
2002	79°43.288	9°47.711	360	25	ok
2003	79°41.916	9°31.826	370	25	ok
2004	79°40.505	9°16.632	370	25	ok
2005	79°39.302	9°02.011	420	25	failed
	79°39.380	9°02.224	410	25	failed
2006	79°38.007	8°47.420	440	25	ok
2007	79°36.686	8°32.142	490	25	weak
2008	79°35.342	8°17.583	600	25	ok
2009	79°34.100	8°02.478	700	25	weak
2010	79°32.764	7°47.644	790	25	failed
2011	79°31.479	7°32.677	880	25	failed
	79°31.526	7°32.380	880	25	ok
2012	79°30.059	7°17.860	1010	25	failed
	79°30.116	7°17.700	1000	25	ok
2013	79°28.803	7°00.464	1140	25	ok
2014	79°27.485	6°47.549	1230	25	ok
2015	79°26.297	6°33.108	1300	25	ok
2016	79°24.776	6°18.167	1280	25	ok
2017	79°23.511	6°03.954	1750	25	ok
2018	79°22.218	5°49.242	1440	25	ok
2019	79°20.876	5°34.145	1440	25	ok
2020	79°19.629	5°19.678	1440	25	ok
2021	79°18.327	5°05.316	1490	25	ok
2022	79°17.156	4°50.717	1550	25	ok
2023	79°15.650	4°36.700	2270	25	ok
2024	79°14.340	4°21.252	2190	50	ok
2025	79°13.068	4°08.268	2250	50	ok

The values for the depth are taken from the Hydrosweep and rounded to 10m

Tab. 5: Locations of all OBS/OBH and lanstations deployed along profile 99300

Profile	Station	Device	Chan.	Deployment		Retrieval		Altitude	Start		Stop		Tape	Signalrange
Nr.	Nr.	Name	Nr.	Lat. (N)	Long. (E)	Lat. (N)	Long. (E)	m	Date	Time	Date	Time	Nr.	in km
99300	301													
99300	302													
99300	303													
99300	304	AWI 02	3	78°46.42	11°46.66	78°46.42	11°46.66	35	25.08.99	14:49	27.08.99	10:07	6	
99300	305	AWI 16	3	78°51.37	11°43.48	78°51.37	11°43.48	70	25.08.99	16:06	27.08.99	10:59	4	
99300	306	AWI 06	3	78°57.41	11°24.31	78°57.41	11°24.31	8	25.08.99	17:41	27.08.99	11:37	5	
99300	307	AWI 04	3	79°08.46	11°18.89	79°08.46	11°18.89	10	25.08.99	14:53	27.08.99	09:44	3	
99300	308	AWI 15	3	79°16.91	11°01.69	79°16.91	11°01.69	10	25.08.99	16:12	27.08.99	10:24	1	
99300	309	AWI 17	3	79°23.42	10°53.81	79°23.42	10°53.81	5	25.08.99	17:24	27.08.99	11:11	2	
99300	310	AWI 11	3	79°31.49	10°41.11	79°31.49	10°41.11	10	25.08.99	19:39	27.08.99	12:35	7	
99300	311	AWI 12	3	79°39.88	10°45.69	79°39.88	10°45.69	5	25.08.99	19:44	27.08.99	12:48	9	
99300	312	AWI 13	3	79°46.27	10°44.35	79°46.27	10°44.35	??	25.08.99	20:34	27.08.99	14:33	8	
99300	313	OBH 1	4	79°50.05	10°09.82	79°50.10	10°09.90	-400	25.08.99	18:47	27.08.99	20:44		
99300	314	OBH 2	4	79°56.69	09°57.18	79°56.40	79°57.80	-480	25.08.99	19:46	28.08.99	11:13		
99300	315	OBH 3	4	80°03.26	09°46.32	80°03.29	09°46.59	-520	25.08.99	20:52	28.08.99	10:52		
99300	316	OBH 4	4	80°09.90	09°32.48	80°09.74	09°32.36	-570	25.08.99	22:22	28.08.99	17:23		
99300	317	OBH 5	4	80°16.72	09°21.69	80°16.70	09°21.96	-610	25.08.99	23:10	28.08.99	16:35		
99300	318	OBH 6	4	80°23.44	09°09.03	80°23.38	09°08.43	-710	26.08.99	00:07	28.08.99	14:51		
99300	319	OBH 7	4	80°30.27	08°55.89	80°30.10	08°56.40	-950	26.08.99	01:32	28.08.99	13:43		

Profile Nr.	Station Nr.	Device Name	Chan. Nr.	Deployment		Retrieval		Altitude m	Start		Stop		Tape Nr.	Signalrange in km
				Lat. (N)	Long. (E)	Lat. (N)	Long. (E)		Date	Time	Date	Time		
99400	401	AWI 05	3	79°07.32	16°16.65	79°07.32	16°16.65	75	01.09.99	14:02	04.09.99	10:00	7	
99400	402	not deployed												
99400	403	AWI 06	3	79°04.75	14°55.12	79°04.75	14°55.12	900	01.09.99	15:27	04.09.99	09:49	8	
99400	404	not deployed												
99400	405	AWI 13	3	79°03.24	13°12.24	79°03.24	13°12.24	900	01.09.99	15:12	04.09.99	09:46	1	
99400	406	AWI 12	3	78°58.64	12°44.72	78°58.64	12°44.72	120	01.09.99	13:49	04.09.99	10:41	2	
99400	407	AWI 1/11	3	78°57.63	12°28.41	78°57.63	12°28.41	90	01.09.99	12:38	04.09.99	10:59	3	
99400	408	AWI 15	3	78°59.63	11°59.63	78°59.63	11°59.63	30	01.09.99	11:16	04.09.99	09:47	6	
99400	409	AWI 17	3	78°57.45	11°24.35	78°57.45	11°24.35	10	01.09.99	10:08	04.09.99	11:55	4	
99400	410	AWI 16	3	78°53.69	10°30.00	78°53.69	10°30.00	10	01.09.99	09:19	04.09.99	12:00	5	
99400	411	OBS A	3											
99400	412	OBH 1	4	78°54.40	09°26.10	78°54.26	09°25.72	-210	31.08.99	17:30	04.09.99	14:51		
99400	413	OBS B	3											
99400	414	OBH 2	4	78°51.08	08°18.68	78°50.66	08°17.22	-820	31.08.99	17:15?	04.09.99	16:01		
99400	415	OBS C	3											
99400	416	OBH 3	4	78°48.17	07°10.17			-1360	31.08.99	18:41	04.09.99	15:32		
99400	417	OBS D	3											
99400	418	OBH 4	4	78°44.72	06°04.77			-2300	31.08.99	16:47	04.09.99	14:24		
99400	419	OBS E	3											
99400	420	OBH 5	4	78°41.46	04°59.24	78°40.60	04°57.30	-2370	31.08.99	15:31	03.09.99	19:43		
99400	421	OBS F	3											
99400	422	OBH 6	4	78°38.37	03°52.74	not retrieved		-2360	31.08.99	14:57	not retrieved			
99400	423	OBS G	3											
99400	424	OBH 7	4	78°35.09	02°47.81	78°34.90	02°48.90	-2560	31.08.99	14:08	03.09.99	13:15		
99400	425	OBS H	3											

Tab. 6: Locations of all OBS/OBH and lanstations deployed along profile 99400

Tab. 7: Location of dynamite shots fired from the EL TANIN along profiles 99300 and 99400

Shotlist of Eltanin

Profile 99300

Shotnumber	Long. (N)	Lat. (E)	Depth (m)	TNT (kg)	Status
3001	79°48.07	10°15.237	360	25	ok
3002	79°50.569	10°08.680	410	25	ok
3003	79°53.656	10°04.647	450	25	ok
3004	79°56.490	9°59.899	480	25	ok
3005	79°59.309	9°54.515	490	25	ok
3006	80°02.277	9°49.452	510	25	ok
3007	80°05.143	9°44.165	540	25	ok
3008	80°07.990	9°39.071	560	25	ok
3009	80°10.814	9°33.879	580	25	ok
3010	80°13.723	9°28.632	580	25	ok
3011	80°16.555	9°22.906	600	25	ok
3012	80°19.498	9°17.355	630	25	ok
3013	80°22.306	9°12.045	670	25	ok
3014	80°25.123	9°07.031	790	25	ok
3015	80°28.040	9°01.290	930	25	ok
3016	80°30.895	8°56.040	910	25	ok
3017	80°33.717	8°50.369	1000	25	?
3018	80°36.558	8°44.664	600	25	ok
3019	80°39.464	8°39.173	860	25	ok
3020	80°42.387	8°33.606	790	25	ok

Profile 99400

Shotnumber	Long. (N)	Lat. (E)	Depth (m)	TNT (kg)	Status
4001	78°55.036	9°33.714	2250	50	ok
4002	78°54.425	9°13.457	2240	50	ok
4003	78°53.646	9°03.317	2180	50	ok
4004	78°52.936	8°48.033	2030	50	ok
4005	78°52.293	8°32.716	1900	50	ok

The values for the depth are taken from the Hydrosweep and rounded to 10m

3

Marine Geology

(H.C. Hass, D. Birgel, C. Didié, M. Forwick, N. Gussone, N. Kukina, N. Lensch, M. Pirrung)

The general goal of the working program of the marine geology group includes reconstructions of the sea-ice cover, paleoproductivity, and paleocurrents as well as paleoclimate reconstructions of the late Quaternary Arctic Ocean and the adjacent continental areas. Special emphasis is placed on the paleoceanographic development of the Yermak Plateau area during the Holocene (Fig. 11). Further emphasis is directed to the physical-property signature of glacial and interglacial sediments of the working area for stratigraphic correlations.

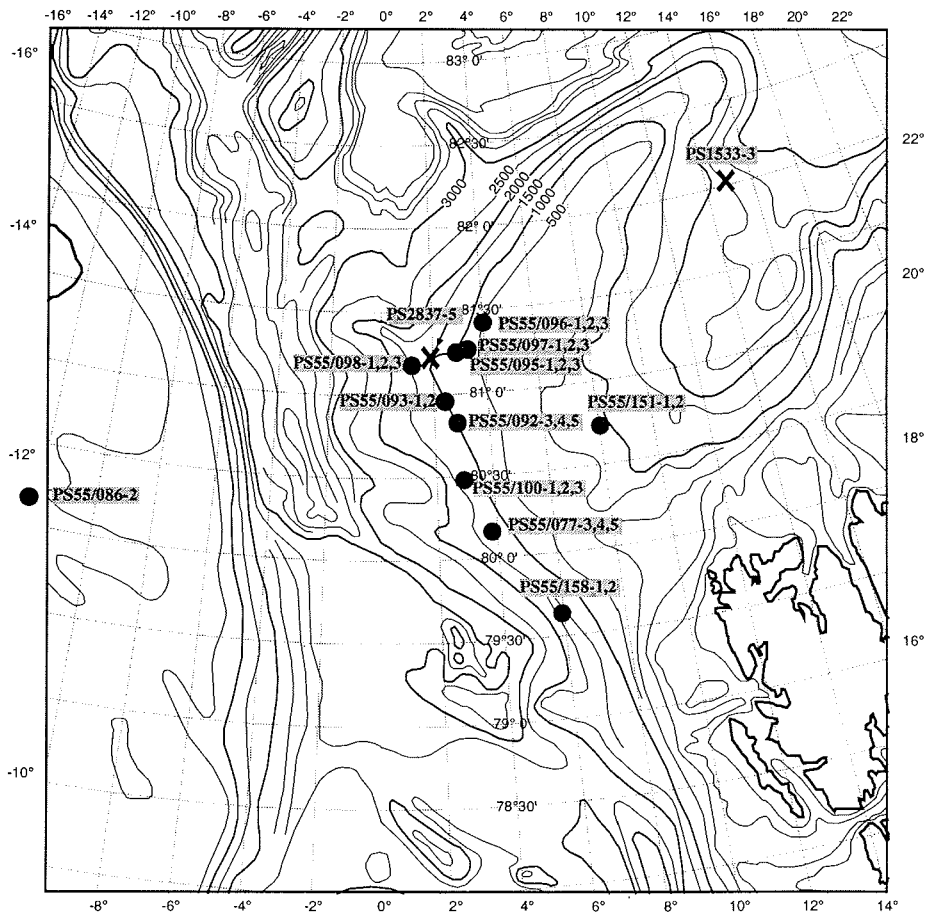


Fig. 11: Main working area with sediment core positions. Crosses mark previously taken sediment cores.

Due to heavy ice conditions the working program that was planned at Morris Jessup Rise was cancelled. Also, the planned coring sites on the Yermak Plateau north of 81°N could not be accessed because of heavy ice and were thus replaced by substitute positions.

The transition from the last glacial to the modern interglacial was a period of strong and rapid fluctuations of the climate system. Warm and cold climate phases such as the Bølling/Allerød warm phase and the Younger Dryas cold spell left significant traces on land and in the marine realm. Recently, a number of minor Holocene climate fluctuations most likely even cyclic in nature that were discovered in the North Atlantic area challenged the general view of a stable Holocene interglacial. Bond et al. (1997) and Bianchi and McCave (1999) related Holocene climate fluctuations to the intensity of thermohaline overturn in the Greenland Sea. To investigate whether or not Holocene climate fluctuations and associated changes in thermohaline overturn left significant traces in high-resolution sediments from the Yermak Plateau was one of the major scientific objectives.

Holocene sedimentation rates in the Arctic Ocean are generally too low for high-resolution investigations of short-term climate fluctuations. Also, minor climate changes may not have had a strong impact outside the mid latitudes. However, the ARK XIII/2 Expedition recovered a sediment core from the upper western slope of the Yermak Plateau at 81° 13' N (PS2837-5, 1042 m water depth) that yielded an exceptional long Holocene section. The core location is under the influence of temperate Atlantic water masses that control the position of the summer ice margin at the sea surface and that also control sediment transport at the seafloor. During ARK XV/2 it was attempted to discover the source and transport ways of the sediments that accumulated at the position of PS2837-5, and to recover a sediment core with even higher sedimentation rates.

The western slope of the Yermak Plateau is very steep and therefore most likely affected by turbidity currents. Thus, positions deeper than the upper shoulder of the slope were generally ruled out. The investigations concentrated at a water-depth interval of 900 to 1500 m. Intensive sediment echosounding (PARASOUND) surveys were carried out along and across the shoulder of the slope of the western - and partly also of the eastern - Yermak Plateau.

Further work aboard "POLARSTERN" included PARASOUND surveys across the Fram Strait, and on the Greenland and Svalbard shelves including the continental slopes. Three surveys in high lateral resolution were carried out (see chapter 5) in order to investigate the horizontal sediment distribution.

Finally, in order to evaluate Ra-226 as an oceanic tracer water samples from different parts of the water column were taken.

In particular the marine geologic research program comprises the following investigations:

- high resolution stratigraphy of the obtained sediment sections (isotope stratigraphy, AMS C-14 age determinations, magnetic susceptibility, physical properties, lithostratigraphy),
- terrigenous sediment supply and paleocurrent reconstructions (high resolution granulometry, bulk and clay mineralogy, heavy minerals, geochemical tracers),
- mapping of the sediment cover (PARASOUND),
- organic carbon flux, marine vs. terrigenous (organic geochemistry, kerogen petrography),
- paleoproductivity in the Arctic Ocean (biomarkers, barium, bio-opal),
- reaction of marine biota to environmental changes (foraminifers, diatoms, coccolithophores),
- correlation of marine sediment sequences with Greenland icecores as well as with previously taken sediment cores from the broad area and the Nordic Seas.

Subbottom profiler used:

- Atlas PARASOUND including an Atlas Deso 25 printer,
- PARADIGMA digitizing and post-processing software (Spiess, 1992).

Coring gear used:

- GKG (giant box corer): 60 cm long, 50 cm x 50 cm.
- MUC (multiple corer): 12 tubes, 60 cm long, 6 cm internal diameter.
- SL (gravity corer): 5 m/8 m/10 m/13 m long, 12 cm internal diameter.
- KAL (kasten corer): 5.75 m/11.5 m long, 30 cm x 30 cm.

Onboard investigations included:

- core descriptions (all box cores, all kasten cores, 1 gravity core),
- spectrophotometric color scans (all box cores, all kasten cores, 1 gravity core),
- smear slide analyses (all box cores, all kasten cores, 1 gravity core),
- x-ray analyses (all box cores, all kasten cores, 1 gravity core),
- physical property analyses: p-wave velocity, wet bulk density, magnetic susceptibility (all cores) (see chapter 3.7).

3.1 Subbottom profiling using PARASOUND

(H.C. Hass, D. Birgel, C. Didié, M. Forwick, N. Gussone, N. Kukina, M. Pirrung)

Introduction

The tasks of the PARASOUND surveys were to:

- provide information on the general acoustic characteristics of the sediments (sediment types). These include penetration depth (based on the sound velocity in water), and structure of the sediment (i.e. layering, thickness of distinguishable layers).

- provide information on the horizontal extension of different sediment types and distinct reflectors in the sediment column.
- provide information to aid selecting core locations.
- provide information on acoustic reflectors that shall be identified in sediment cores.

The goals include to:

- contribute to a mapping of sediment characteristics of the Yermak Plateau,
- classify sediment types,
- to discover areas with sediments of high temporal resolution,
- to reconstruct sediment-transport pathways to positions that are characterized by high sedimentation rates.

Technical features

The ship-mounted PARASOUND system (Krupp Atlas Electronics, Bremen, Germany) generates two primary sound waves at frequencies of 18 kHz and of 20-23.5 kHz. As a result of the parametric effect, a secondary frequency between 2.5 and 5.5 kHz is produced with a very narrow beam width of 4° which provides much higher resolution at depth compared to other sediment-echosounding devices.

The PARASOUND system is attached to an analogue printer (Atlas DESO 25). The analogue signal is digitized and postprocessed using the PC-based PARADIGMA software. Digital data are stored on tape and printed simultaneously on a color printer. Important data such as time, geographic position, and water depths are continuously plotted on a third printing device.

The PARASOUND system was operated for 24 h during most of the expedition. It was stopped during part of the profiling work of the geophysics working group when identical profile lines were sailed several times or when the reflection signal strength was almost zero at steep slopes.

Conditions during the survey

Ice conditions were very heavy north of 80°N within the Fram Strait. Ice ramming was necessary most of the time. Thus PARASOUND records show the typical features including a high noise level and an artificial hummocky relief due to the ship's back and forth movements. Aside from the ice, the slopes to the west and especially to the east of the Fram Strait were often too steep so that the narrow-beam system failed to record reasonable signals. Ice-free areas investigated during the expedition include the Norwegian Sea from Tromsø to about 80°N in the middle of the Fram Strait, a large area up to the north (82°N) and to the east until about 25°E to the north of Svalbard as well as the NE Water Polynya off the NW Greenland coast.

Examples of seismic facies, sediment types, relief, and sediment-core positions

Shelves and Yermak Plateau <1000 m of water depth

The shallow Greenland shelf was investigated between 79° and 81°45' N. Water depths ranged between 20 and 300 m. The relief was even to wavy, either showing a seafloor that was obviously affected by grounding ice (plough marks, Fig. 12) or a quite even seafloor without any depression or ridge. Larger channels up to 100 m deep at the shelf edge with no or only limited fill of acoustically transparent material occurred irregularly (Figs. 13, 14). Signal penetration ranged from 0 to about 10 m. An acoustically hard reflector characterized the entire area investigated by PARASOUND. At places a wavy hard reflector was overlain by a likewise hard and very uneven surface layer (Fig. 15). It is suggested that Till material forms the upper hard reflector. One gravity core (PS55/086-2) was taken at a position where the geophysical working group had seismic evidence for an outcropping salt dome. The actual position for coring was chosen according to PARASOUND data that suggested a very hard reflector with no sound penetration. Although the core penetrated about 5 m there was only ca 47 cm of clayey sediment in the core tube.

The upper shoulder <1000 m of water depth of the western Yermak Plateau was investigated between 80°40' and 81°30'N, and at 80°40'N/8°E. It generally shows a thick and acoustically well structured sediment cover that tends to become thinner and diffuse upslope and slightly thicker and acoustically better structured below ca. 1000 m water depth. There were few channels; all of them filled with material similar to the adjacent areas. There are many places where the influence of gravity flows becomes evident sometimes even at shallower water depths (Fig. 16).

The northern and western Svalbard shelves showed relief and acoustic characteristics similar to those of the Greenland shelf: basically one acoustically hard layer and no or very limited signal penetration. Channels are common; most of them show no fill other than the acoustically hard material of the surrounding areas. There are also small and larger ridges that can be interpreted as till or moraine material. The Svalbard shelf area around 20°E displays mostly diffuse reflectors and a very uneven relief. Series of steep more than 80 m high ridges may be interpreted as moraine ridges.

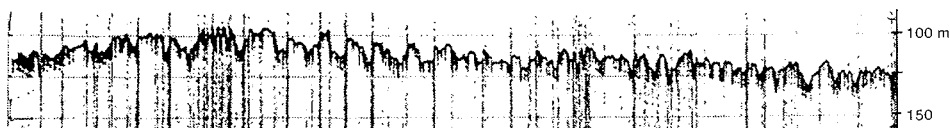


Fig. 12: Ploughmarks on the Greenland shelf at 79°56'N, 10°27'W.

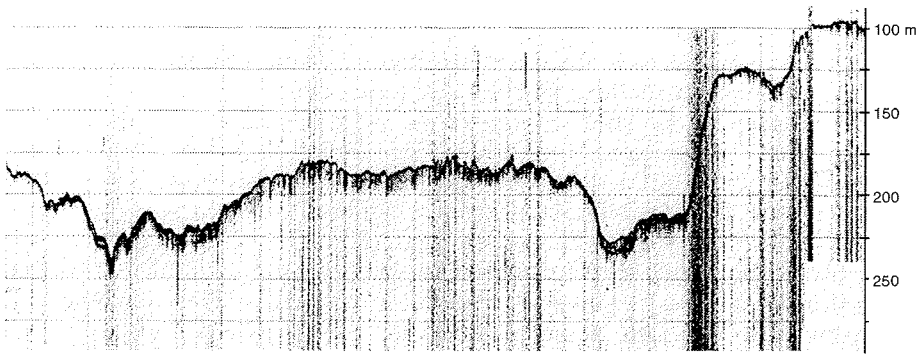


Fig. 13: System of channels on the Greenland shelf at 79°47'N, 13°49'W (right channel).

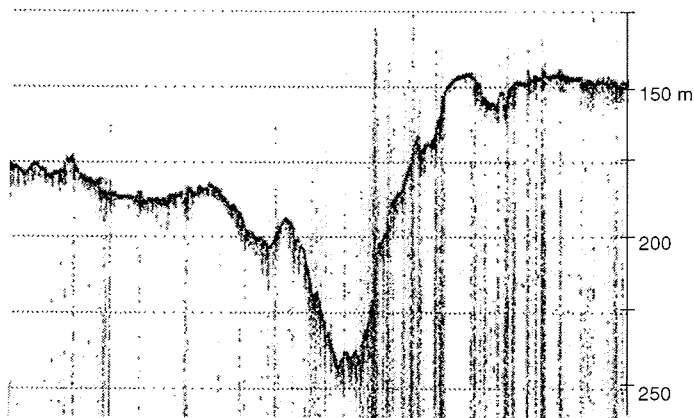


Fig. 14: Channel on the Greenland shelf at 79°8'N, 12°57'W.

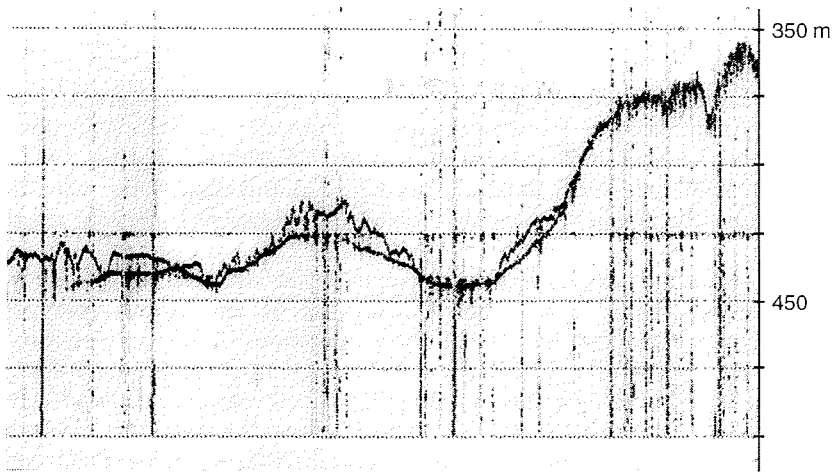


Fig. 15: Paleosurface covered with gravel on the Greenland shelf at 79°58'N, 6°58'W.

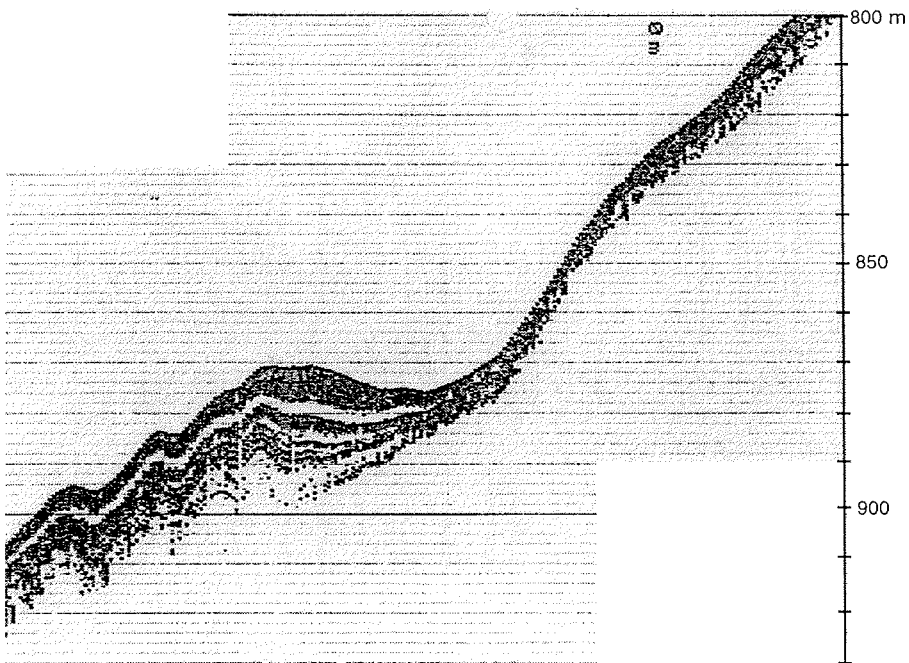


Fig. 16: Slumping on the shallow western shoulder of the Yermak Plateau at 80°19'N, 04°05'E.

Slopes

PARASOUND profiles were acquired across and along the western and northern Svalbard continental slope, the western and eastern slopes of the Yermak Plateau, and the eastern Greenland continental slope. However, during most of the profiling across the western Svalbard and Greenland slopes no recording was possible because the signal was lost as a result of extreme steepness of the slopes.

There is no sediment type, structure or acoustic feature that would fit to all the areas mentioned at the same depth intervals of the slopes. Nevertheless, characteristic structures can be found. The slope shoulder of the western Yermak Plateau between 80°N and 80°15'N is covered by thick sediments that show a number of distinct acoustic reflectors (Fig. 17). These can be followed downslope until 3500 m water depth (locally different) where the seafloor changes into a vague hyperbolic structure that may be caused by slumps (see next chapter). Some times depressions show higher sound penetration. It can be assumed that this is the result of slumps and/or gravity currents that tend to fill morphologic depressions. Layers pinching out to the slope of small depressions and acoustically transparent sediment bodies support this assumption (Fig. 18).

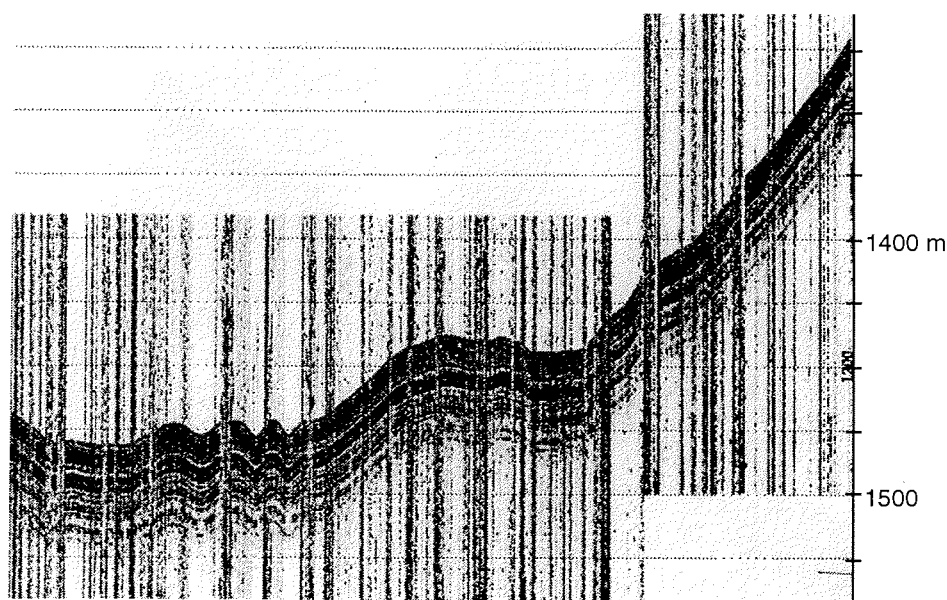


Fig. 17: High sedimentation rates on the western flank of the Yermak Plateau at 80°28'N, 2°56'W.

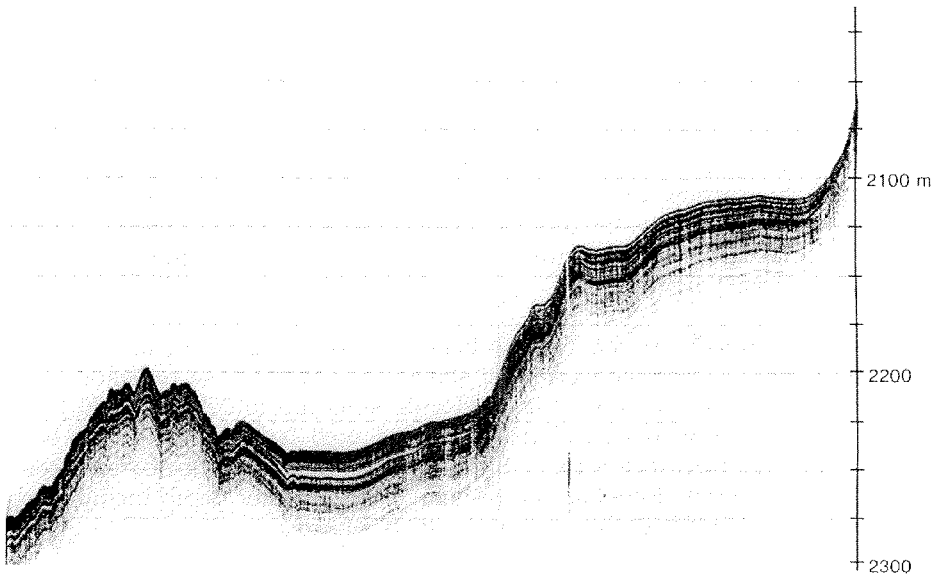


Fig. 18: Influence of gravity flows within depressions (acoustically transparent sediment body) in the southeastern Fram Strait at 76°54'N, 9°57'E.

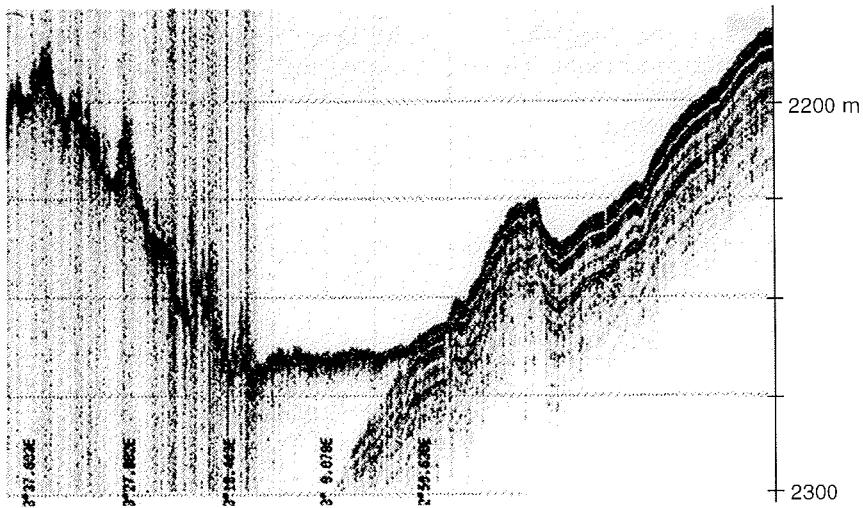


Fig. 19: Acoustically well structured sediments dip under unstructured sediments on the deep southeastern slope of the Yermak Plateau at 81°11'N, 12°50'E.

To look for undisturbed sediment cores the upper part of the slope shoulder (around 1000 m) seems to be most promising. The highest resolution core that has ever been taken from the Yermak Plateau (PS2837-5; Stein and Fahl, 1997) was recorded from the western Yermak Plateau at a water depth of 1044 m. Thus, 26 sediment cores were taken from 9 stations along the upper western slope shoulder of the Yermak Plateau during this expedition. Seven cores from three positions were taken at water depths above 1000 m to investigate the shallower part of the slope shoulder to confirm that here Holocene resolution is worse than below 1000 m water depth.

The lower eastern slope of the Yermak Plateau between 12°E and 13°E appears to be different. Here, a very uneven relief shows only one diffuse reflector. Around 2300 m of water depth thick well-layered sediments dip under this hard reflector (Fig. 19). Upslope towards Svalbard thick and well layered sediments become thinner until they turn into a very thin and hard surficial reflector between 700 and 500 m water depth. Relief structures above 700 m water depth include iceberg plough marks and unfilled channels of a variety of sizes.

Because of heavy ice conditions and steep slope, the PARASOUND data from the Greenland slope from two profile lines are too sparse and too noisy for further interpretations.

Deep-sea areas >2500 m of water depth

Most of the deep sea areas were characterized by influences of turbidites that leave discrete layers and of slump and debris flows that produce diffuse large sediment bodies with a chaotic internal structure (Fig. 20). Sometimes the initial layering was still visible on the deep slope although large parabolic structures indicate large scale sliding sediments. These structures were found in the area of the Molloy Deep and north of Svalbard (Figs. 21, 22). However, in places discrete layering continued down to >3000 m.

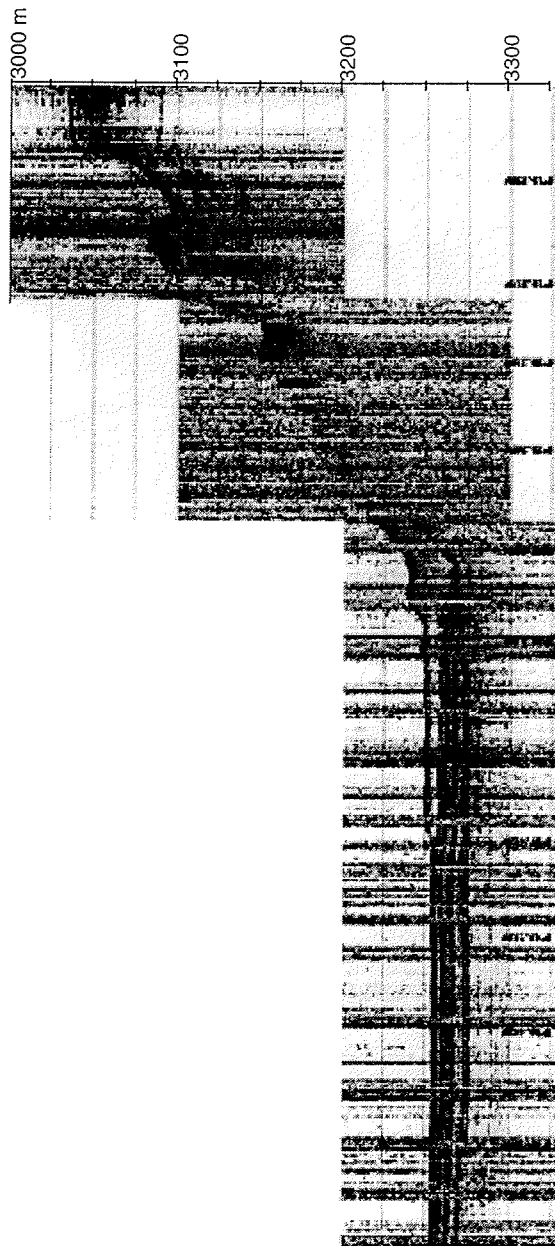


Fig. 20: Debris flow in the central Fram Strait at 80°56'N, 0°30'E.

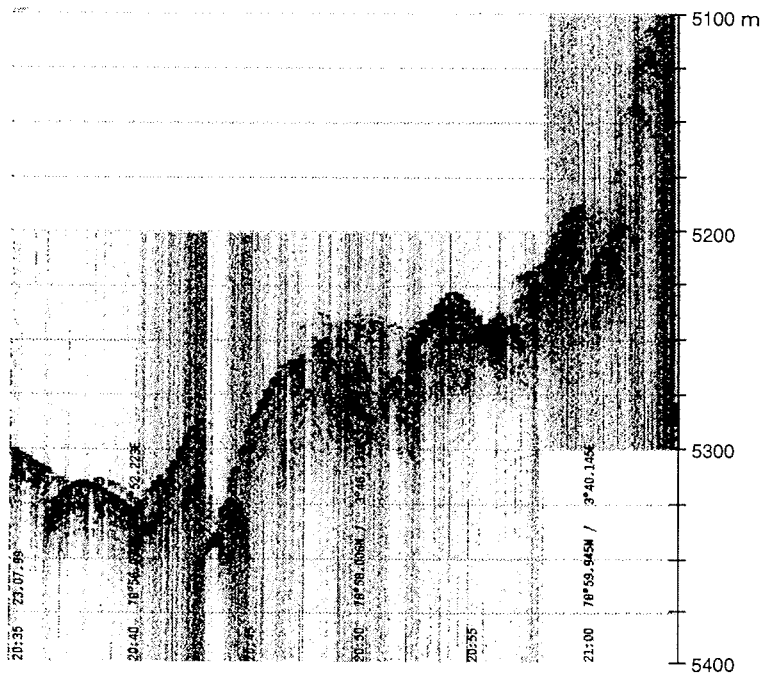


Fig. 21: Chaotic sediment structure in the Molloy Deep at 78°58'N, 3°46'E.

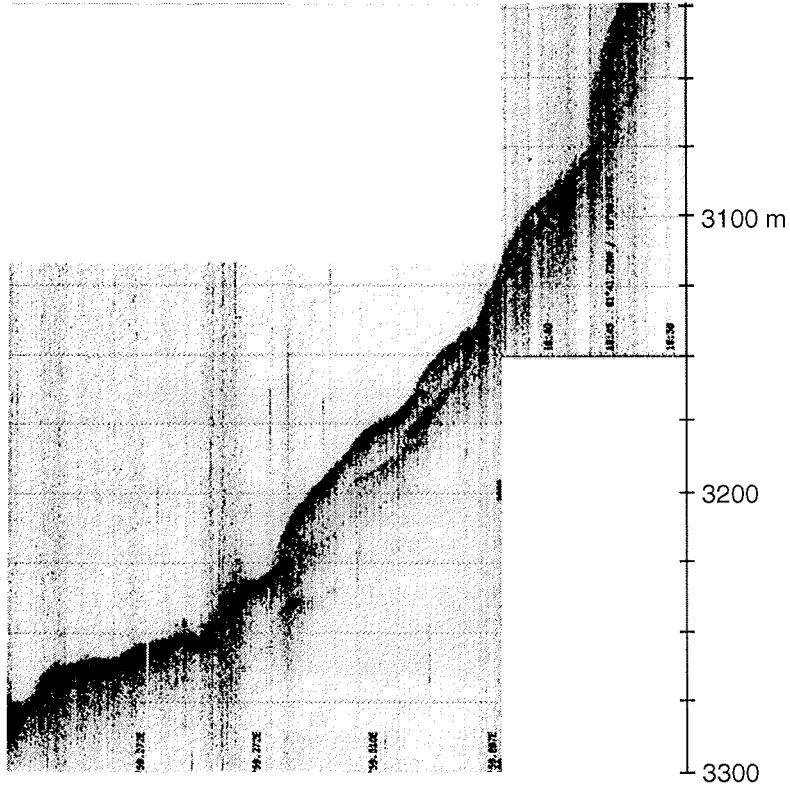


Fig. 22: Slope affected by gravity processes northeast of Spitsbergen at $81^{\circ}43'N$, $19^{\circ}59'E$.

3.2 Geological sampling

(H.C. Hass, D. Birgel, C. Didié, M. Forwick, N. Gussone, N. Kukina, N. Lensch, M. Pirrung)

A total of ca. 65 m of sediment was recovered (Figs. 11, 23; Tab. 8). Most of the stations were on the upper western shoulder of the Yermak Plateau. Gravity cores as well as giant box cores were taken at every station. The heaviest gear of the geology working group, the kasten corer, was only deployed at very promising localities.

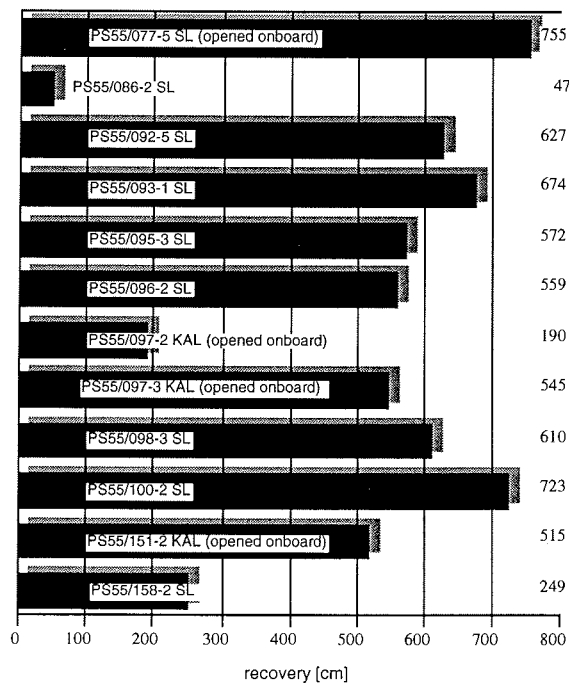


Fig. 23: Lengths of kastencores (KAL) and gravity cores (SL).

Tab. 8: List of geological stations.

Station number	Gear	Latitude deg.	Longitude deg.	Water depth (m)	Recovery (m)
PS 55/077-3	MUC	80°09.00'N	3°49.00'E	1475	0.32
PS 55/077-4	GKG	80°09.40'N	3°51.81'E	1512	0.48
PS 55/077-5	SL (13m)	80°09.12'N	3°55.44'E	1488	7.55
PS 55/086-1	MUC	80°12.56'N	12°18.83'W	187	0.25-0.30
PS 55/086-2	SL	80°12.77'N	12°19.37'W	184	0.47
PS 55/092-3	MUC	80°49.69'N	2°51.07'E	1021	0.30
PS 55/092-4	GKG	80°49.62'N	2°49.98'E	1037	0.50
PS 55/092-5	SL (13m)	80°49.53'N	2°49.37'E	1045	6.27
PS 55/093-1	SL (13m)	80°57.14'N	2°27.65'E	1083	6.74
PS 55/093-2	GKG	80°56.91'N	2°26.85'E	1089	0.48
PS 55/095-1	MUC	81°16.00'N	3°22.00'E	750	0.30
PS 55/095-2	GKG	81°16.75'N	3°22.98'E	769	0.50
PS 55/095-3	SL (10m)	81°16.43'N	3°23.67'E	768	5.72
PS 55/096-1	MUC	81°26.44'N	4°03.41'E	765	0.30
PS 55/096-2	SL (10m)	81°26.35'N	4°02.93'E	765	5.59
PS 55/096-3	GKG	81°26.25'N	4°02.25'E	769	0.49
PS 55/097-1	GKG	81°16.21'N	3°18.42'E	775	0.50
PS 55/097-2	KAL (12m)	81°15.79'N	3°13.37'E	799	1.97
PS 55/097-3	KAL (6m)	81°15.55'N	3°00.37'E	860	5.49
PS 55/098-1	MUC	81°10.00'N	1°17.00'E	1680	0.30
PS 55/098-2	GKG	81°10.74'N	1°12.29'E	1823	0.33
PS 55/098-3	SL (10m)	81°10.94'N	1°09.34'E	1880	6.10
PS 55/100-2	SL (10m)	80°29.23'N	2°56.73'E	1538	7.23
PS 55/100-3	GKG	80°28.87'N	2°56.01'E	1541	0.515
PS 55/151-1	GKG	80°43.43'N	8°02.71'E	962	0.49
PS 55/151-2	KAL (6m)	80°43.47'N	8°01.32'E	971	5.15
PS 55/158-1	GKG	79°38.05'N	6°00.06'E	1544	0.50
PS 55/158-2	SL (10m)	79°37.38'N	5°58.07'E	1596	2.49

The initial planning was to arrive from west at the western Yermak Plateau margin at ca. 1000 m water depth thereby investigating with PARASOUND the slope from very deep to shallower water depths at a latitude of 80°45'N in order to get information on the sediment conditions on the slope. Then a transect close to the 1000 m isobath up to approximately 81°45'N should have followed including some zig-zag PARASOUND profile between 900 and 1500 m water depths in order to survey the area where Core PS2837-5, a core with an exceptional high resolution, was taken during the ARK XIII/2 expedition (Stein and Fahl, 1997, Fig. 11). During the way north coring stations were already pre-planned. The cores should have been preliminarily processed on the multisensor core-logging device in order to select the best location for a kasten core. Unfortunately, ice conditions were so extreme that the pre-planned locations were unable to reach. The first two cores (PS55/092 and PS 55/093) were more or less on the transect but the following core (PS55/095) was already taken at an

alternate location since deeper water depths could have only been reached after time-consuming ice ramming. At the location of the following core (PS55/096, again an alternate) the transect had to be terminated after "POLARSTERN" stuck in heavy multiyear ice. Thus, locations north of 81°30'N were not reached. Meanwhile first results from the core logger were available suggesting highest sediment accumulation at the location of PS55/095 (which turned out to be a misinterpretation, though). Thus, it was decided to take a kasten core at this position on our way back south. However, the exact position could not be reached anymore and the first deployment of the kasten corer failed because of heavy ice. After some time during which the ship drifted a second kasten core (PS55/097-3) was successfully recovered. The next core (PS55/098) was taken intentionally at a water depth of 1823 m. Later, during the cruise the geological transect along the shoulder of the Yermak Plateau was completed with two more stations (PS55/100; PS55/158) adding to PS55/077 that was taken at the beginning of the expedition. Another kasten core (PS55/151) was taken at the eastern slope shoulder at 971 m water depth. This position was selected because PARASOUND suggested high sedimentation rates.

Surface sediment sampling using a multiple corer (MUC)

In order to achieve undisturbed surficial sediments a multiple corer (MUC) was deployed at most (6) of the geological stations. The MUC was equipped with a video device in order to get information on the seafloor properties before touching the ground. It was run by the biology group (I. Schewe). Recovery was always between 20 and 35 cm. The surficial sediments contained silty or sandy-silty clay at all stations.

Six tubes were available for the geology working group. The following sampling scheme was applied: One of the tubes was deep frozen at -30°C, then extruded into a plastic bag and stored deep frozen again. This core is for geochemical analyses. One of the tubes was extruded using a custom-built extruder. While it was slowly extruded it was simultaneously cut into 1 cm-slices. These were packed into small plastic bags and stored deep frozen. These samples are also for geochemical analyses. Three tubes were extruded, cut into 1 cm-slices and stored at 4 °C. Two sets of samples are for sedimentologic analyses, one is for mineralogic analyses. It was unsuccessfully attempted to measure one of the tubes on the corelogger.

Surface sediment sampling using a giant box corer (GKG)

Relatively undisturbed samples of the upper 50 cm were obtained by means of a giant box corer (GKG). The GKG was deployed at 10 geological stations. Recovery was always at 50 cm which is the maximum core length. The following working and sampling scheme was applied:

Core description

Surface: one frame of 10 cm² + Bengalrose (foraminifer analysis);
one frame of 10 cm² stored deep frozen (geochemistry);
30 - 50 cm³ stored deep frozen in a glassbottle (geochemistry);
2 x 30 - 50 cm³ (sedimentology), one syringe sample (physical properties).

Core: Two tubes (12 cm in diameter; AWI), one 50 cm liner (GEOMAR), one set of syringes at variable intervals (physical properties), one set of 25 cm liners (x-ray analyses), one set of smear-slide samples in 5 cm intervals.

Sediment sampling using a gravity corer (SL)

The gravity corer (SL) was deployed at nine geological stations. A total of 48.16 m of sediments were recovered. In order to compare core-logger results with the sediment Core PS55/077-2 was opened onboard. None of the other cores could be opened due to lacking laboratory capacity. These cores were cut in meter pieces and stored at 4 °C. One set of smear slides was taken at the base and top, respectively, of each meter. Every meter-piece tube of Core PS55/077-2 was cut vertically in work and archive halves, respectively. After the core description smear slide samples were taken every 10 cm and one continuous set of x-radiographs samples were taken.

Sediment sampling using a kasten corer (KAL)

The kasten corer (KAL) was deployed at three stations. The total recovery was at 12.63 m. After core description a total of four 1 m liners per core-meter and a continuous set of x-radiograph samples were taken. Further samples for smear slides (every 10 cm) and a set of samples for density measurements and one set for REM analyses were taken. All liners were stored at 4 °C.

3.3 Sediment characteristics

(H.C. Hass, D. Birgel, C. Didié, M. Forwick, N. Gussone, N. Kukina, M. Pirrung)

Surface sediments showed little variation. The ultimate surfaces of the GKGs appeared to be undisturbed. Obviously no material was quantitatively washed out. On the surface living and dead fauna was still in live positions indicating undisturbed material. Several types of lebensspuren were found as well. Living brittle stars and polychaet tubes were abundant on all surfaces. Benthic foraminifers and arthropod holes were commonly found whereas bivalves, gastropodes and shrimps were rare. The common grain size was silty clay. GKG PS55/158-1 and GKG PS55/151-1 form exceptions with increased sand components and aside from scattered black IRD the surface was inhabited by gastropodes, bivalves and deep-sea shrimps. A further exception forms GKG PS55/100-3 that showed huge amounts of agglutinated foraminifers (1 - 3 cm in length) in the topmost two centimeters. Generally, there was an oxidized surface layer about 1 to 3 cm in thickness. In GKG PS55/151-1 this surficial layer was about 38 cm thick thus promising very high resolution (which could not be confirmed by further investigations, though). East of the Fram Strait IRD was mostly composed of deeply weathered shale.

The long cores that were opened and described (PS55/97-2, 3; PS55/151-2; PS55/077-5) were very similar revealing grey silty clay with some scattered coarser layers and few color changes (see Fig. 24). Thus, on a macroscopic basis

paleoenvironment interpretations were difficult. However, there is one macroscopic marker layer that was found in every core. It is a yellowish layer with clay aggregates ("cottage cheese structure") followed by a coarser fining-upward layer. Earlier investigations (Spielhagen, unpublished; Stein and Fahl, 1997) revealed that this layer marks the last glacial maximum in the area of the Yermak Plateau. Thus, this marker layer can be used for stratigraphic correlation along with the results from the multisensor core logging device (Fig. 25, see also chapter 3.7).

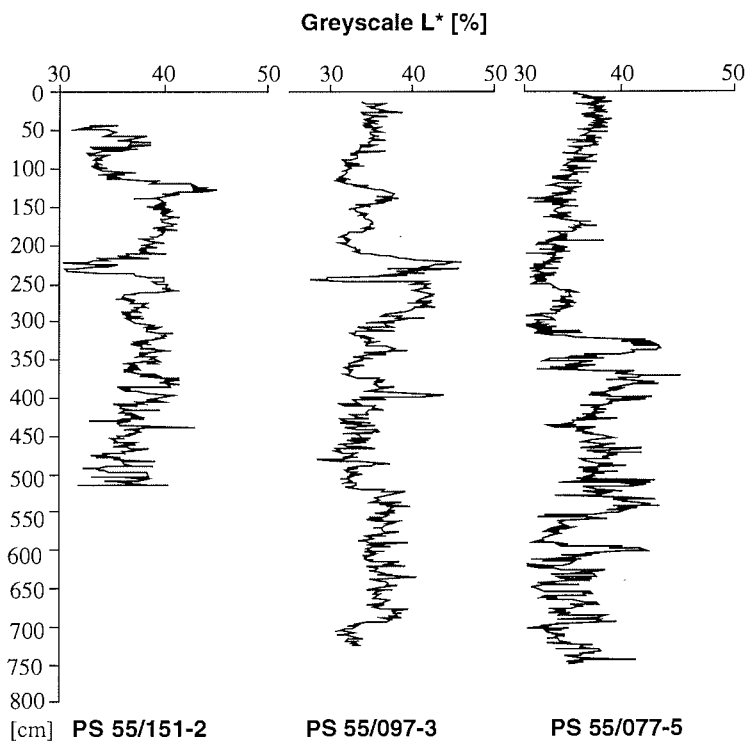


Fig. 24: Greyscale records of two kastencores (PS55/097-3, PS55/151-2) and one gravity core (PS55/077-5) that were opened onboard.

3.4 Smear-slide analyses (N. Koukina)

Smear-slide analyses were carried out on sediments from eight long cores (s. App. 3 tabs. 9 - 16, figs. 25 - 26). A total of 135 slides were investigated under the light microscope. Smear-slide investigations were performed to estimate the mineralogic compositions and to determine the contents of biogenic and terrigenous components. Based on these analyses terrigenous particles dominate the sediments recovered during ARK XV/2. The principal minerals include quartz, feldspar, terrigenous carbonate and clay minerals. Quartz contents ranged from 15% (PS55/092-5) to 53% (PS55/097-3). Quartz/feldspar ratios ranged from 0.95 (PS55/077-5) to >3 (PS55/093-5, PS55/095-3, PS55/092-5). Feldspar contents were up to 30%. Terrigenous carbonates (i.e. calcite, dolomite) occurred between 0.1% (PS55/092-5) and 10.9% (PS55/077-5). Opaque minerals tend to increase down the core. The highest amounts of opaques (5.3%) were observed in Core PS55/097-3 between 270 and 430 cm core depth. Biogenic carbonate was between 0.1 and 6.3% with a maximum at 0 - 140 cm in Core PS55/077-5. Heavy minerals determined in the various cores include amphiboles, pyroxenes, epidote, biotite, garnets, chlorite, titanite, Fe-Mn-nodules, hydroxides, and iron and black ores. Amphiboles and pyroxenes dominate the spectrum although in intervals of some cores Fe-hydroxides (i.e. limonite and hydrogetite) dominate the association. Further investigations at the home laboratory will intensify the mineralogic studies.

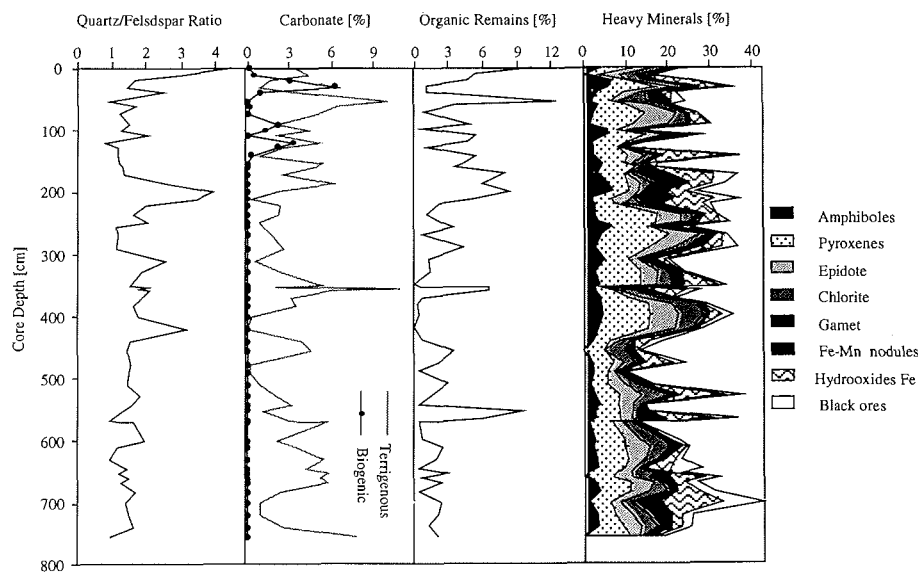


Fig. 26: Selected results from smear-slide analyses (Core PS55/077-5 SL).

3.5 Watersampling for Ra-226 analysis (N. Gussone)

At station PS 55/074 (79°21'12"N, 2°16'02"E) water samples for the determination of Ra-226 were taken. Because of the fact, that the residence time of Ra-226 (half live 1600 a) is in the same order of magnitude as the circulation time of the ocean water, it can be used as an oceanic tracer. The samples were taken with a CTD-rosette in 12 l niskin-bottles at different water depth (2450 m, 2350 m, 2200 m, 2050 m, 1800 m, 1600 m, 1300 m, 1100 m, 900 m, 750 m, 500 m, 100 m). The water was filled in precleaned 20 l PE-container and treated with supra pure nitric acid. A Ra-228 spike was added to the samples for later analyses of Ra-226 by isotopic dilution mass spectrometry.

3.6 Summary (H.C. Hass)

Although the time available for the geological program was quite short and ice conditions were severe even the preliminary results are of great wealth for the marine geology group. Some of the target areas could not be reached due to ice conditions (i.e. Morris Jessup Rise and some of the pre-planned stations at the Yermak Plateau), however, the sediment cores recovered and the PARASOUND profiles taken are likely to be able to answer some of the questions that were open at the beginning of the expedition. Regarding the preliminary stratigraphic correlations from the core logging data and the macro- and microscopic sediment investigations it turns out that high sedimentation rates at the shoulder of the western Yermak Plateau are neither a function of water depth (below 1000 m, that is) nor a function of latitude. Since the significantly increased Holocene sedimentation rates of Core PS2837-5 are not caused by slumps or other mechanisms of gravity induced processes (Hass et al., in press) further investigations of geological data will also focus on oceanographic and high-resolution bathymetric data.

Aside from the results of the sediment cores ARK XV/2 revealed valuable data from PARASOUND subbottom profiles. Many different sediment transport and deposition processes were interpreted and will thoroughly be processed at the home laboratory. Relief structures as well as different layering structures were discovered throughout the expedition. These significantly aid the interpretation of the sediment cores. P-wave velocity data measured in the sediment cores will be compared with processed PARASOUND data in order to shed light on the acoustic sediment properties.

3.7 Physical Properties of the Sediments (M. Pirrung)

Introduction

During the cruise ARK XV/2 the physical properties of 64 m of sediment cores were logged with a MultiSensorCoreLogger. Density, P-wave velocity and magnetic susceptibility of the cores can be correlated with other cores from the area and tentative age models are presented.

General

Logging of physical properties like density, P-wave velocity and magnetic susceptibility allows a first interpretation of sediment properties of unopened cores. Changes in these parameters reflect changes in sediment composition, so an indication for the lithology of the cores can be given (Thomson & Oldfield 1986, Weber et al. 1997). For example, a layer rich in ice rafted debris (IRD) will show higher density, lower P-wave amplitude, higher P-wave velocity and - depending from the magnetisation of the debris - higher or lower magnetic susceptibility than the surrounding pelitic sediment. As physical properties have been measured on many cores of the Greenland-Iceland-Norwegian Sea (Frederichs 1995, Niessen et al. 1997, Nowaczyk 1991), a correlation with other cores is possible.

Material

The sites of the sediment cores are on the western margin and the central part of the Yermak Plateau in the Greenland Sea, for location see fig. 11. Tab. 17 lists the logged sediment cores of Giant Box Corer (GKG, liner 12 cm inner Ø or liner 9.3 * 7.7 cm), Gravity Corer (SL, liner 12 cm Ø) and Kastenlot (KAL, liner 9.3 * 7.7 cm).

Methods

The Geotek MultiSensorCoreLogger (MSCL14) allows the logging of core thickness, P-wave travel time, attenuated gamma counts, magnetic susceptibility and temperature. For determining gamma densities, gamma rays of a ¹³⁷Cs-source are used. Magnetic susceptibility is measured with a BARTINGTON MS2C coil sensor. Calibration of the sensor was weekly controlled with a BARTINGTON calibration core (3896 * 10⁻⁶ SI, ser. no. 208). Technical details of the Multi Sensor Core Logger are given in Tab. 18. As the processing with the new GEOTEK MSCL 4.2 software was not possible, the version 3.0 was reinstalled. Because of software problems, data of the box cores, of SL PS55/086-2, PS55/158-2 and of the KAL PS55/097-2 and PS55/151-2 could not be processed and are not shown in this report. After data processing, P-wave amplitude, P-wave velocity (calculated for 20°C), gamma density, magnetic susceptibility, acoustic impedance and fractional porosity can be analysed. For further processing of the density values, a KALEIDAGRAPH makro from Frank Niessen (AWI Bremerhaven) was used. Calibration was done with aluminium, graphit, nylon and water pieces of varying thickness, for details see Weber et al. (1997).

Unprocessed susceptibility data were manually corrected for sensor drift, end effect at the top and the base of the cores and the sensor coil to core diameter ratio in EXCEL to get the volume susceptibility k (dimensionless, all values presented here are in 10^{-6} in the SI-System). For drift control of the MS2C sensor, the cores were taken out of the sensors and an empty liner was measured in the MS2C sensor every 15 - 20 cm, when the liner had passed the P-wave transducers. Due to the sensor offsets, this was possible only in the lower 60 cm of one meter liners. The preliminary point sensor correction coefficient was determined for 4 cores which were measured with loop and point sensor by calculating the ratio of volume susceptibility measured with the MS2C and the MS2F susceptibility, see tab. 18.

For a first overview, the cores taken with the gravity corer were logged with 5 cm interval. Between July, 29th and August, 12th, the drift of air measurements with the MS2C susceptibility sensor rose from 5 - 10 $\cdot 10^{-6}$ SI per hour up to 5800 $\cdot 10^{-6}$ SI per hour, far beyond any variation in the cores. Similar problems with the susceptibility measurements were already reported from ARK XIII/2 by Niessen et al. (1997). The reason for this problem was found in the adhesive between the two plastic covers of the MS2C sensor, which was partially corroded and gave no protection against water seeping from the cores into the coil. After drying the sensor in a drying box and taping all adhesive parts, the drift was relatively normal again, two air measurements in 10 sec interval varied between 0 and 5 $\cdot 10^{-6}$ SI. In addition, rare erroneous peak values of several thousand $\cdot 10^{-6}$ SI were observed which didn't occur on the MS2 display and were probably produced by erroneous data transfer to the processing panel.

For detailed logging, the cores were stored in the laboratory until the temperature difference between the air of the room and of the core was smaller than 2°C. All cores were logged with 1 cm interval. Before and after each core, an empty liner was logged for determination of the intensity i_0 of the gamma source. After each gravity core, an additional liner filled partially with aqua demin. and partially with aluminium for control of P-wave velocity and density data was logged.

In addition to the logger measurements, the magnetic susceptibility was measured with a BARTINGTON spot sensor F on the opened SL liner (measured with MSCL) and on liners pressed into GKG (measured manually) and KAL (MSCL). Sediments were covered with a PE-foil. Every 10 cm the sensor was lifted for air measurement to correct the drift. Discrete samples were taken from GKG and KAL with a syringe and filled into a 12.5 ml NUNC plastic box (13.6 ml volume), avoiding air bubbles as far as possible. On these samples, the magnetic volume susceptibility k at 460 and 4600 Hz and the frequency dependent susceptibility k_{fd} will later be determined with a BARTINGTON bulk sensor B. The low field susceptibility will be used for a better determination of the point sensor correction coefficient as the comparison of loop and point sensor measurements is not so exact. Wet bulk density, water content and dry density will be measured and specific susceptibility c will be determined in the laboratory.

Results

The sediment cores of the western flank of the Yermak Plateau can be correlated by means of magnetic volume susceptibility (fig. 27), gamma density (fig. 28), p-wave velocity (fig. 29) and acoustic impedance, the product of density and P-wave velocity (fig. 30). By comparison of the magnetic susceptibility data with that of PS1533-3 of the northeastern flank of Yermak Plateau and with PS2837-5 from the western flank of Yermak Plateau (for their location see fig. 11 (chap. 3.0), a preliminary stratigraphy can be given, see fig. 31. An age model for PS1533-3 based on paleomagnetic, AMS C-14, oxygen isotope and Be-10 data was reported by Nowaczyk et al. (1994). For PS2837-5 Niessen et al. (1997) suggested a preliminary stratigraphy based on density data, and an unpublished age model based on oxygen isotope data of the planctic foraminifer *N. pachyderma* was established by Robert Spielhagen (GEOMAR Kiel, pers. comm.). In the figs. 27 - 30 units I to VI are shown, which are assumed to correlate with the Marine Isotope Stages (MIS) I to VI. Horizons with higher p-wave velocity and higher density are interpreted as layers rich in IRD.

In unit I P-wave velocity, density and susceptibility are low and almost constant. In core PS55/100-2 the thickness of unit I is highest with about 260 cm. The impedance of this unit in PS55/100-2 is low and homogenous. A rise in impedance at 2.2 m correlates with the base of a transparent layer in the Parasound data. In GKG cores, the susceptibility of the uppermost 50 cm is almost homogenous.

In unit II P-wave velocity and density are higher and are more variable than in unit I. In PS55/100-2 a maximum in the impedance curve at 3.3 - 3.6 m can also be seen as reflector in the Parasound profile. There is a characteristic feature on the susceptibility curves: a maximum surrounded on top and base by a minimum. The lower minimum correlates in PS55/097-3 (184 - 188 cm) with an olive black sandy silty clay layer described by Schubert et al. (1997) in other cores from the Yermak Plateau and which has an age of 21 - 23 kyr.

In unit III and V the susceptibility is in general higher than in unit II, P-wave velocity is mostly lower than in unit II. A sharp peak in the impedance of PS55/100-2 at 5.0 m depth can be correlated with the top of a reflector rich zone in the Parasound data that reaches until about 9 m depth. The high density and P-wave velocity peak at 5.0 m is probably caused by ice rafted debris.

Unit IV is generally low in susceptibility and has similar variations in density and P-wave velocity as unit III and V. Unit VI has low susceptibility in its uppermost part. The lower part is high in susceptibility, density and P-wave velocity, the top of this lower part was taken as top of MIS VI by Niessen et al. (1997). Susceptibility correlates well with PS1533-3, so the limit MISV/VI is drawn at the transition from high to low values in fig. 27.

Laterally, corresponding parts of the units I - VI show only small variations which points to similar lithology in the cores. Only the southernmost core

PS55/077-5 differs by a larger number of peaks in the density and P-wave velocity curves which indicates a higher amount of ice rafted debris in this core.

The thickness of the unit II is about 2 to 3 times that of unit IV, being highest in the three southernmost cores. The thickness of unit III and V is variable in the three northernmost cores and about equal in the other cores. The sedimentation rate seems to increase from MIS V to I. This increase in sedimentation rate is also evident in cores from the northeastern Yermak Plateau (for ex. PS1533-3) and in cores on the slope off Eastern Greenland (Nam 1997). The reason for the increase in sedimentation rate in the Norwegian Greenland Sea is probably the rapid change of colder arid and warmer humid phases during the last glacial/interglacial cycle providing high input of terrigenous material.

The physical properties of the cores taken during ARKXV/2 will be available in the PANGAEA database on web page <http://www.pangaea.de>.

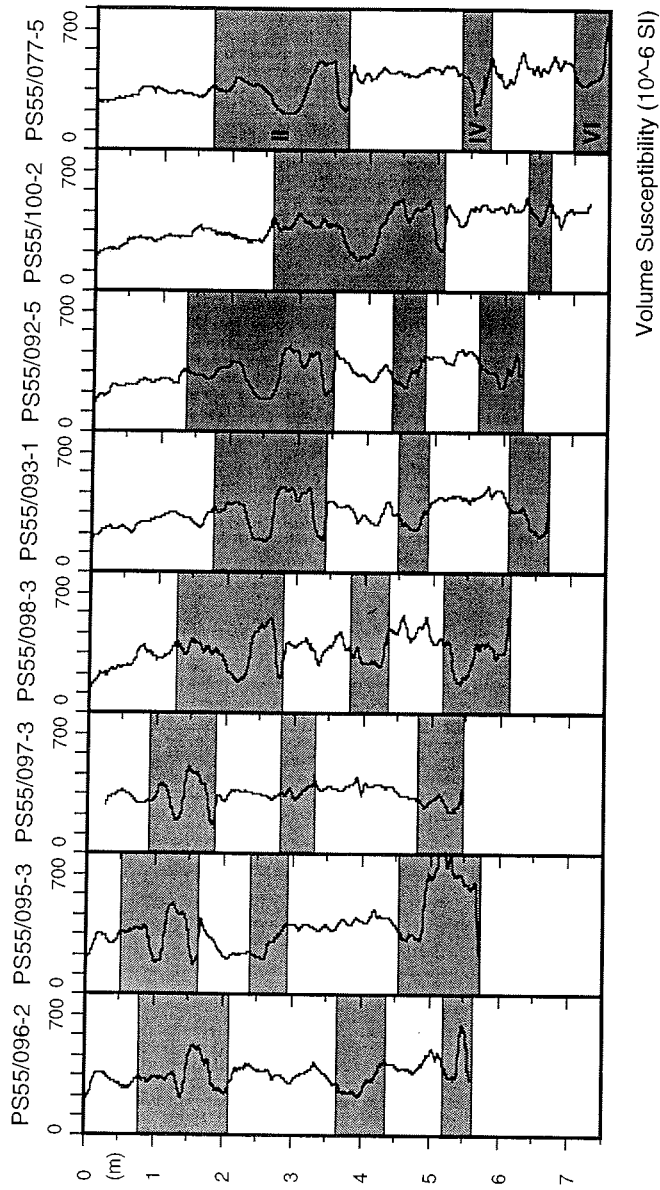


Fig. 27: Volume susceptibility of cores on the western margin of the Yermak Plateau from ARK-XV/2. Cores are sorted from north (left) to south (right). Units II, IV and VI roughly correlate with colder marine isotope stages II, IV and VI.

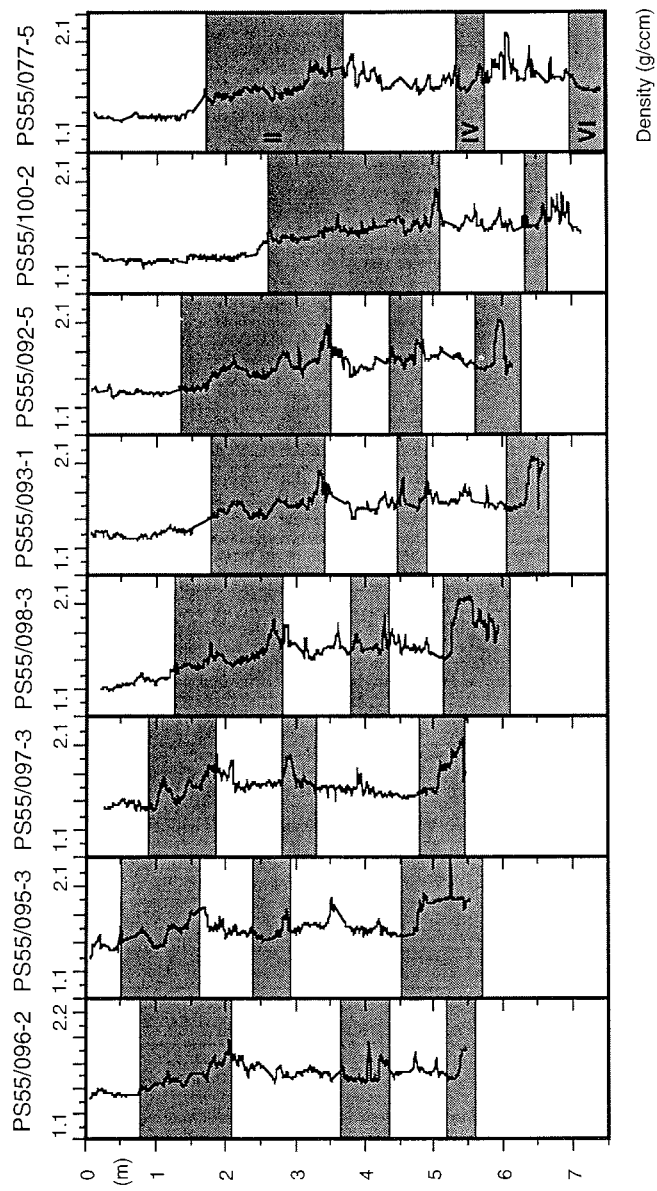


Fig. 28: Density of cores from ARK-XV/2.

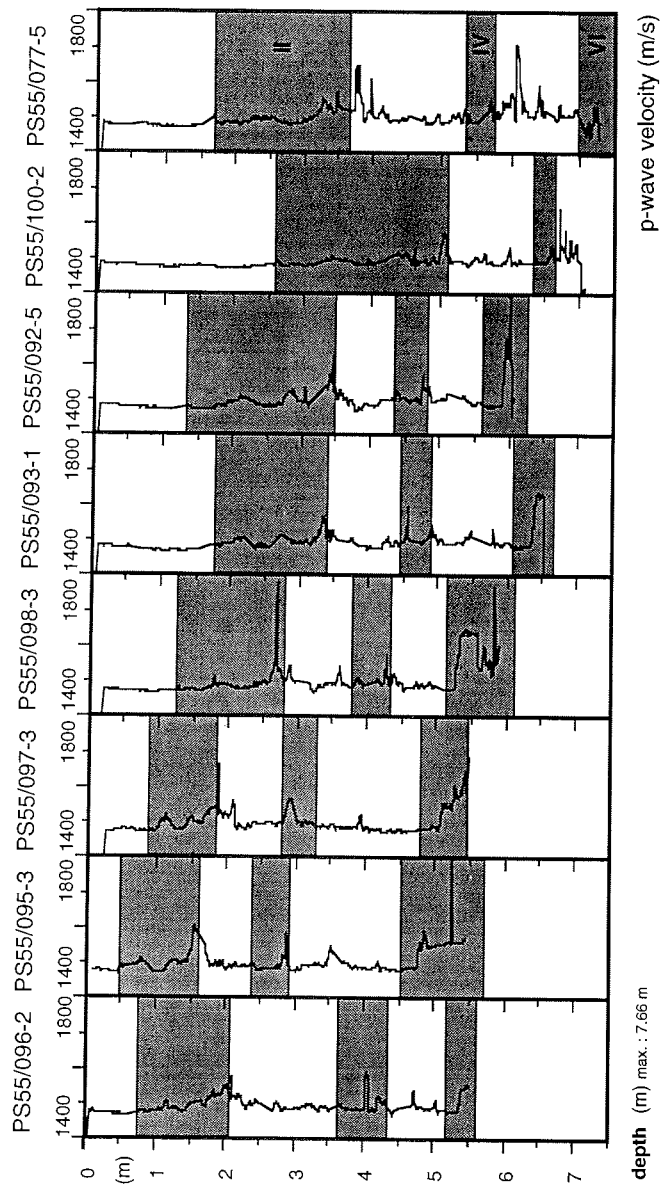


Fig. 29: P-wave velocity of cores from ARK-XV/2.

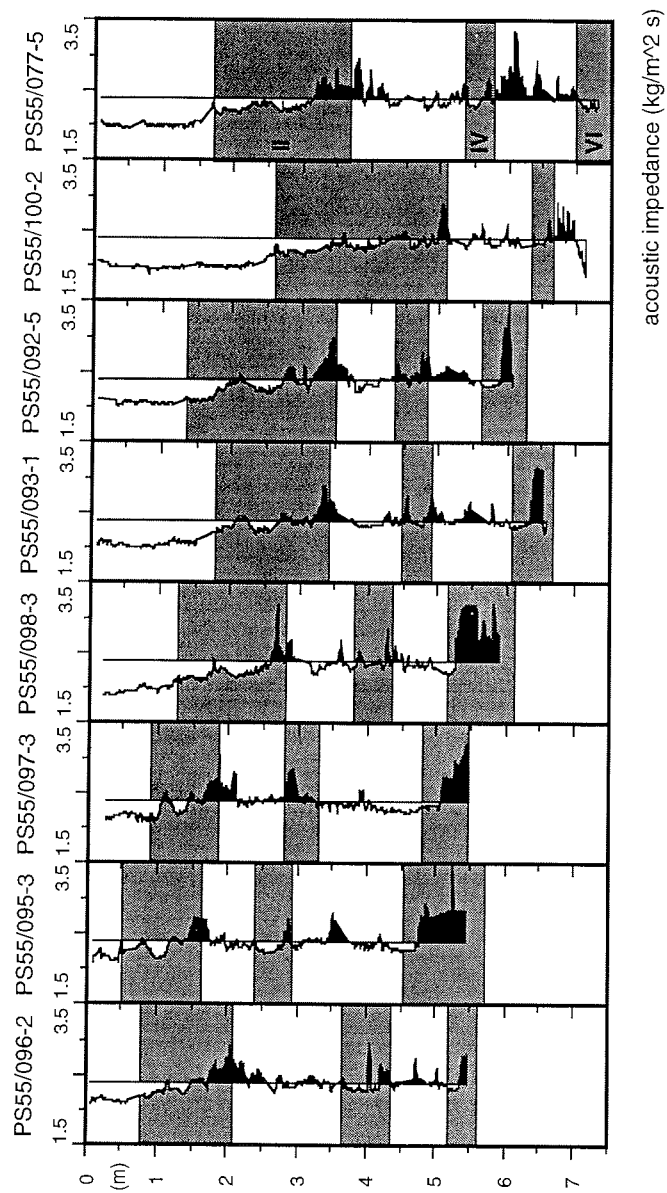


Fig. 30: Acoustic impedance of cores from ARK-XV/2.

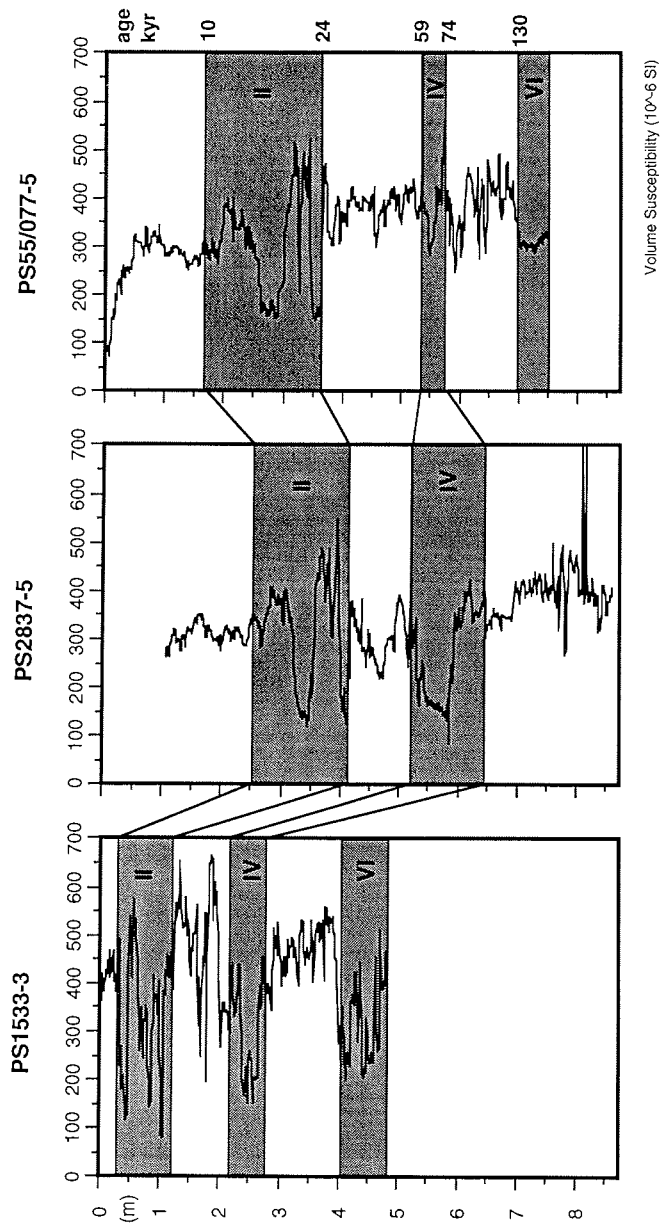


Fig. 31: Correlation of volume susceptibility (point sensor) of PS1533-3 from the northeastern margin with PS2837-5 and PS55/077-5 from the western margin of the Yermak Plateau. Marine isotope stages II, IV and VI are marked in grey. Age model of PS1533-3 after Nowaczyk et al. (1994), age model of PS2837-5 modified after Niessen et al. (1997) and Robert Spielhagen (pers. comm.).

Tab. 17: Logged sediment cores during ARKXV/2. Susceptibility measured with coil sensor, * = susceptibility also measured with point sensor.

GKG	SL	KAL
PS55/077-4*	PS55/077-5*	PS55/077-2*
PS55/092-4*	PS55/086-2	PS55/077-3*
PS55/093-2*	PS55/092-5	PS55/151-2*
PS55/095-2*	PS55/093-1	
PS55/096-3*	PS55/095-3	
PS55/097-1*	PS55/096-2	
PS55/098-2*	PS55/098-3	
PS55/100-3*	PS55/100-2	
PS55/151-1*	PS55/158-2	
PS55/158-1*		

Tab. 18: Specification of the Multi Sensor Core Logger (MSCL14) used during ARK XV/2.

<p>P-wave Velocity and Core diameter</p> <p>Plate Transducer diameter: 5 cm Transmitter pulse frequency: 500 kHz Transmitted pulse repetition rate: 1 kHz Received pulse resolution: 50 ns P-wave travel-time offset: 7.73 ms (SL, 2*2.5 mm wall thickness), 8.66 ms (KAL, 2*3 mm wall thickness)</p>
<p>Density</p> <p>Gamma ray source: Cs-137 Source activity: 356 MBq Source energy: 0.662 MeV Collimator diameter: 5.0 mm (SL), 2.5 mm (KAL) Gamma detector: Gammasearch2, model SD302D, ser. no. 3019 , John Caunt Scientific Ltd., 20 sec counting time</p>
<p>Magnetic Susceptibility</p> <p>Loop sensor type: BARTINGTON MS-2C, ser. no. 130 Loop sensor diameter: 14 cm Alternating field frequency: 565 Hz, counting time 10 s, precision $0.1 \cdot 10^{-5}$ SI Magnetic field intensity: about 80 A/m RMS Loop sensor correction coefficient: 6.391 (SL), 13.649 (KAL) Krel: 1.56 (SL, 12 cm diameter), 0.73 (KAL, 9.57 cm calculated diameter)</p> <p>Point sensor type: BARTINGTON MS2-F, ser. no. 188 Point sensor correction coefficient: 18.88 Krel: 0.53</p>

4 Petrology (E. Hellebrand)

Three regions were sampled by eight dredging stations during cruise ARK XV/2: one at Molloy Ridge, four at Lena Trough, and three at newly discovered basement highs on the Yermak Plateau. The scientific motivation and the samples will be described for each region.

Lena Trough

From a petrological viewpoint, the Lena Trough is a unique region for testing several aspects of magma generation and crustal architecture at early-stage ultraslow-spreading mid-ocean ridges. The N-S trending graben, with axial depths exceeding 4000 m, is, possibly, the last remaining part of the global mid-ocean ridge system that is petrologically completely unexplored. Because of the thick sediment cover in the axial graben, our sampling targets were the valley walls. By sampling these steep, sediment-free walls we intended to address two important questions:

- What is the nature of the basement in the Lena Trough? I.e., are we dealing with a 'real' mid-ocean ridge setting, or, do we merely find rifted slivers of continental origin?
- If there is mid-ocean ridge type spreading at the Lena Trough: is it magmatic or amagmatic? I.e., do we find mid-ocean ridge basalt that was generated by decompression melting beneath an active spreading center, or, does the seafloor rather consist of exhumed, serpentized mantle material, as found at Molloy Ridge, more to the south?

Interpretations strongly depend on bathymetric coverage, magnetic data and seismic results, which provide information about the spreading rate, the obliquity of the ridge and the vicinity of 'cold' continental lithosphere. These are some of the 'forcing functions', thought to influence melting and melt migration beneath spreading centers. Knowing these controlling factors is necessary to understand how the formation of ocean crust in general functions.

Further, the ice-covered Fram Strait offers an excellent opportunity to develop an optimal sampling strategy for heavy ice conditions. Because of total lack of experience under these circumstances, these hard rock sampling 'tests' are crucial for planning a systematic basement rock recovery program at other ice-covered regions, such as the Gakkel Ridge in the Arctic Ocean.

Yermak Plateau

Two basic theories are currently in debate for the composition and age of the northern Yermak Plateau basement:

- The crust is the northern continuation of the Caledonides as exposed on northernmost Spitsbergen. This includes a broad lithological spectrum

ranging from deformed and metamorphosed sediments to Paleozoic granites and Mesozoic extrusives.

- Magnetic data suggest a largely magmatic nature for the northern Yermak Plateau. According to this theory, the intrusion of basic magma occurred in early Tertiary times. Furthermore, the only published deep seismic data across the northernmost Yermak Plateau predict a shallow Moho at depths around 10 - 15 km, suggesting an oceanic origin for this region.

While expanding the bathymetry database during this cruise, unexpected highs were discovered on the eastern margin of the Yermak Plateau. Some of these steep 'seamounts' rise more than 1000 m out of the otherwise gently sloping topography. Seismic reflection experiments across these structures revealed a clear non-sedimentary nature. Along the relatively steep slopes the sediment cover was below detection limit of the geophysical method (~<20 m), implying that basement outcrops could be sampled by dredging.

The newly found basement highs were therefore immediately adopted as highly important sampling targets that could shed the first petrological light onto this speculative and opaque matter.

Results

The dredging locations are shown in Fig. 32. Most important result is that the collected basement rocks confirm that the Lena Trough is an active mid-ocean spreading center, which is consistent with the currently available geophysical data.

A total of nearly 600 kg hard rocks were collected in 5 dredge hauls, using a barrel dredge with 50 cm diameter. On average, each dredging station lasted almost 5 hours. In the Lena Trough, the ice conditions were very bad and thus the dredging time-consuming. Yet, 10 - 20 m wide leads between large ice floes proved sufficient to dredge up slope (500 to 1000 m difference in altitude) for a distance of 1 to 2 nautical miles.

Nearly all major and minor lithologies found on the ocean floor are represented in the dredge hauls, ranging from serpentinized upper mantle rocks, fresh pillow basalt to hydrothermal sulfide deposits. These basement rocks must be partially covered by ice-rafted debris and other sediments, which were also collected in variable amounts. The detailed locations and content of the individual dredge hauls are listed below and in Tables 19, 20 and 21.

Station 075 was carried out under ideal ice-free conditions at Molloy Ridge (Fig. 32). The dredge contained 170 kg of rocks, that represent a mixture of ice-rafted debris (61 %, by weight) and highly serpentinized peridotites (39 %) of mantle origin. The ice-rafted debris mainly consists of low-grade metamorphic schists and quartzites, as well as fine-grained yellow sandstones. Minor amounts of red

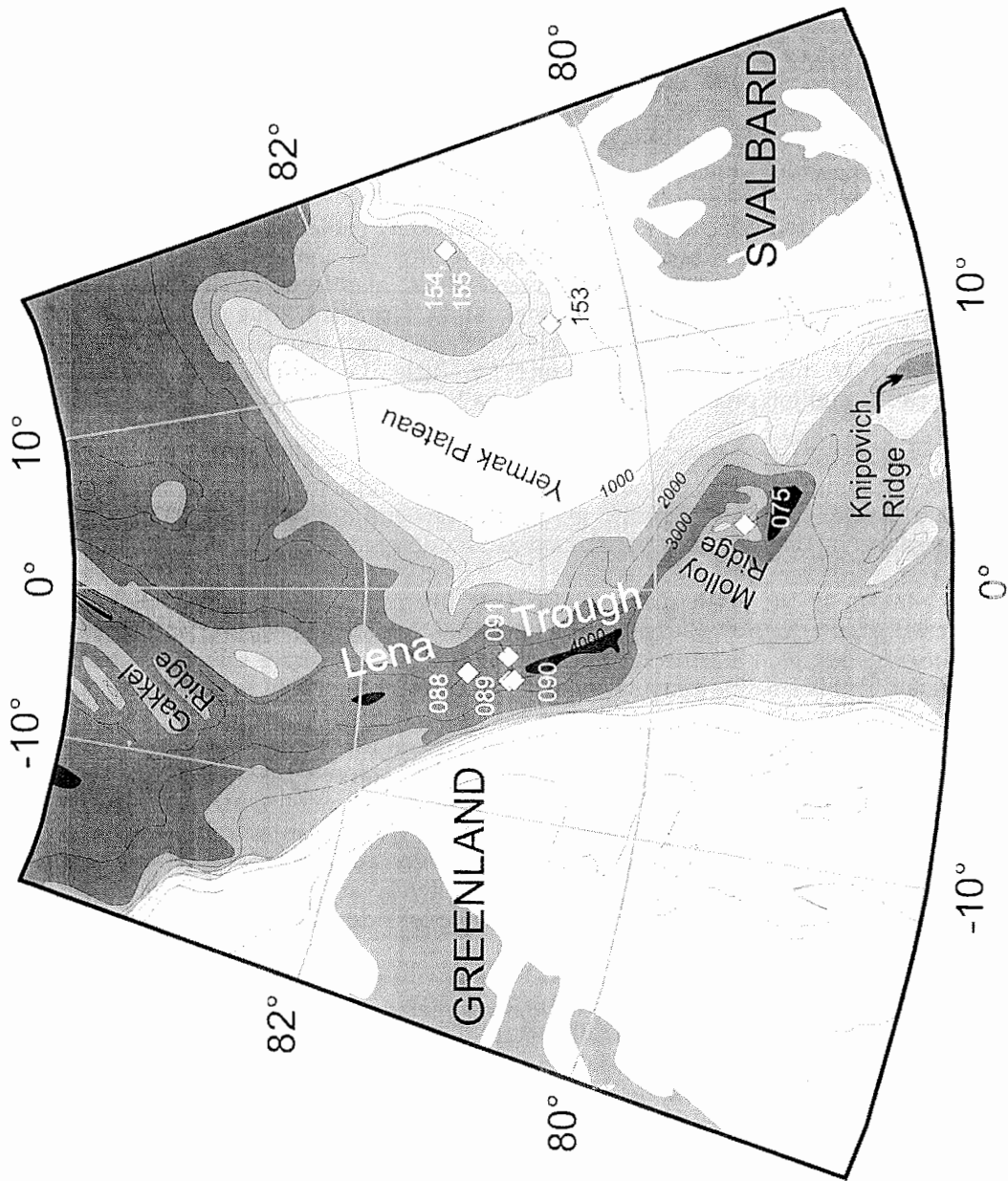


Fig 32: Dredging locations at Molloy Ridge, Lena Trough and Yermak Plateau. 500 m isobaths.

granite, well-rounded vein quartz pebbles, and some higher grade metamorphic rocks could also be identified.

The precursor rock of the collected peridotites is mainly plagioclase-free lherzolite. Three out of 42 samples contain traces of plagioclase, two samples have higher abundances. In one plagioclase-rich lherzolite, plagioclase is extremely heterogeneously distributed and mainly associated with olivine. A clear distinction between harzburgite and lherzolite could not be made for pervasively altered samples. Here, the clinopyroxene content was estimated from pyroxene pseudomorph textures. Important for further analyses is the degree of alteration. Therefore an estimate is given, which mantle minerals (i.e. olivine, orthopyroxene, clinopyroxene, Cr-spinel, and, if present, plagioclase) are not replaced by alteration silicates. In Table 20, these rough estimates were given an index, which means that either none (-), little, i.e. sufficient for electron microprobe and ion probe analysis (+/-), or a lot (+) of that mineral is preserved.

Different alteration stages are preserved. Most samples are cut by late CaCO_3 veins. In some samples, fibrous antitaxial aragonite veins (up to 4 mm thick) form a dense, irregular network, giving the serpentinite host rock a brecciated appearance. In Table 20, they are defined as pseudo-breccias.

This station is the sixth dredge haul that brought up serpentinitized mantle material at the Molloy Ridge, confirming that seafloor spreading at this mid-ocean ridge segment is entirely amagmatic. So far, no extrusive material has been collected at this small segment. The exact location of the ridge axis remains open for speculation, although this term is not appropriate at an amagmatic spreading center. Most likely, the serpentinites were exhumed along one (or multiple) low-angle detachment fault, as seen at many magma-starved regions of the MAR, SWIR and even CIR. The symmetry of this detachment fault is unknown. Because of its uniform mantle lithology, Molloy Ridge is an end member in the global spectrum of ocean ridge types that lie between a layered, Penrose type ocean crust for fast spreading ridges, and the completely amagmatic spreading type ocean crust for extremely slow-spreading (?oblique) ridges away from hotspots.

Station 088 was without doubt a most unexpected highlight of the cruise. At $81^{\circ}22'N$, $3^{\circ}30'W$, located at the eastern flank of the Lena Trough (Fig. 32) more than 100 kg of massive hydrothermal sulfides and low-temperature Fe-oxides/hydroxides were collected. The same dredge haul yielded chunks of blue to grey-blue clays. Blue-green serpentinite fragments with pyroxene pseudomorphs are preserved in some cores of these clay chunks. No extrusive rocks were present, and neither was there any macroscopic evidence for vent biota.

These hydrothermal sulfide deposits are spectacular and important for several reasons:

- This site is only the 7th found along the Mid-Atlantic Ridge.

- It is the second mantle serpentinite-hosted hydrothermal sulfide deposit on the ocean floor. The other one is the Rainbow field south of the 15°20'N Fracture Zone on the Mid-Atlantic Ridge. That region is characterized by large outcrops (exceeding several 100 km²) of extremely depleted mantle rocks.
- This hydrothermal field is located in the slowest-spreading tectonic setting found so far.
- It is the first site ever discovered by dredging, which raises the question, whether it was only an extremely lucky haul, or, maybe representative for a larger area. Based on submersible observations and other studies along the EPR and MAR, there appears to be a negative correlation between the spreading rate on the one hand, and the size and the lifespan of hydrothermal systems on the other hand. E.g., the TAG field on the Mid-Atlantic Ridge near 26°N, an active hydrothermal system, which was drilled during Leg 158 of the Ocean Drilling Program, is located in an 5 km x 5 km area of intense active/fossil hydrothermal activity. The size of individual mounts is equivalent to exploited massive sulfide deposits on land. Spectacular black smoker fields are well known at the East Pacific Rise, but the fields are always relatively small and short-lived. The discovery was not preceded by any water column measurements and was therefore informally named the 'Lucky Bastard Field'.

Station 089 sampled the east-facing flank of a N-S trending ridge on the western valley wall of the Lena Trough (Fig. 32). Its contents were less spectacular, but provided valuable insight in the expected magma-starved nature of the Lena Trough. A total of 78 kg highly serpentinitized mantle peridotites and minor amounts of ice-rafted debris were collected. In contrast to the Molloy Ridge peridotites from Station 075, all mantle rocks are plagioclase-free, indicating very efficient melt extraction beneath the spreading center. Another indication for efficient melt transport is a pyroxene-poor dunitic sample, which is further characterized by a high modal Cr-spinel content. The spinel grains in this dunite are aligned.

Texturally, most samples are moderately to strongly foliated. Three (ultra-) mylonitic peridotites are well preserved, with very low degrees of serpentinization, as often observed for these relatively rare rocks.

Station 090 sampled the same N-S trending ridge but a few kilometers south of Station 089 (Fig. 32). Fresh pillow basalts and minor amounts of serpentinite with a total weight of 210 kg showed that magmatic processes at very slow-spreading ridges can be temporal and spatially variable on a relative small scale.

The extrusives are mainly large pillow basalt fragments. One smaller sheet flow piece was also identified. Most samples have a glassy rim. Large phenocrysts are absent. Only plagioclase occurs as small (around 100 µm on average, maximum 300 µm) irregular microphenocrysts. The groundmass consists of plagioclase needles and glass. The quality of the glass is variable, ranging from very fresh for the sheet flow sample, to highly devitrified for some other samples. Fresh glass

fragments – sufficient for most geochemical analyses – can be recovered from most samples, though. Abundant subrounded vesicles, ranging between 30 and 300 μm in diameter, are present in all samples. Some larger, irregular vugs (between 3 and 50 mm) can only be found in a few basalts. The presence of the vesicles is not common for Mid-Ocean Ridge Basalts, since most basalt is undersaturated in water at ocean floor pressures. This might mean a very low degree of partial melting in the mantle.

The serpentinite fraction consists of 8 samples between few grams and 2 kg. The biggest sample is a red, serpentinitized harzburgite with very low modal pyroxene and large spinel grains. Most samples are too small to estimate the modal compositions. The low pyroxene content in most samples suggests a high degree of melting. One red breccia contains only serpentinite fragments and is cemented by calcium carbonate. It is similar to the serpentinite pseudobreccias of Station 075, but it contains more small fragments and appears to be very heterogeneous, suggesting a different origin.

Station 091 was located at the eastern valley wall of the Lena Trough, symmetrically to Station 89 and 90 (Fig. 32). The dredge only contained sandy and clayey sediments with minor amounts of ice-rafted debris.

Stations 153, 154 and 155 were located on the Yermak Plateau. Dredge station 153 collected only clays at the steep southern wall of Mosby Peak.

The next two stations sampled the southwall of a cone-shaped seamount at the eastern margin of the Yermak Plateau. The first haul yielded 1.2 times the volume of the dredge; very cohesive clays and only minor amounts (3 kg) of what was preliminary determined as IRD, in spite of many bites (max.: 11.4 tons on whinge). This indicated outcropping basement, worthwhile to spend a second attempt, which yielded 15 kg of well-foliated metasediments, and 2 kg IRD. These very-low grade metamorphic rocks are alternating slate-dolomite bands. The thickness of these bands ranges between less 50 μm and several centimeters. Synsedimentary folding was found in one sample. Two hand specimens from station 154 are identical. Further, dredge 154 contained two small (3 cm Δ) Mn-nodules, one fractured Mn-nodule was found in dredge 155. The dropstones in both dredges consist of brown sandstones, carbonates, and well-rounded granites.

Conclusions

All major aims of the petrology group were accomplished

- We succeeded to dredge under heavy ice conditions, i.e. 80 - 95% ice coverage, and obtain very good recovery using a barrel dredge of 50 cm diameter.
- Basement rocks – esp. mantle-derived rocks and fresh basalts – were collected, strongly supporting that the Lena Trough is an active mid-ocean spreading center, linking the well-studied Knipovich Ridge in the northernmost Atlantic, and the nearly unexplored Gakkel Ridge in the Arctic Ocean.

- Evidence for recent or present hydrothermal activity in the Lena Trough turned out to be an unexpected bonus result of our dredging campaign. The implications of this discovery are far-reaching and the 'Lucky Bastard Site' will without doubt become a study object for forthcoming multi-disciplinary investigations.
- One successful dredge at a basement high on the central Yermak Plateau offered first petrological insight on the nature of this highly debated region: Low- to medium-grade metamorphosed sediments, similar to outcropping lithologies along the northernmost Spitsbergen coastline. Existing theories, proposing a magmatic crustal nature for this region, may need to be revised.

Tab. 19: Dredging statistics

Station	Date		Time (UTC)	Latitude	Longitude	Water depth (m)	Max. pull (tons)	Content
PS 55 / 075	24.7.99	start	6:30	79°21.3'N	1°48.0'E	3119	10.8	serpentinite, IRD
		end	10:40	79°22.0'N	1°41.0'E	2133		
		duration:	4:10			h: 986		
PS 55 / 088	4.8.99	start	14:05	81°21.6'N	3°34.0'W	3703	7.3	sulfides, serpentinites
		end	19:10	81°21.7'N	3°19.4'W	3011		
		duration:	5:05			h: 692		
PS 55 / 089	5.8.99	start	9:40	80°58.0'N	2°37.0'W	3640	6.4	serpentinite
		end	14:30	80°58.0'N	2°37.0'W	2956		
		duration:	4:50			h: 684		
PS 55 / 090	5.8.99	start	16:45	80°54.5'N	2°27.4'W	3950	7.2	fresh basalt, serpentinite
		end	22:30	80°53.9'N	2°30.5'W	3500		
		duration:	5:45			h: 450		
PS 55 / 091	6.8.99	start	2:30	80°58.5'N	1°43.7'W	3410	5.4	sediment, IRD
		end	6:45	80°58.9'N	1°35.4'W	2650		
		duration:	4:15			h: 760		
PS 55 / 153	28.8.99	start	6:30	81°14.91'N	11°41.81'N	2013	4.0	sediment
		end	9:20	81°17.10'N	11°34.31'E	1453		
		duration:	2:50			h: 560		
PS 55 / 154	28.8.99	start	13:50	81°37.31'N	15°32.31'E	2382	11.4	sediment, IRD
		end	17:00	81°39.49'N	15°32.92'E	1570		
		duration:	3:10			h: 812		
PS 55 / 155	28.8.99	start	18:40	81°37.22'N	15°32.70'E	2307	8.6	sediment, IRD, banded slate
		end	21:20	81°38.12'N	15°32.13'E	1682		
		duration:	2:40			h: 625		

Sample Nr.	Lithology ^(a)	Size (cm)	color ^(b)	% serp	fresh min's ^(c)					modal plag (%)	foliation ^(d)	comment ^(e)
					ol	opx	cpx	sp	pl			
075-1	harzburgite	30 x 25 x 20	bik-gr	90-95	+/-	+	+	+	-	0.1	-	
075-2	plag-lherzolite	20 x 20 x 20	br	60-90	+	+	+	+	+	0.2 - 20	-	extremely heterogeneous
075-3	lherzolite	40 x 20 x 20	r-br	95-99	-	+/-	+/-	+	-	0	-	
075-4	lherzolite	15 x 10 x 10	r-br	95-99	-	+/-	+/-	+	-	0	-	
075-5	lherzolite	30 x 25 x 20	ye-br	95-99	-	+/-	+	+	-	0	-	many thick cc veins
075-6	lherzolite	25 x 15 x 15	r-br	95-99	-	+/-	+	+	-	0	-	
075-7	gabbro/peridotite	10 x 4 x 4	ye-br	90-95	+/-	+	+	+	+/-	-	-	diffuse contact
075-8	lherzolite	4 x 4 x 3	ye-br	90-95	+/-	+/-	+	+	-	0	-	
075-9	lherzolite	3 x 2 x 1	ye-br	90-95	+/-	+/-	+	+	-	0	-	
075-10	lherzolite	5 x 2 x 1	ye-br	90-95	+/-	+/-	+	+	-	0	-	
075-11	lherzolite	3 x 2 x 1	ye-br	90-95	+/-	+/-	+	+	-	0.1	-	
075-12	lherzolite	4 x 3 x 2	ye-br	90-95	-	-	+	+	-	0	-	
075-13	lherzolite	10 x 10 x 6	r-br	60-90	+/-	+	+	+	-	0	-	
075-14	lherzolite	10 x 10 x 5	br	90-95	-	+/-	+/-	+	-	0	-	
075-15	harzburgite (?)	12 x 10 x 8	ye-br	100	-	-	?	+	-	0	-	
075-16	harzburgite (?)	5 x 4 x 3	grey	100	-	-	?	+	-	0	-	
075-17	harzburgite (?)	3 x 3 x 1	gr-br	100	-	-	?	+	-	0	-	
075-18	lherzolite	5 x 4 x 4	ye-br	95-99	-	+/-	+/-	+	-	0	-	cc pseudo-brecciated
075-19	harzburgite (?)	10 x 8 x 8	ye-br	95-99	-	-	+/-	+	-	0	-	cc pseudo-brecciated
075-20	pl-bearing lherz.	10 x 7 x 5	br	95-99	-	+/-	+	+	-	3	-	pl blebs heterogeneously distributed
075-21	harzburgite (?)	8 x 3 x 3	br	90-95	-	+	+	+	-	0?	-	amphibole-bearing
075-22	harzburgite (?)	3 x 3 x 2	ye-br	100	-	-	-	+	-	0	-	
075-23	lherzolite	6 x 6 x 4	br	95-99	-	+/-	+/-	+	-	0	-	cc pseudo-brecciated
075-24	lherzolite	10 x 10 x 8	ye-br	90-95	-	+/-	+	+	-	0	-	cc pseudo-brecciated
075-25	harzburgite (?)	7 x 5 x 3	ye-br	100	-	-	-	+	-	0	-	cc pseudo-brecciated
075-26	lherzolite	4 x 3 x 2	ye-br	95-99	-	-	+/-	+	-	0	-	
075-27	harzburgite (?)	3 x 2 x 2	ye-br	100	-	-	-	+	-	0	-	
075-28	harzburgite (?)	10 x 5 x 1	ye-br	95-99	-	-	+/-	+	-	0?	-	
075-29	harzburgite (?)	3 x 3 x 2	ye-br	100	-	-	-	-	-	0?	-	
075-30	harzburgite	4 x 4 x 2	ye-br	95-99	-	+	+	+	-	0	-	
075-31	pl-bearing lherz.	5 x 4 x 3	ye-br	95-99	-	+/-	+	+	-	1	-	
075-32	pl-bearing hzb. (?)	6 x 4 x 3	br	95-99	-	+/-	+/-	+	-	1	-	
075-33	lherzolite (?)	7 x 5 x 2	ye-br	100	-	-	-	+	-	0	-	
075-34	pl-bearing hzb. (?)	5 x 3 x 3	ye-br	95-99	-	+/-	+/-	+	-	< 1	-	amphibole-bearing

Tab. 20: Schematic petrographic description of collected serpentized peridotites

Sample Nr.	Lithology ^(a)	Size (cm)	color ^(b)	% serp	fresh min's ^(c)					modal plag (%)	foliation ^(d)	comment ^(e)
					ol	opx	cpx	sp	pl			
075-35	harzburgite (?)	6 x 4 x 3	br	100	-	-	-	+	-	0	-	amphibole-bearing
075-36	lherzolite	4 x 3 x 2	ye-br	95-99	-	-	+/-	+	-	0	-	
075-37	harzburgite	3 x 3 x 2	ye-br	95-99	-	-	+/-	+	-	0	-	
075-38	lherzolite	3 x 2 x 1	red-br	95-99	-	+/-	+	+	-	0	-	
075-39	pyroxenite	10 x 3 x 2	ye-br	30-60	+/-	+	+	+	+/-			1 mm Fe-Mn coating coarse-grained
				mode:	17	80	2	1				5 mm Fe-Mn coating
075-40	lherzolite	5 x 4 x 3	ye-br	100	-	-	-	+	-	0	-	
075-41	harzburgite (?)	10 x 8 x 5	ye-br	100	-	-	-	+	-	0	-	
075-42	lherzolite	12 x 4 x 3	ye-br	90-95	-	+	+	+	-	0	-	
089-1	harzburgite	60 x 30 x 30	ye-gr	90-95	+/-	+	+	+	-	0		
089-2	lherzolite	25 x 20 x 20	blk-br	100	-	-	-	-	-	0		
089-3	harzburgite	25 x 20 x 15	ye-gr	95-99	+/-	+	+	+	-	0	++	elong. Opx -> foliation
089-4	dunite	25 x 20 x 15	ye-gr	95-99	-	+/-	+/-	++	-	0		spinel micropods (max: 12 mm)
089-5	harzburgite	10 x 10 x 6	ye-gr	95-99	-	-	+/-	+	-	0	++	elong. Opx -> foliation
089-6	harzburgite	8 x 6 x 4	ye-gr	100	-	-	-	+	-	0		
089-7	harzburgite	10 x 8 x 7	ye-br	95-99	-	+/-	+/-	+	-	0		
089-8	peridotite	12 x 8 x 3	ye-br	90-95	+/-	+	+	+	-	0		5mm CaCO3-vein
089-9	harzburgite	8 x 6 x 6	ye-br	95-99	-	+/-	+/-	+	-	0		
089-10	serpentinite breccia	8 x 5 x 3	grey-br	100	-	-	-	?	-	0		dunite-fragments
089-11	harzburgite	8 x 8 x 6	ye-br	95-99	-	+	+	+	-	0		
089-12	harzburgite	5 x 4 x 4	ye-gr	100	-	-	-	+	-	0		diffuse cpxite vein?
089-13	harzburgite	5 x 5 x 4	ye-gr	95-99	-	+/-	+	+	-	0		
089-14	harzburgite	5 x 4 x 4	ye-br	95-99	-	+/-	+/-	+	-	0		
089-15	peridotite	10 x 6 x 2	wh-gr	100	-	-	-	+	-	0		
089-16	peridotite	12 x 6 x 3	ye-br	100	-	-	-	+	-	0		
089-17	mylonitic peridotite	4 x 2 x 2	grey-br	<20?		+/-					+++	rare ultra-elong. opx-clasts
089-18	mylonitic peridotite	8 x 6 x 6	grey-br	<20?		+/-					+++	
089-19	harzburgite	9 x 5 x 4	blk	90-95	+/-	+/-	+/-	+	-	0	-	
089-20	?talc-schist	7 x 6 x 3	wh-gr	-	-	-	-	-	-		+	crenulated foliation
089-21	harzburgite	12 x 8 x 6	ye-br	95-99	-	+	+/-	+	-	0	-	
089-22	harzburgite	4 x 3 x 2	blk	90-95	+/-	+	+	+	-	0	-	
089-23	mylonitic peridotite	10 x 8 x 7	grey-gr	<10							+++	weathering color bright yellow
089-24	lherzolite	5 x 4 x 4	gr-br	90-95	+/-	+	+	+	-	0	+	

Sample Nr.	Lithology ^(a)	Size (cm)	color ^(b)	% serp	fresh min's ^(c)					modal plag (%)	foliation ^(d)	comment ^(e)
					ol	opx	cpx	sp	pl			
089-25	lherzolite	4 x 3 x 3	ye-br	95-99	-	+/-	+	+	-	0	+/-	
089-26	harzburgite	10 x 10 x 3	gr-br	95-99	+/-	+/-	+	+	-	0	-	
089-27	lherzolite	7 x 7 x 4	gr-br	95-99	-	+/-	+	+	-	0	++	
089-28	lherzolite	10 x 6 x 4	gr-br	95-99	+/-	+/-	+	+	-	0	+/-	
089-29	harzburgite	20 x 15 x 12	gr-br	95-99	-	+/-	+/-	+	-	0	++	
089-30	harzburgite	20 x 18 x 15	gr-br	95-99	-	+/-	+/-	+	-	0	++	
090-12	harzburgite	20 x 15 x 15	red	95-99	-	+/-	+/-	+	-	0	-	very px-poor, large spinels
090-13	peridotite	7 x 5 x 3	gr-wh	100	-	-	-	-	-	0	-	
090-14	peridotite	4 x 3 x 3	ye-gr	95-99	-	+/-	+/-	+	-	0	++	px-poor, spinel-rich (2% modal)
090-15	peridotite	5 x 3 x 3	gr-wh	100	-	-	-	-	-	0	-	
090-16	?dunite	3 x 2 x 2	red-gr	100	-	-	-	+/-	-	0	+	?mylonite, no px visible
090-17	harzburgite	10 x 7 x 3	gr-wh	100	-	-	-	+	-	0	+	
090-18	peridotite	4 x 3 x 1	gr-wh	100	-	-	-	-	-	0	-	
090-19	harzburgite	4 x 2 x 2	red-gr	90-95	+	+	+/-	+	-	0	+	
090-20	harzburgite	3 x 2 x 1	red	95-99	-	+/-	+/-	+	-	0	-	
090-21	serpentinite breccia	9 x 5 x 4	red-pink	80-100	+/-	+	+	+	-	0	-	red angular dunite clasts in CaCO ₃
090-23	peridotite	2 x 1 x 1	red	95-99	+/-	+/-	+/-	+	-	?	+	
090-24	'ophicalcite'	2 x 1 x 1	wh	-	-	-	-	-	-	-	-	few serp. fragments in carbonate
090-25	harzburgite	7 x 5 x 4	grey-gr	95-99	+/-	+	-	+	-	0	+	very px-poor
090-26	peridotite	2 x 1 x 1	gr	100	-	-	-	-	-	0	-	

a) 'peridotite' when sample too small or too altered

b) green (gr), brown (br), yellow (ye), black (bl), white (wh)

c) fresh minerals: olivine (ol), orthopyroxene (opx), clinopyroxene (cpx), spinel (sp), plagioclase (pl)

(-): no primary mineral preserved; (+/-): some preserved, sufficient for analysis; (+): well-preserved

d) (-): no foliation; (+/-): weak foliation; (+): well-developed foliation; (++): strong foliation; (+++): mylonite

e) cc = calcium carbonate; px = pyroxene; elong. = elongated

Tab. 21: Schematic petrographic description of collected basalts

Nr.	Sample			Glass Surface Quality ^(a) (-cm ²)	phenocrysts ^(b)		vesicles in glass abundance ^(c) (µm)	Comment
	Lithology	Size (cm)	Weight (kg)		pl	cpx ol size (mm)		
090-1	pillow basalt	40 x 30 x 30	20	900	+	+/- - - <0.2	+	50-200
090-2	pillow basalt	50 x 35 x 30	30	1000	+/-	+/- - - <0.2	+	50-200
090-3	pillow basalt	35 x 30 x 30	16	900	+	+/- - - <0.2	+/-	50-200
090-4	pillow basalt	40 x 40 x 20	21	800	+	+/- - - <0.2	+	50-200
090-5	pillow basalt	50 x 30 x 30	24	900	+	+/- - - <0.2	+/-	50-200
090-6	pillow basalt	40 x 20 x 15	9	30		+/- - - <0.2		
090-7	pillow basalt	30 x 30 x 20	9	500	+/-	+/- - - <0.2	+	50-200
090-8	pillow basalt	20 x 10 x 10	2	200		+/- - - <0.2		
090-9	pillow basalt	35 x 25 x 15	10	300	+/-	+/- - - <0.2	+	200-500
090-10	pillow basalt	30 x 25 x 15	8	300	+/-	+/- - - <0.2	+	50-200
090-11	pillow basalt	20 x 20 x 10	3	0		+/- - - <0.2		
090-22	sheet flow	20 x 15 x 10	2.5	300	++	+/- - - <0.2	+/-	50-200
090-27	pillow basalt	20 x 18 x 12	3	150	-	+/- - - <0.2	+	50-200
090-28	pillow basalt	25 x 15 x 15	3.5	150	-	+/- - - <0.2	+	50-200
090-29	pillow basalt	20 x 12 x 8	2	100	+/-	+/- - - <0.2	+/-	50-200

1050

- a) Glass quality: ++: no sign of devitrification, limited palagonitization, abundant perfect glass shards
 +: initial devitrification in some shards, variable palagonitization, some perfect glass shards
 +/-: devitrification in many shards, strong palagonitization, (very) few perfect glass shards
 -: devitrification in all shards, strong palagonitization, no perfect glass shards

- b) Phenocrysts: +/-: rare (less than 1% modal)
 -: absent

- c) Vesicle abundance
 +: many vesicles in most glass shards
 +/-: few vesicles in most glass shards

5 Hydrosweep DS2 Bathymetry

(S. Daschner, C. Hohmann, W. Voß)

The expedition ARK XV/2 was intended to collect and process navigation, bathymetry and side-scan sonar data. The task of the bathymetric group on board of RV "POLARSTERN" during the cruise ARK XV/2 was to expand the systematically surveyed area in the central Fram Strait to the north and north-east, in order to map the transition of the Spitsbergen Fracture Zone to the Lena Trough. In addition, the multibeam surveys from previous expeditions in 1991 and 1997 should be completed and expanded.

On July, the 21st, 1999 RV "POLARSTERN" departed from Tromsø. After leaving the Norwegian EEZ at 74° N, the HYDROSWEEP was activated, continuous data recording was performed during the leg. The planning of the survey was performed in close co-operation with the geophysical and geological working groups on board. Reaching the latitude of 74° N at the end of the expedition, the Hydrosweep data acquisition was terminated.

5.1 Hydrographic Survey Equipment on RV POLARSTERN

The multibeam echosounding system HYDROSWEEP DS2 operates at a frequency of 15.5 kHz and measures athwartships orientated cross sections of the seafloor topography in depths between 11 and 10.000 metres. The opening angle of the swath, which consists of 59 pre-formed-beams (PFB), is 90°. Thus the width of the strip covers twice of the water depth underneath the ship. The multibeam system is automatically calibrated for the sound speed in a special procedure, called cross-fan calibration. The mean water sound velocity is determined in a least squares process by comparing the swath measurements along the ship's main axis to the profile as observed by the centre beam.

The system was operated continuously during the entire cruise with some minor exceptions, caused by system failures. Other reasons causing interrupts of the data logging was given when the ship was steaming through heavy sea ice, when no reasonable signals could be recorded.

The Differential Global Positioning System (DGPS) on board is supplied by the SkyFix system using Inmarsat satellites as a broadcast link to receive differential data. The used differential corrections are generated at the SkyFix computing centres in Norway and Scotland. The working area of POLARSTERN between Spitsbergen and Greenland is only partly covered by the Inmarsat satellites. Therefore, DGPS corrections were especially north of 80° N only partly available. During the DGPS operation the positioning accuracy is between ±5 and 10 m, in the Standard Positioning Services of GPS supplies only an accuracy of ±100 m.

5.2 Surveys

The first systematic HYDROSWEEP survey was performed at the Molloy Fracture Zone (between 80°N 0°30'W to 80°20'N 2°30'E) in order to complete measurements in this area from earlier cruises in 1990 and 1997. Despite bad ice conditions, the collected data were reasonable quality.

The planned survey in the Fram Strait, west of Greenwich Meridian, was cancelled because of extreme heavy ice conditions. Therefore, an alternative program east of the Yermak Plateau was initiated. The task of the systematic survey in this area was the mapping of the continental slope and the topographic structures east of the Yermak Plateau.

A first box survey was carried out (81°N to 81° 45'N and 10° 30'E to 15°E) parallel to the continental slope, covering the Mosby Peak seamount in the north-west corner of the box (fig. 33). Mosby Peak is a major submarine feature located at the continental slope and is elevating more than 1000 m above the surrounding terrain. Beforehand the morphology of this area was only known from side scan sonar data, published in the Fram Strait Atlas (Crane et. al. 1995).

A second box has been surveyed in the area between 81°35'N 15°E to 81°55'N 18°20'E parallel to the continental slope. A new submarine seamount (proposed name POLARSTERN Peak) ranging between 2700 and 1550 meters, was discovered at the position of 81°38'N 15°32'E (fig. 34). After the multibeam survey a seismic profile across this structure was acquired.

To study the morphology of the continental slope between 17°E and 25°E a third areal survey east of the Yermak Plateau was performed covering the region between 81°35'N and 82°N. A total profile length of 550 nautical miles was surveyed, this corresponds to an area of 4000 km². A single bathymetric profile was measured from 81°20'N to 80°45'N along the 1500 m isobath to investigate the continental slope east of Yermak Plateau (fig. 35).

On the transit back to Spitsbergen a short multibeam survey of the Sophia-Trough (80°45'N, 10°E) was performed.

5.3 Data processing

Controlled by the Hydrosweep operating system, the multibeam raw data are stored on magnetic tapes every ten minutes. The navigation data and the centre depths are additionally stored in POLDAT (POLARstern DATAbank), the data archive on "POLARSTERN".

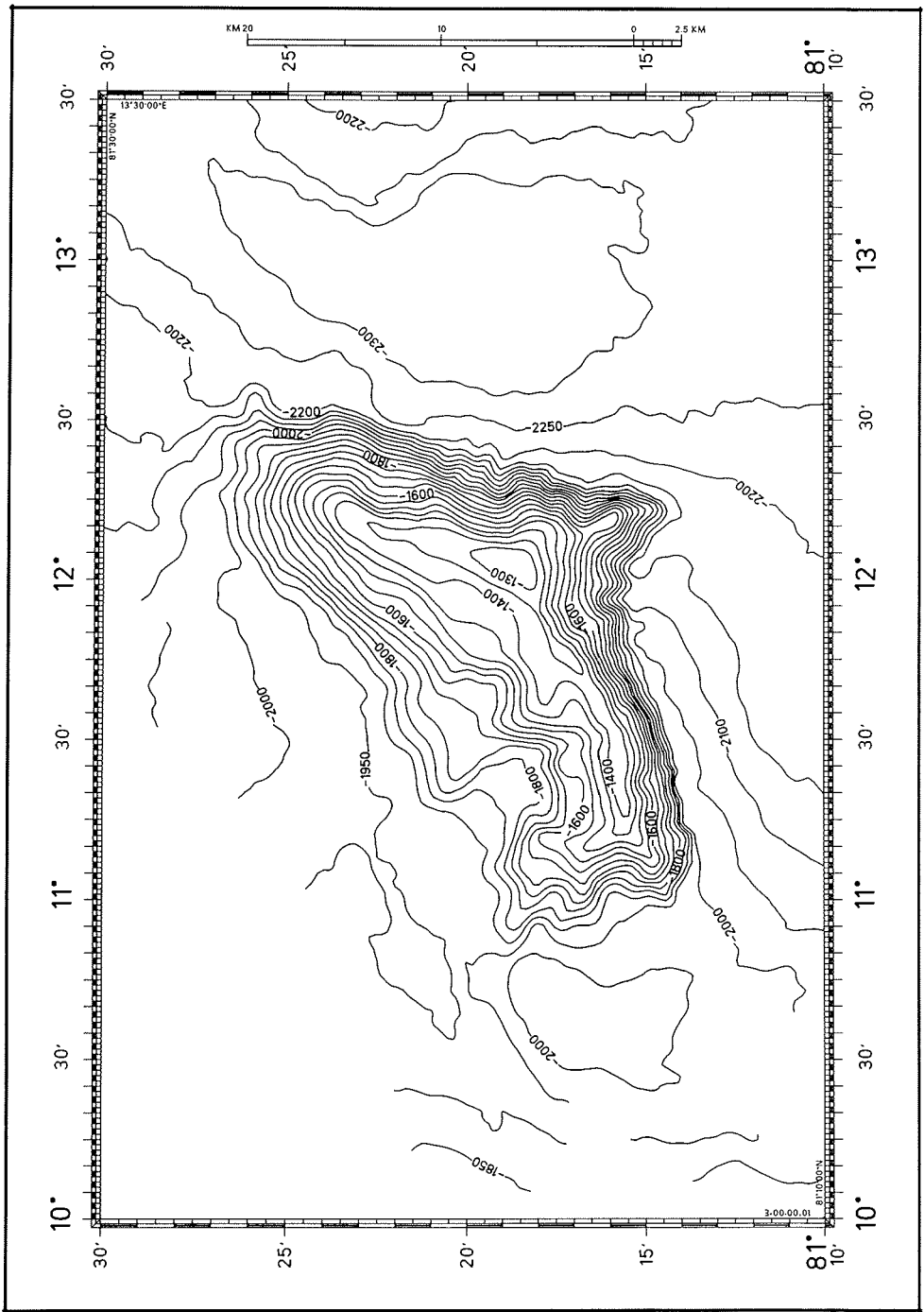


Fig. 33: Bathymetric chart of Mosby Peak

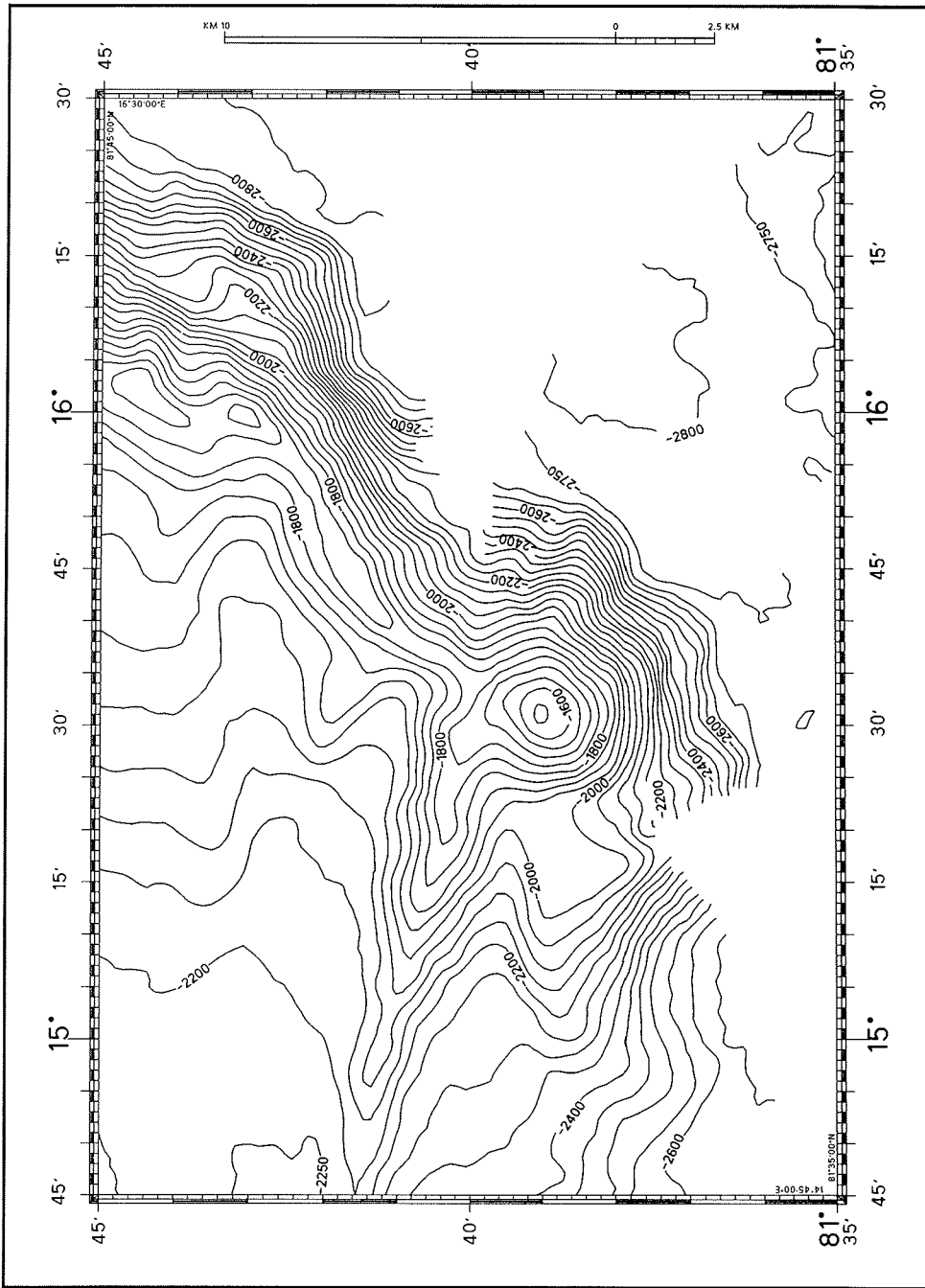


Fig. 34: Bathymetric chart of Polarstern Seamount, a new discovery during ARK-XV/2

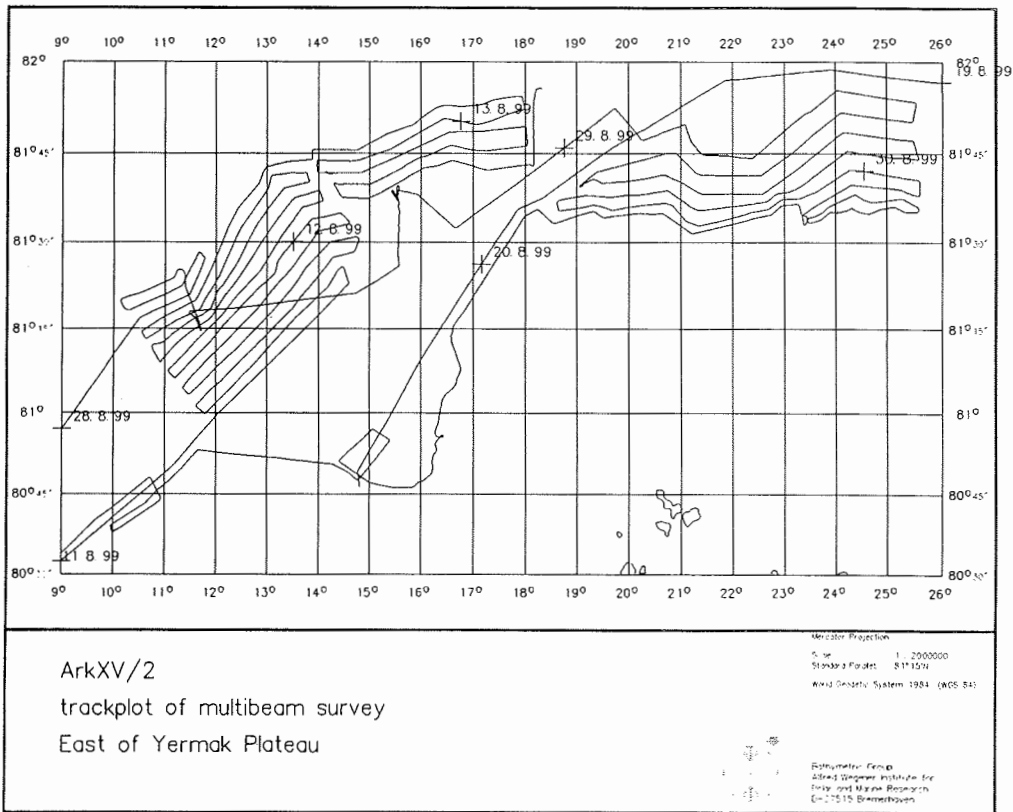


Fig. 35: Trackplot of the Multibeam survey north of Svalbard

The navigation data are checked using HYDROMAP off-line. The differences in the ship's positions are checked and, if necessary, edited. Within the next step during postprocessing on board the depths are edited using the graphic editor HDCS (Hydrographic Data Cleaning System). In this process obviously wrong depths are flagged, and systematic errors of the outer-beams, sometimes caused by a false mean water sound velocity, are corrected. Especially while steaming through sea ice, wrong echoes, caused by ice or aeration at the transducers are recorded. In addition, the operation of large volume airguns negatively influenced the data quality, a periodical interference was observed in the received signal. After data cleaning, the raw data files were converted into the .hyd-format, which is used for further processing.

5.4 Plotting bathymetric charts

In general, bathymetric charts are used before and during scientific expeditions with "POLARSTERN". For this purpose the AWI Bathymetric Plotting Sheets of

the Fram Strait in the scale 1:200000 which are maintained by the AWI bathymetric group are utilized.

The index of the bathymetric plotting sheets is derived from the catalogue of the General Bathymetric Charts of the Ocean (GEBCO), published by the International Hydrographic Organisation (IHO) in 1983. The GEBCO Sheets no. 581, 582, 589 and 590 are divided into subsheets with 1° N-S and 5° W-E extension.

These plotting sheets contain all multibeam measurements between 1984 and 1987 collected with SEABEAM and between 1990 and 1997 with Hydrosweep. The data from this cruise will be included in those sheets.

5.5 Final results and future work

Preliminary bathymetric charts were compiled from the areal surveys around Mosby Peak and POLARSTERN Peak (Fig. 33, 34) using standard postprocessing tools of AWI. Finally large scale products will be prepared at the AWI using the Hydrographic Information System CARIS (Computer Aided Resource and Information System).

During ARK XV/2, about 7180 nautical miles were sailed, a total area of 40.000 km² was surveyed. East of the Yermak Plateau, for the first time measurements with the multibeam echosounding system HYDROSWEEP were performed. This systematical survey covers an area of ~ 10.000 km².

The collected data will be used for the creation of the new "International Bathymetric Chart of the Arctic Ocean" (IBCAO) which is planned in co-operation with IHO and Intergovernment Oceanographic Commission (IOC). A significant contribution to this work is the Fram Strait Atlas, scale 1:100.000, and the multibeam data collected by "POLARSTERN".

6 Planktonic foraminifera (E. Stangeew, J. Netzer)

During the first part of the POLARSTERN cruise (ARK-XV/1) a total of 14 multinet stations (st. 001 - 066) were taken, 9 stations along a transect at 75°N (Abb. 37). Several different watermasses were covered, such as PW, GSW and RAC. During the second part of the cruise (ARK-XV/2) a total of 10 CTD- and multinet stations (st. 077 - 176) were collected, 8 stations (Abb. 36) along a transect in the Fram Strait (80°N).

The multinet samples with depth intervals of 0 - 50, 50 - 100, 100 - 200, 200 - 300 and 300 - 500 m were conserved in ethanol (90%). Water samples from the CTD rosette were taken for analysis, at 0, 25, 50, 100, 200, 300, 400 and 500 m were sampled for analysis of $d^{18}O$ and $d^{13}C$ and nutrients. SiO_4 and PO_4 levels were determined photometrically (model UV 150-01) for the same depths and are given as $\mu M/l$. Chl *a* concentrations from 0, 25, 50, 75, 100, 130, 160 and 200 m were analysed with the fluorometer (model AU-10) and are given as $\mu g/l$.

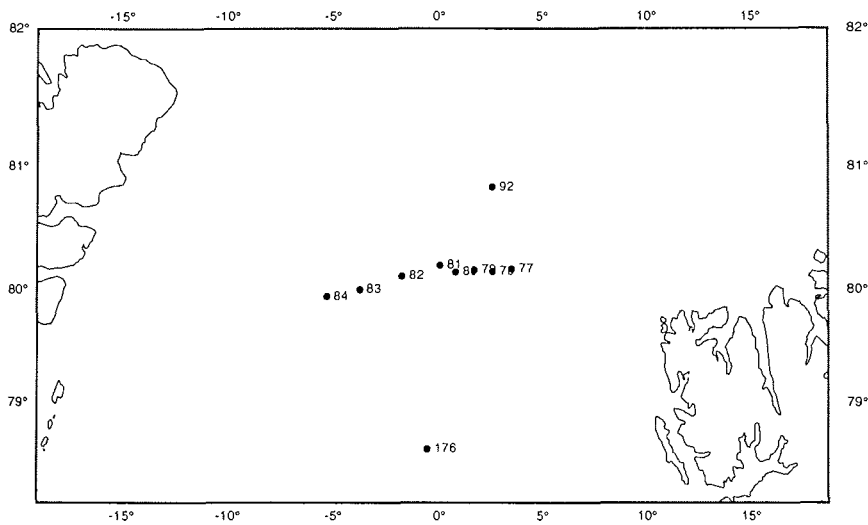


Fig. 36: Multinet stations (ARK-XV/1 and ARK-XV/2)

Results

Nutrient and pigments: The vertical distribution of nutrients over the top 500 m of the watercolumn reflect a typical summer situation in the Greenland sea , with extremely low levels of SiO_4 and PO_4 .

st. 001 - 004 (Abb. 37): The lowest nutrient levels were observed at 50 to 100 m depth, with concentrations of $2.0 \mu\text{M}/\text{l}$ SiO_4 and $0.2 \mu\text{M}/\text{l}$ PO_4 . With increasing depth the SiO_4 levels rose to $6.5 \mu\text{M}/\text{l}$, while the concentration of PO_4 was seen to fluctuate very little around $3.0 \mu\text{M}/\text{l}$. The maximum concentration of chlorophyll *a* at these stations was $1.3 - 2.3 \mu\text{g}/\text{l}$ at 25 and 50 m respectively. The levels of phaeopigments are faintly correlated with those of chl *a*.

st. 018 - 066 (CTD-transect, Abb. 38): The lowest nutrient levels were seen between the surface and 25 m depth, with $0.3 - 3.3 \mu\text{M}/\text{l}$ SiO_4 and $0.2 \mu\text{M}$ PO_4 ; in greater depths the concentration increased to a max. of $7.2 \mu\text{M}/\text{l}$ SiO_4 and $0.3 \mu\text{M}/\text{l}$ PO_4 . The concentration of chl *a* shows a similar depth distribution, decreasing from 3.7 to $0.2 \mu\text{g}/\text{l}$. Phaeopigment levels in the watercolumn again were highest at around 20 - 25 m depth with max. values of $0.1 \mu\text{g}/\text{l}$.

St. 002

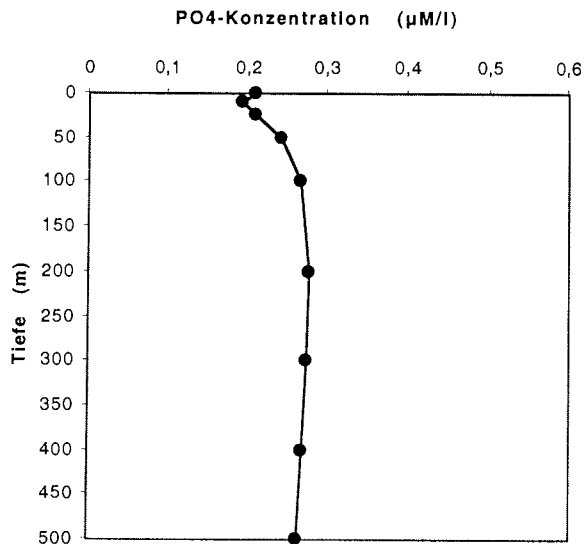
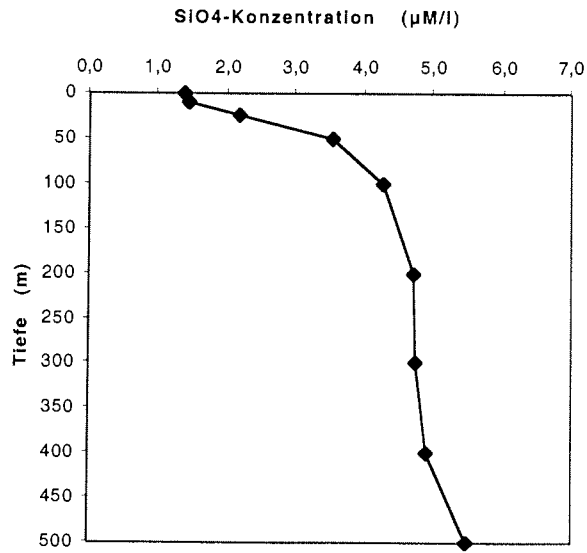


Fig. 37: Nutrient and pigment concentrations and depth distribution at st. 002 (ARK-XV/1)

St. 002



St. 002

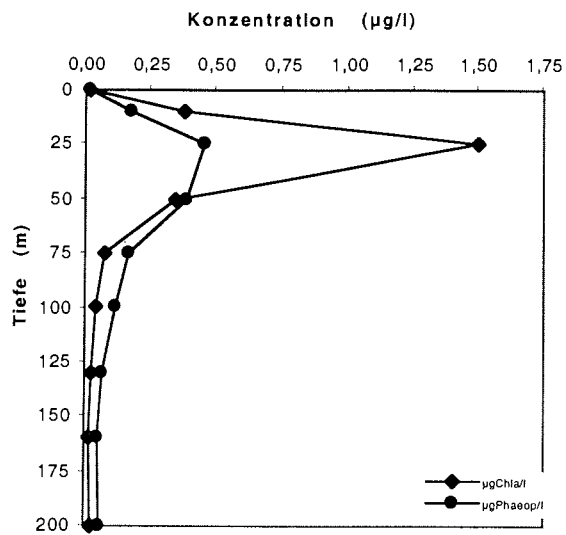


Fig. 37 (continuation)

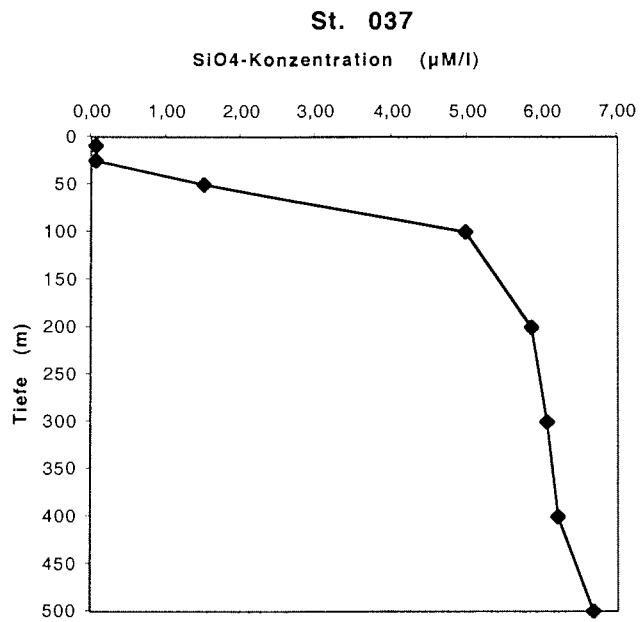
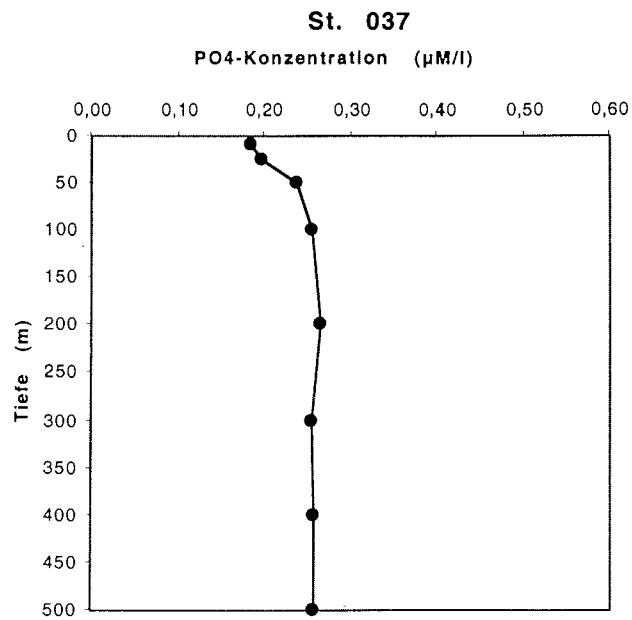


Fig. 38: Nutrient and pigment concentrations and depth distribution at st. 037 (ARK-XV/1)

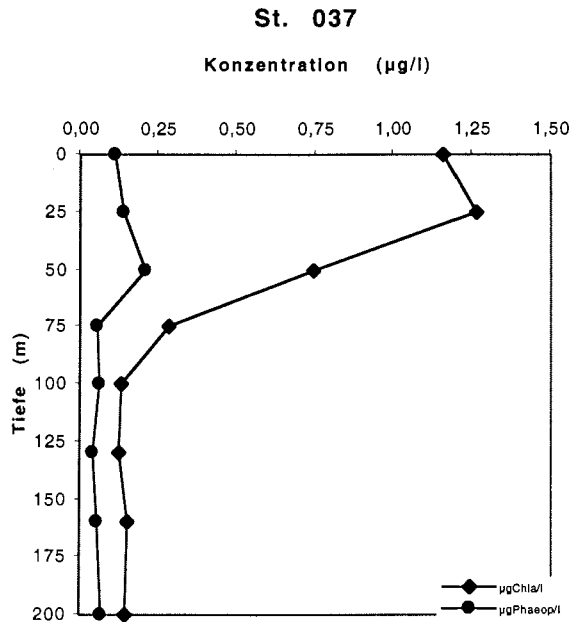


Fig. 38 (continuation)

ARK-XV/2

nutriens and pigments:

st. 077 - 082 (Abb. 39): This stations show generally low nutrient concentrations in the surface water. The mixed layer extends to app. 100 m depth, with extremely low levels of SiO_4 between 1.4 - 1.6 $\mu\text{mol/l}$ and for PO_4 between 0.1 - 0.2. Generally, low levels of chl *a* were found with variable depth distribution. Maximal values are found at 0 - 25 m depth and vary between 0.3 and 1.2 $\mu\text{g/l}$. Only at st. 078 exeptional high chl *a* concentrations were found. The concentration of phaeopigments was also rel. low on these stations and decrease with increasing wather depth.

st. 083 - 084 (Abb. 40): Polar water is located at the surface with relatively high nutrient concentrations of 8.0 - 10.0 $\mu\text{mol/l}$ for SiO_4 and 0.25 $\mu\text{mol/l}$ for PO_4 respectively. The polar watermass extends down to app. 100 m and Atlantic water is found below with comparatively lower SiO_4 and PO_4 levels. The chl *a* concentrations were low, in spite of high nutrient concentrations, with a max. at 0.3 $\mu\text{g/l}$ on the surface and high level of phaeopigments.

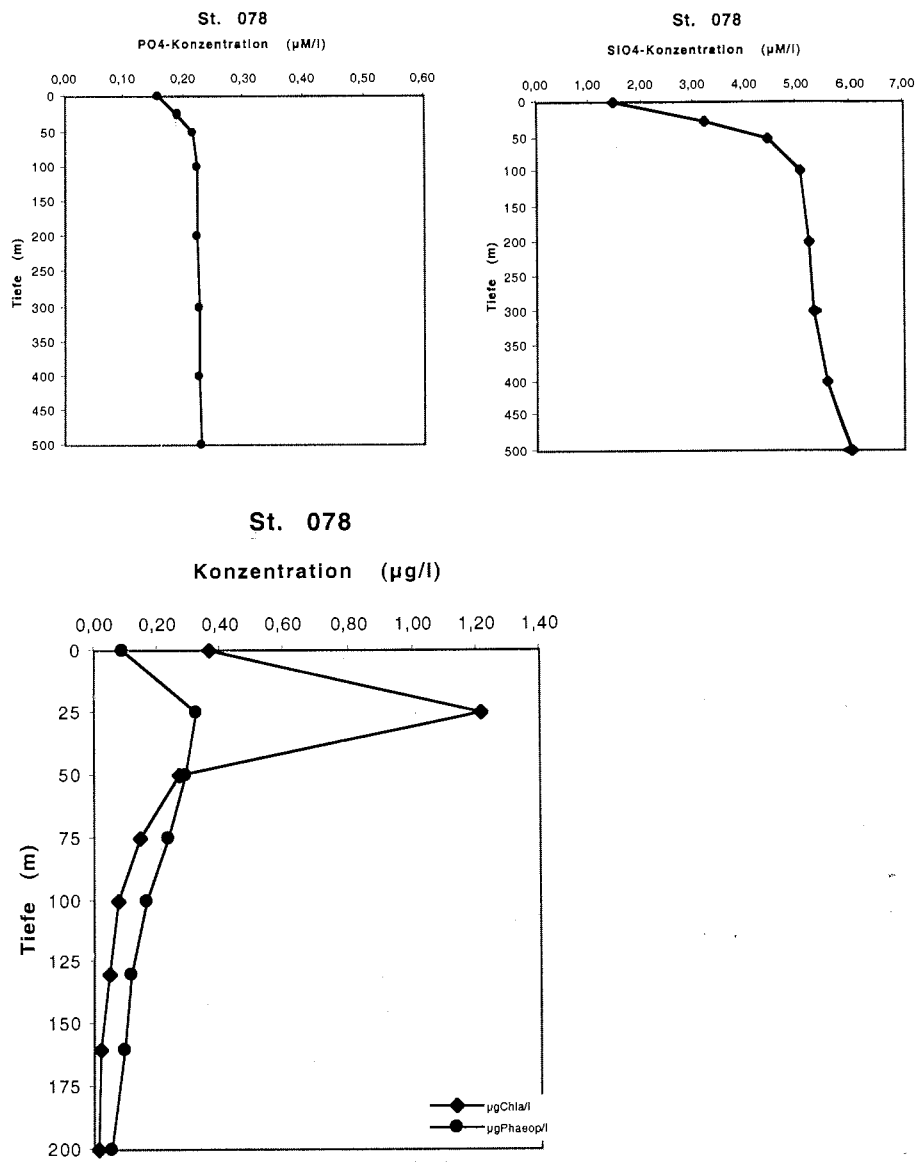


Fig. 39: Typical nutrient and pigment concentrations and depth distribution in the eastern part (st. 078) of transect (ARK-XV/2)

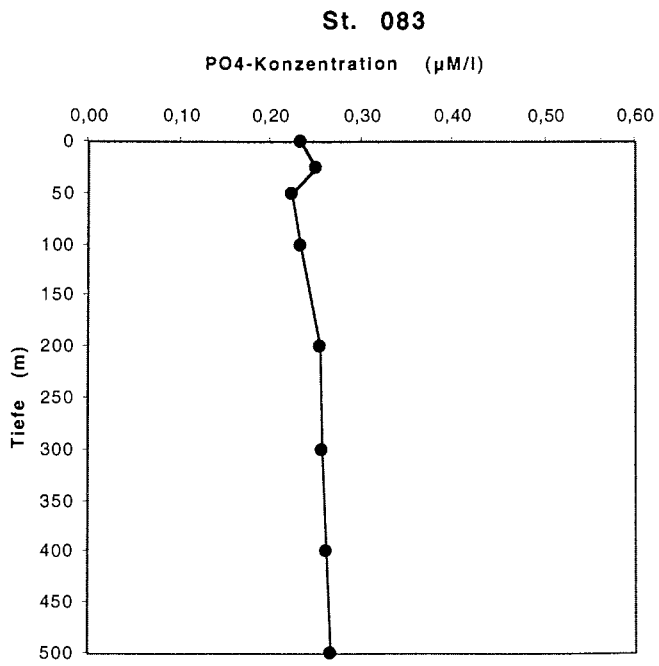
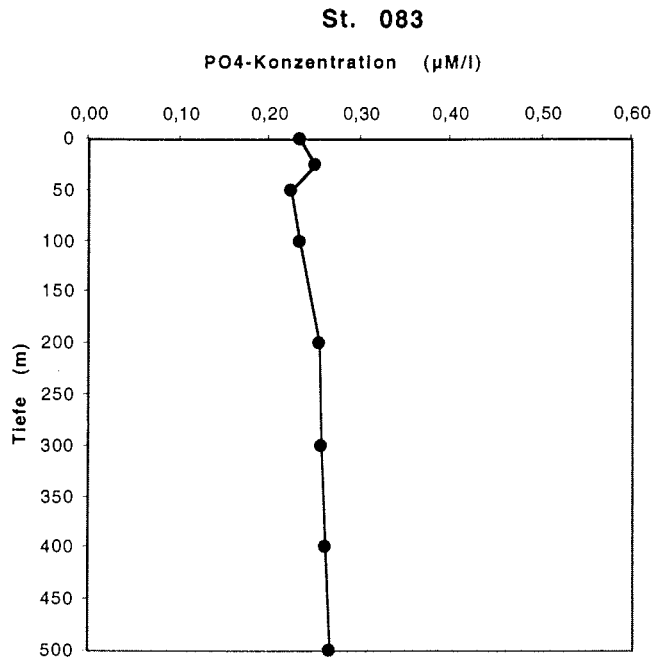


Fig. 40: Typical nutrient and pigment concentrations and depth distribution in the western part (st. 083) of transect (ARK-XV/2)

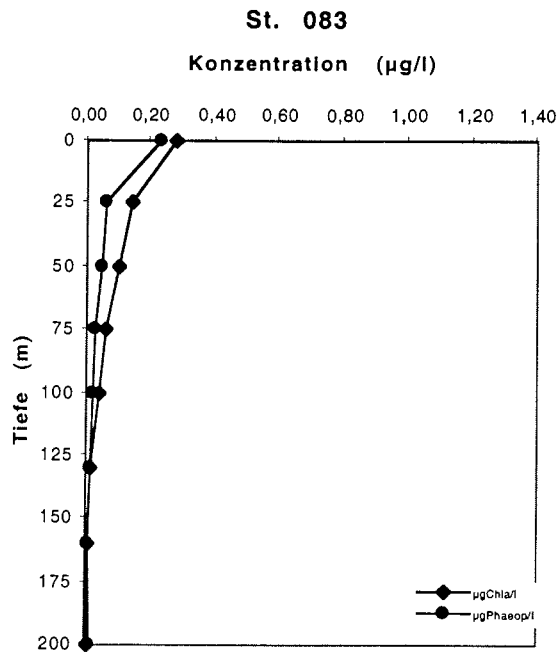


Fig. 40 (continuation)

Foraminiferal assemblage (Abb. 41):

The multinet samples have been processed to determine counts, species composition and depth distribution of planktonic foraminifera. The highest abundances of planktonic foraminifera were observed in the ice-free water in the eastern part of the transect, tending to lower values towards the western part. Two species, *T. quinqueloba* and *N. pachyderma* (s), dominate the foraminiferal assemblage in this region. From east to west a gradual dominance change from *T. quinqueloba* to *N. pachyderma* (s) was observed. While the percentage of the subpolar species *N. pachyderma* (d) and *G. bulloides*, slightly increases towards the west, the other species *G. glutinata*, *G. uvula*, *O. riedeli* and *G. falconensis* decreases, accounting for a total of < 1% throughout the transect. The foraminiferal composition shows no dependence on ice-coverage and is bound to different water masses (surface polar water and atlantic water). For most stations, maximal abundances between 50 and 200 m water depth were observed. The maximal abundances shows no correlation with a chlorophyll *a* concentration. In the eastern part of the transect *N. pachyderma* (s) shows max. abundances at 50 - 200 m water depth, while in the western of the transect *N. pachyderma* (s) shows max. abundances at 0 - 100 m. Most individuals of *N. pachyderma* (s) with secondary calcit crust and kummerform were found in the 100 - 200 m depth interval.

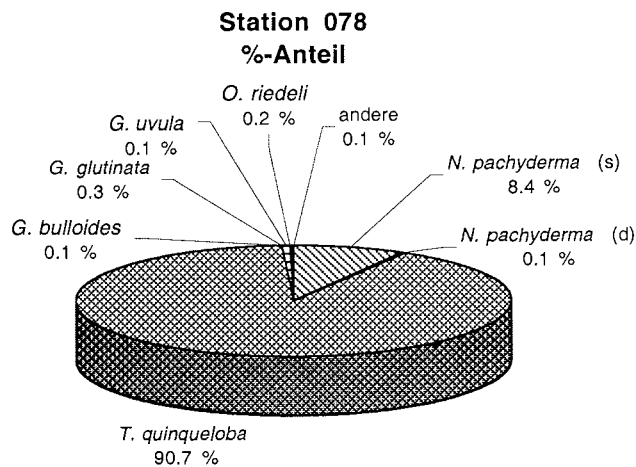


Fig. 41: Percentage and depth distribution of planktonic foraminifera in the eastern part (st. 078) and western part (st. 083) of transect (ARK-XV/2)

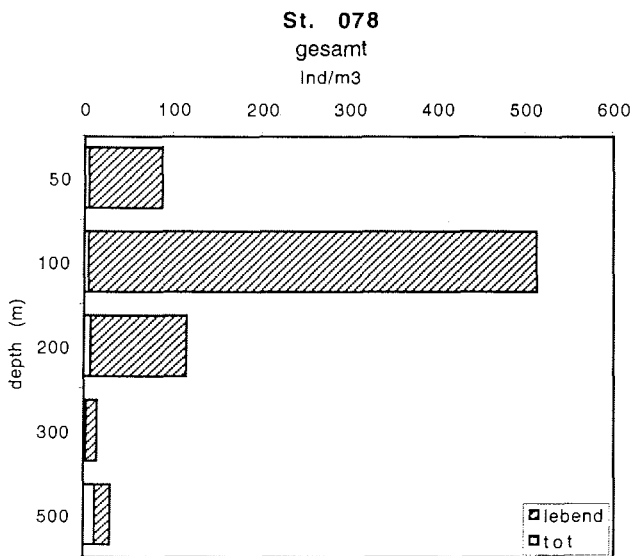
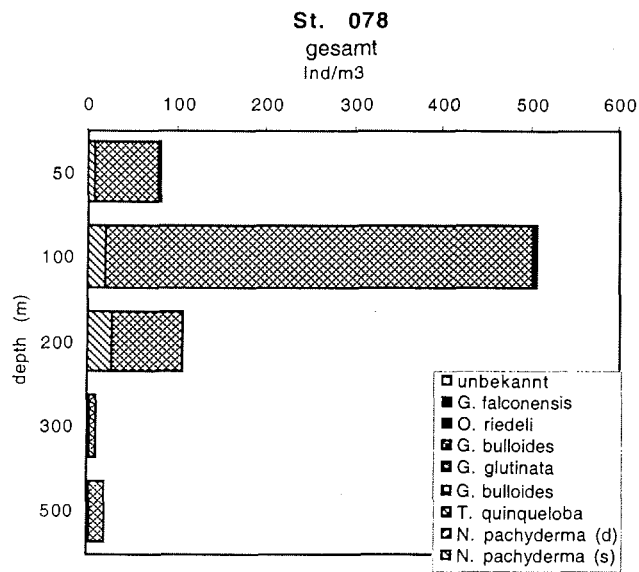


Fig. 41 (continuation)

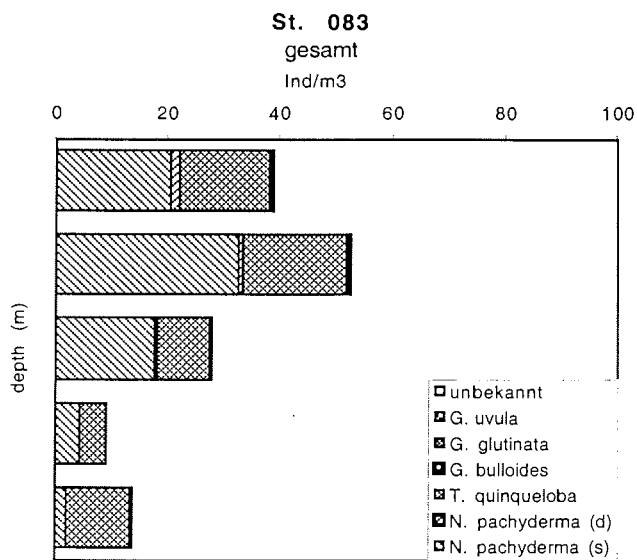
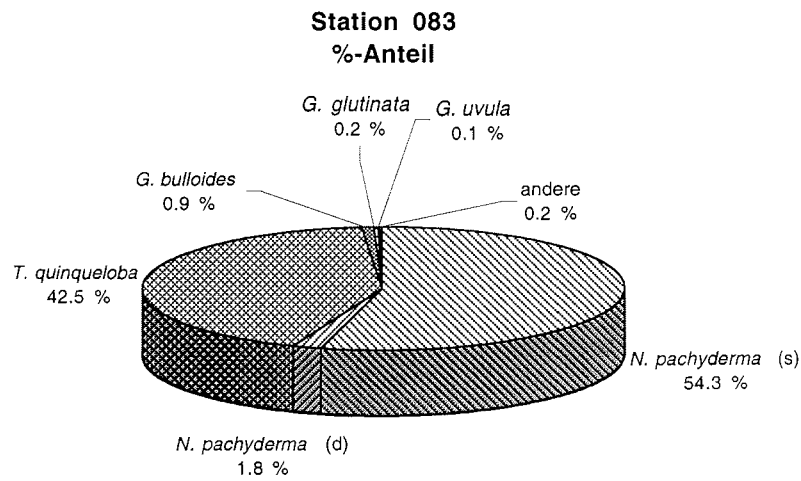


Fig. 41 (continuation)

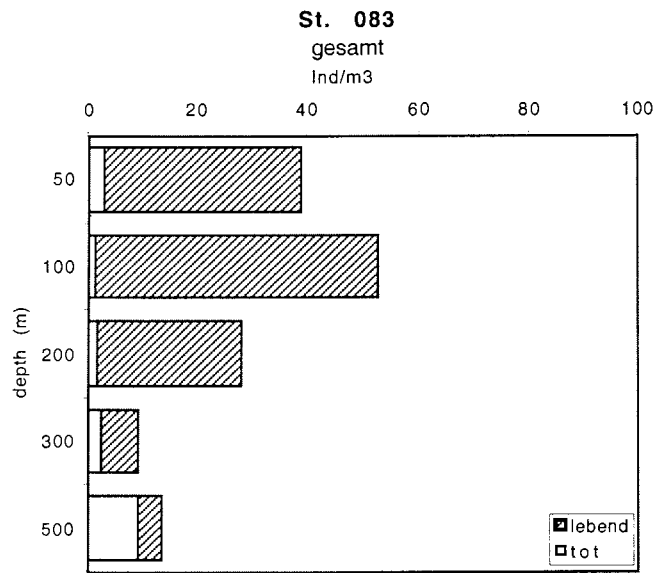


Fig. 41 (continuation)

7 The ice edge and its influence on the smallest benthic biota (I. Schewe, S. Meyer)

"Possibly the most important limiting factor in deep-sea ecology is food availability" (Gage and Tyler, 1991). The extreme limited input of organic matter from primary production to the seafloor of the Arctic Ocean is caused by its perennial ice-coverage and a strongly developed density layer in the upper waters. Thus, the deep Arctic Ocean is probably one of the most oligotrophic marine ecosystems on earth.

The Fram Strait can be understood as a transition zone to the central Arctic Ocean. The benthic environment in this area is influenced by various biotic and abiotic factors on a geographic small scale. Algal blooms on the near ice edge supply the deep sea benthos in the eastern parts of the Fram Strait with comparatively large amounts of particulate organic matter (POM), northward transported by the inflow of warm and nutrient rich Atlantic water. On the other hand, the western parts of the Fram Strait are dominated by an outflow of cold and oligotrophic waters from the central Arctic Ocean, carrying only small amounts of POM. These influences are reflected in different distribution patterns of benthic organisms. Especially the microscopic small organisms (<1000 µm) are able to react rapidly to short-term variations in food availability. Consequently, they are especially suitable for indicating spatial and temporal differences.

A performed east-west transect crossing the Fram Strait around 80°N (transect-A) serves as an extension of benthic transects, already sampled in summer 1997 during the ARK/XIII 2 cruise over the Yermak Plateau and across the Fram Strait (Fig. 42). Its position located nearby the summer ice edge in 1999, shall give information about the influence of algal blooms on the benthic deep sea ecosystem in this area. An additional transect running in south-north direction on the western Yermak Plateau slope along a water depth of about 1000 m (transect-B) was performed to elucidate benthic reactions to a northerly directed lateral input of POM to the seafloor, having its origin at the ice edge.

The quantitative assessment of bacteria, nano- and meiofauna organisms and the analysis of a series of biogenic sediment compounds will allow to obtain substantial information on the ecological status of the benthic environment. Sediment bound chloroplastic pigment equivalents (CPE, chlorophyll a and its degradation products) were determined to quantify the vertical and/or lateral organic matter input from primary production. Differences in activities and biomass within the sediments were assessed by a series of biochemical assays commonly used in ecological investigations of the deep sea benthos. To evaluate bacterial exoenzymatic activities, esterase turnover rates were determined with the fluorogenic substrate fluorescein-di-acetate (FDA). Rather labile macromolecules like adenylates (i.e. ATP, ADP and AMP) as well as phospholipides have been or will be analysed specifically as indicators for total microbial biomass (TMB, i.e. small sediment inhabiting organisms).

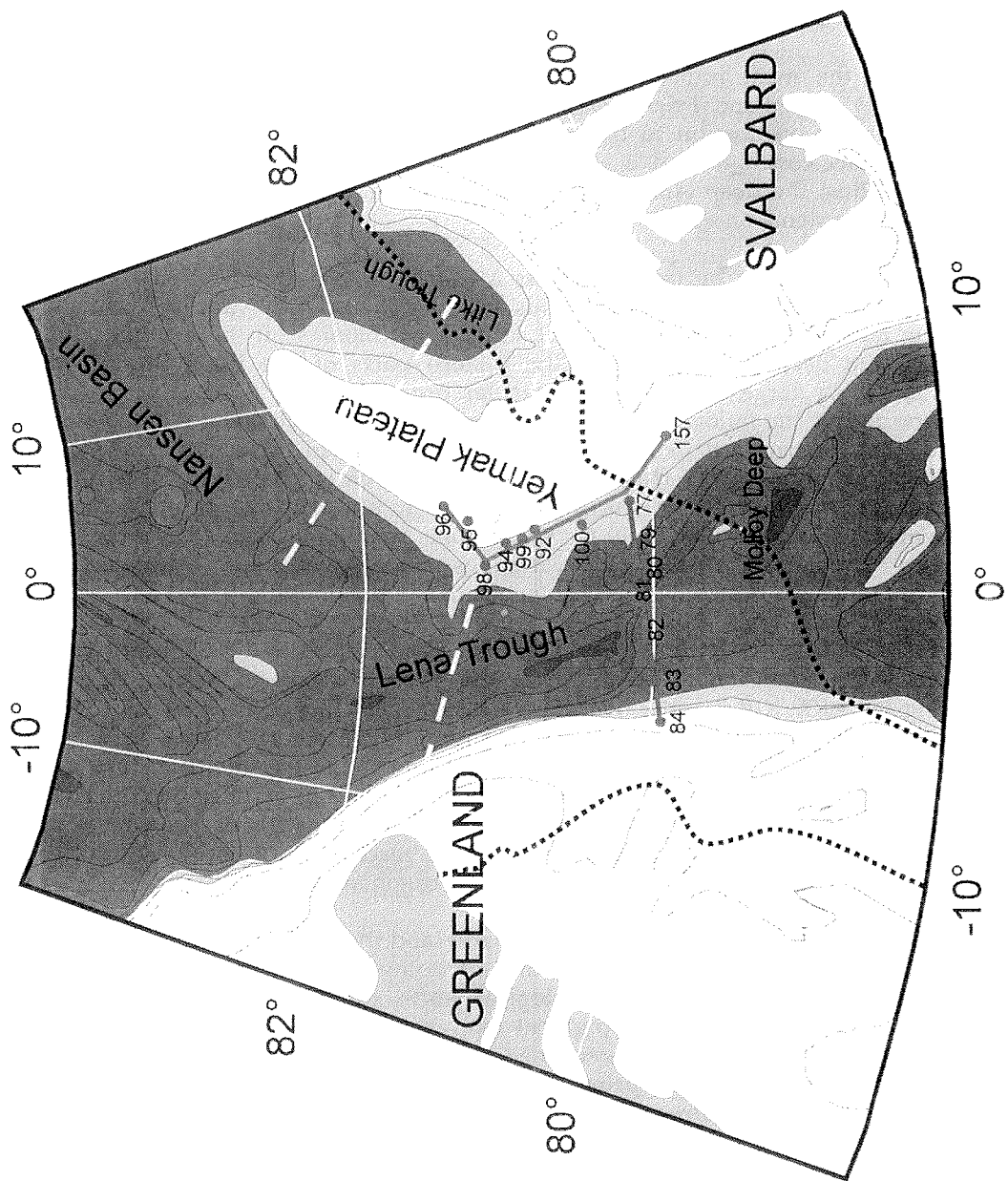


Fig. 42: Location of sampled stations during ARK-XV/2

Sediment samples were obtained by a multicorer (MUC), taking up to 12 sediment cores per haul with an inner diameter of 6 cm. The MUC was equipped with a video camera system to get first visual impressions of the benthic realm and to allow a (semi-)targeted sampling at the seafloor. Immediately after recovery of the MUC, the sediment-overlying water was drained off, to analyse oxygen concentrations in bottom waters (Winkler-Titration). The uppermost five centimetres of the sediment cores were subsampled using plastic syringes with cut off anterior ends. Three (pseudo-)replicate subsamples from different MUC tubes were taken for each parameter investigated. Samples were either processed directly on board or fixated with formalin and glutaraldehyde or stored at -20°C for later analyses at the home laboratory.

Preliminary results, determined onboard, showed some clear trends in the data. Especially chloroplastic pigment data cleared up the transport of plant material to the sea floor (Fig. 43). Crossing the Fram Strait (transect-A) the input of "fresh" phytodetritus, presumably transported within the northward flowing Atlantic waters, was noticeable up to $1^{\circ}30'W$. In spite of their slighter water depth, the concentrations of fresh chlorophyll *a* as well as of phaeopigments were quite lower on the more westerly located stations, than on the deeper eastern stations. This indicates the dominance of the oligotrophic Arctic water, transporting only very small amounts of POM. Pigment concentrations along the northwards directed transect-B (Fig. 44) clearly decrease with increasing distance from the ice edge (increasing latitude). This correlation proves the assumption of long range laterally transported phytodetritus along the Yermak Plateau into the Arctic deep sea. Because of heavy ice conditions unfortunately it was not possible to expand this transect to the north.

Preliminary results of the biomass estimations show interesting tendencies. They do not follow trends, described for the distribution of sediment bound chloroplastic pigments. Biomasses of smallest sediment inhabiting organisms generally follow water depth depending gradients to a great extend. However, on transect-A they do not show the same decline of values on the most western stations, as noticed for pigment values. On transect-B biomass concentrations don't show any significant trend, in spite of decreasing input of fresh phytoplankton. These results may have their origin in the unspecific method for determining organism biomasses. A wide range of different organisms, which may have different metabolism strategies, is covered by the used method.

Anyway, further inspections are imperative and especially direct evaluations of meiofauna, nanofauna and bacteria will help to understand these first results.

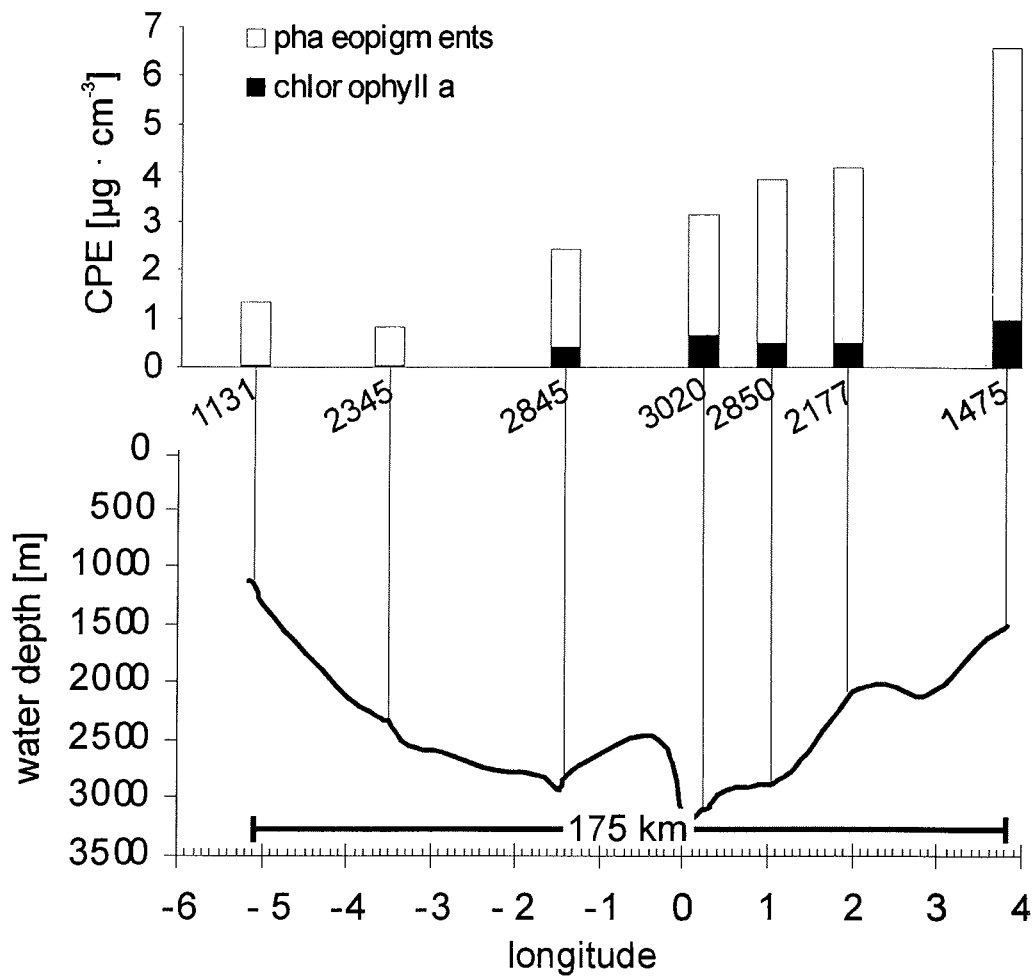


Fig. 43: Sediment bound chloroplastic pigments in the uppermost sediment layer (0 - 1 cm) crossing the Fram Strait (transect A).

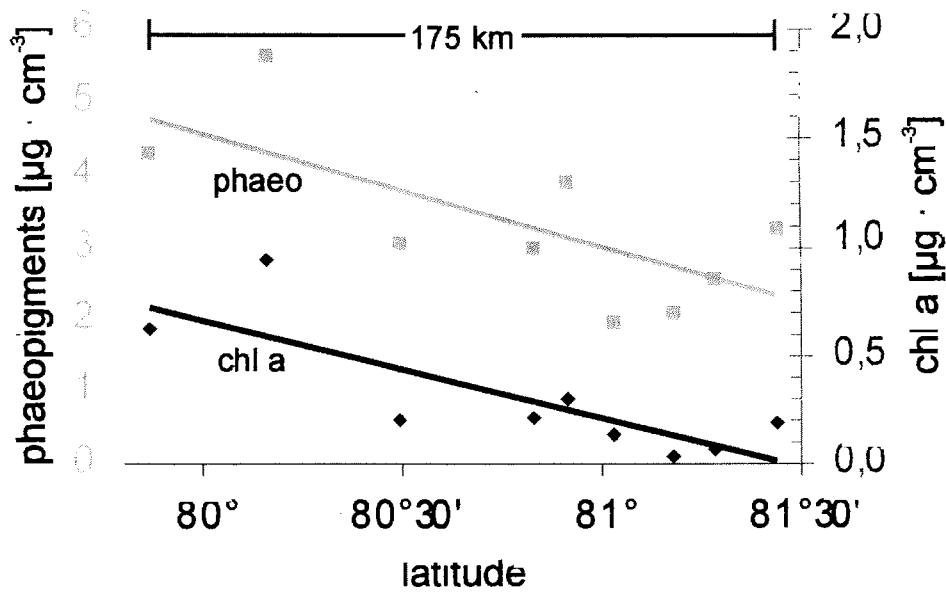


Fig. 44: Sediment bound chloroplastic pigments in the uppermost sediment layer (0 - 1 cm) along the Yermak Plateau 1000 m line (transect B)

8 The GEUS/AWI programs during POLARSTERN cruise ARK-XV/2 (O. B. Olesen)

The aim of the GEUS and GEUS/AWI programs were threefold:

- To visit the New Islands
- To collect data and instruments from 79Fjord-glacier.
- To perform CTD measurements in Dijnphna Sund.

New Islands

The islands, of which the name Tobias Øer has been proposed (Tobias was a Greenlandic dog sledge driver during the Danmark Ekspeditionen 1906 – 1908), were discovered during a helicopter flight by two AWI oceanographers, Budeus and Schneider, who also landed there in 1997 during the POLARSTERN cruise ARK-XIII/3 in this area. Attempts by Danish authorities to reach the islands with helicopter from a base camp at 79Fjord-glacier in 1998 unfortunately failed due to prolonged bad weather. The generous offer by AWI to make participation in the POLARSTERN cruise ARK XV/2 available for the execution of the three programs mentioned above were therefore most welcome.

On July 27. the islands were visited by Ole Olesen, GEUS; Anette Gierlichs, AWI; Uwe Lahrmann and Marc-Oliver Hillebrandt, HSV.

The islands form an arch situated along the western flank of an ice island which rises to 10 – 20 m above the sea ice. There appear to be 6 separate islands but due to recent snow falls and overcast weather it was not possible to assess whether some of them are interconnected. The biggest of the islands, the last but one to the south, is about 100 x 20 m if looked upon as an entity. However, in reality it is a collection of smaller islands the highest point being no more than a meter above the melt water lake surrounding them (Fig. 45 shows the two southernmost islands).

The islands consist of mostly very well rounded crystalline boulders with diameters of 20 – 30 cm (fig. 46) in a sand/silt matrix which is completely water-logged, making the surface highly unstable. This instability was very quickly discovered upon landing on the biggest of the islands, as both helicopter skis and boots of the landing party slowly but surely were sinking into the ground upon the slightest movement.

The preponderance of crystalline, wear resistance and well rounded rocks clearly shows that the material must have been water transported for a considerable distance, but at the time of writing the samples collected have not yet been categorized as to place of origin.

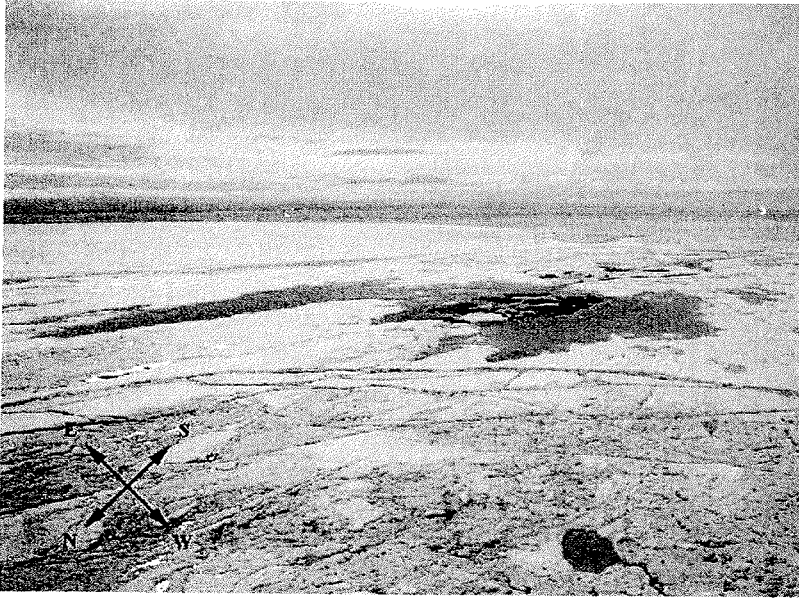


Fig. 45: View of the two southernmost islands surrounded by sea ice. Note ice-island east of islands upper left side of picture (Fot. Anette Gierlichs).



Fig. 46: Surface of island in fig. 45. Well rounded boulders (diameter up to 20 – 30 cm) in a matrix of waterlogged sand/silt. Note ice-island in background (Fot. Anette Gierlichs).

Using the GPS (Bendix King type KN89B) of the helicopter the position of the largest island was measured to: 79° 20,45' N; 15° 50,39' W, which places the islands within the boundaries of the shallowest part of the Westwind Shoal. Judging from their appearance and placing it is reasonable to assume that they have been assembled by sea or glacier ice pushing material from the top of the Westwind Shoal, against the western flank of the ice island which in itself is resting on the shoal.

If the sea ice pressure ridges, which are surrounding both islands and ice island, are taken as the outer perimeter, the size of the area is roughly 2.7 km E-W and 2.2 km N-S as determined by using the helicopter GPS while flying over the area.

Gravity measurements were attempted on the biggest island but due to the instability of the surface the measurements had to be moved to the ice island and was carried out at:

79° 20,04'N; 15° 48,57' approx. 10 m.a.s.l. by A. Gierlichs (Tab. 22)

Data & instrument collection at 79Fjord-glacier

In 1996 GEUS and in 1997 – 1998 both GEUS and AWI conducted glaciological investigations on 79Fjord-glacier. An integral part of the programme was the building of 6 automatic climate stations, dispersed from the terminus of the glacier to a position 115 km inland to the west. In 1998 an echo sounder was added. Situated beneath the floating tongue it looked upwards towards the glacier bottom for the recording of possible bottom melting. This station also measured salinity and temperatures 5 and 15 m under the glacier i.e. about 115 and 125 below sea level.

As the field season in 1998 encountered very bad weather, which caused the loss of 70% of the helicopter flying time needed for the full program, this resulted in the necessity to leave the area without having recovered neither data nor instruments from the stations at the retreat from the area.

The recovery of data and instruments were achieved in two operations using first one and then both of the POLARSTERN helicopters. Of the total of 7 stations 6 were recovered. Of these 4 were still in more or less working conditions (some sensors had stopped functioning). One had toppled and one had lost battery power. The last and westernmost station was not visited because of the distance to the position and the great likelihood that its batteries would be dead, making data recovery impossible unlikely.

All in all it must be concluded that the operation, to recover data and instruments, was far better than expected.

As the main object of the original 79Fjord-glacier project was to assess whether melting from the bottom of the floating tongue is a reality, a preliminary graph of the results (raw data) from the echo sounder experiment is shown (Fig. 47).

The sounder was situated approx. 31 km behind the glacier-front and 4 km from its northern margin, where the ice thickness is in the order of 100 m.

The instrument used was a Datasonics, Inc. PSA-916 Sonar Altimeter with a 200 kHz frequency and a 14° conical beam. The claimed resolution is ± 2.5 cm. The altimeter was placed under the ice via a 12 cm diameter drill-hole and suspended by a kevlar line with a 10 kg iron weight to keep the assembly vertical. Data logger and batteries remained on the glacier surface.

Although the data has not yet been subjected to proper corrections, it is safe to conclude that bottom melting do take place in this part of the glacier and for the three month the altimeter worked, a melting of more than 2 m of ice occurred.

CTD measurements in Dijnphna Sund

The CTD-measurements in Dijnphna Sund unfortunately had to be cancelled due to the prevailing ice conditions and the tight time schedule of the overall program. The CTD-measurements would have served as a supplement to measurements from the sound in 1998.

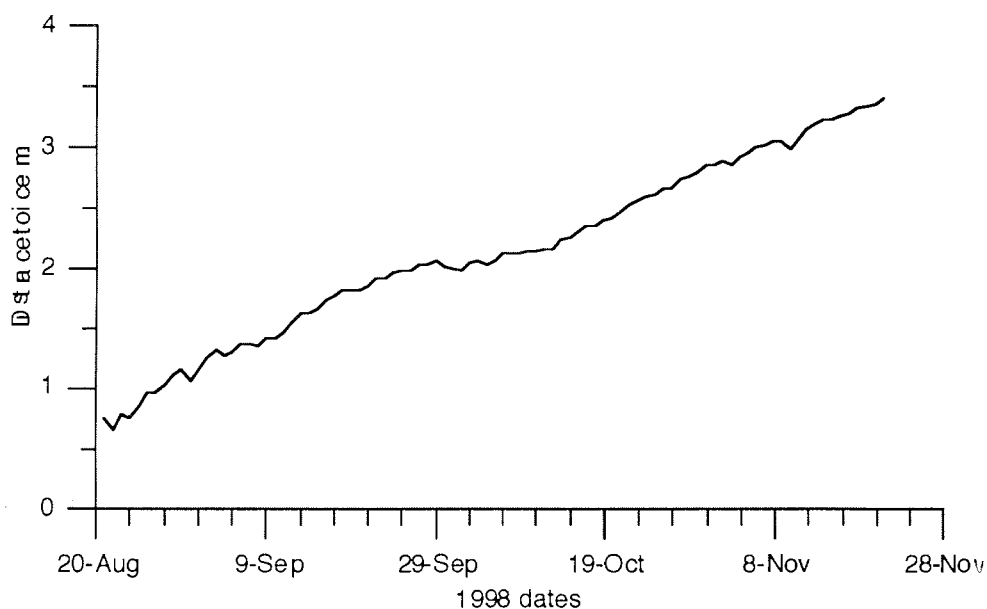


Fig. 47: Graph of echo-soundings (raw data) from beneath 79Fiord-glacier. Sounder directed upwards towards the bottom of the floating glacier tongue.

Datum	Time [h]		Latitude [deg]	Longitude [deg]	Location	SCU	Feed-back	Less Scale Fix	Scale Fix Diff.	Calib. Factor	Calib. Diff.	Cal. Fix Value	Rel. Grav. Value [mgal]
21.07.99	21:37	LT	69.6482 N	18.9612 E	Tromsø, Polizeistat.	6056.950		6000.0	56.950	1.02323	58.27295	6141.60	6199.87295
21.07.99	21:40	LT	69.6482 N	18.9612 E	Tromsø, Polizeistat.	6056.940		6000.0	56.940	1.02323	58.26272	6141.60	6199.86272
21.07.99	21:42	LT	69.6482 N	18.9612 E	Tromsø, Polizeistat.	6056.940		6000.0	56.940	1.02323	58.26272	6141.60	6199.86272
21.07.99	21:45	LT	69.6482 N	18.9612 E	Tromsø, Polizeistat.	6057.080		6000.0	57.080	1.02323	58.40597	6141.60	6200.00597
21.07.99	21:47	LT	69.6482 N	18.9612 E	Tromsø, Polizeistat.	6057.080		6000.0	57.080	1.02323	58.40597	6141.60	6200.00597
21.07.99	21:48	LT	69.6482 N	18.9612 E	Tromsø, Polizeistat.	6057.090		6000.0	57.090	1.02323	58.41620	6141.60	6200.01620
21.07.99	21:52	LT	69.6482 N	18.9612 E	Tromsø, Polizeistat.	6056.990		6000.0	56.990	1.02323	58.31388	6141.60	6199.91388
21.07.99	21:54	LT	69.6482 N	18.9612 E	Tromsø, Polizeistat.	6056.980		6000.0	56.980	1.02323	58.30365	6141.60	6199.90365
21.07.99	21:56	LT	69.6482 N	18.9612 E	Tromsø, Polizeistat.	6056.960		6000.0	56.960	1.02323	58.28318	6141.60	6199.88318
21.07.99	21:58	LT	69.6482 N	18.9612 E	Tromsø, Polizeistat.	6056.960		6000.0	56.960	1.02323	58.28318	6141.60	6199.88318
21.07.99	22:02	LT	69.6482 N	18.9612 E	Tromsø, Polizeistat.	6056.830		6000.0	56.830	1.02323	58.15016	6141.60	6199.75016
21.07.99	22:03	LT	69.6482 N	18.9612 E	Tromsø, Polizeistat.	6056.850		6000.0	56.850	1.02323	58.17063	6141.60	6199.77063
21.07.99	22:25	LT			Tromsø, Hafen	6060.000	0.79	6000.0	60.793	1.02323	62.20522	6141.60	6203.80522
21.07.99	22:27	LT			Tromsø, Hafen	6061.000	-0.148	6000.0	61.000	1.02323	62.41703	6141.60	6204.01703
21.07.99	22:34	LT			Tromsø, Hafen	6060.370		6000.0	60.370	1.02323	61.77240	6141.60	6203.37240
25.07.99	10:51	UTC	79.334 N	15.8095 E	New Islands	6518.500	3.676	6500.0	22.176	1.02199	22.66365	6652.98	6675.64365
25.07.99	10:52	UTC	79.334 N	15.8095 E	New Islands	6517.400	4.676	6500.0	22.076	1.02199	22.56145	6652.98	6675.54145
25.07.99	10:53	UTC	79.334 N	15.8095 E	New Islands	6526.100	-3.97	6500.0	26.100	1.02199	26.67394	6652.98	6679.65394
25.07.99	10:53	UTC	79.334 N	15.8095 E	New Islands	6526.400	-4.293	6500.0	26.400	1.02199	26.98054	6652.98	6679.96054
25.07.99	11:03	UTC	79.334 N	15.8095 E	New Islands	6521.590		6500.0	21.590	1.02199	22.06476	6652.98	6675.04476
25.07.99	11:10	UTC	79.334 N	15.8095 E	New Islands	6521.510		6500.0	21.510	1.02199	21.98300	6652.98	6674.96300

Tab. 22: Onshore gravity measurements during ARK-XV/2

Datum	Time [h]		Latitude [deg]	Longitude [deg]	Location	SCU	Feed-back	Less Scale Fix	Scale Fix Diff.	Calib. Factor	Calib. Diff.	Cal. Fix Value	Rel. Grav. Value [mgal]
10.09.99	12:01	UTC	69.6482 N	18.9612 E	Tromsø, Polizeistat.	6055.951		6000.0	55.951	1.02323	57.25074	6141.60	6198.85074
10.09.99	12:05	UTC	69.6482 N	18.9612 E	Tromsø, Polizeistat.	6056.172		6000.0	56.172	1.02323	57.47688	6141.60	6199.07688
10.09.99	12:07	UTC	69.6482 N	18.9612 E	Tromsø, Polizeistat.	6056.165		6000.0	56.165	1.02323	57.46971	6141.60	6199.06971
10.09.99	12:12	UTC	69.6482 N	18.9612 E	Tromsø, Polizeistat.	6056.066		6000.0	56.066	1.02323	57.36841	6141.60	6198.96841
10.09.99	12:14	UTC	69.6482 N	18.9612 E	Tromsø, Polizeistat.	6056.169		6000.0	56.169	1.02323	57.47381	6141.60	6199.07381
10.09.99	12:17	UTC	69.6482 N	18.9612 E	Tromsø, Polizeistat.	6056.172		6000.0	56.172	1.02323	57.47688	6141.60	6199.07688
10.09.99	13:56	UTC			Tromsø, Bunkerpier	6056.619		6000.0	56.619	1.02323	57.93426	6141.60	6199.53426
10.09.99	13:59	UTC			Tromsø, Bunkerpier	6056.730		6000.0	56.730	1.02323	58.04784	6141.60	6199.64784
10.09.99	14:04	UTC			Tromsø, Bunkerpier	6056.626		6000.0	56.626	1.02323	57.94142	6141.60	6199.54142
10.09.99	14:08	UTC			Tromsø, Bunkerpier	6058.174		6000.0	58.174	1.02323	59.52538	6141.60	6201.12538
10.09.99	14:11	UTC			Tromsø, Bunkerpier	6059.261		6000.0	59.261	1.02323	60.63763	6141.60	6202.23763

RMS gravity values at certain locations:

Datum	Time [h]		dezimal Stunden [h]	Rel. Grav. Value [mgal]	Instrument. Drift [mgal]	Abs. Schwere [mgal]	Location
21.07.99	20:50:00	UTC	0	6199.89427	0.00000	982552.534	Tromsø, Polizeistation
21.07.99	21:29:30	UTC	0.66	6203.73155	0.00043	982556.372	Tromsø, Hafen
25.07.99	11:00:30	UTC	86.18	6676.80122	0.06219	983029.503	New Islands
10.09.99	12:09:00	UTC	1212.32	6199.01940	0.87487	982552.534	Tromsø, Polizeistation
10.09.99	14:03:30	UTC	1214.28	6200.41731	0.87628	982553.933	Tromsø, Bunkerpier

References

- Bianchi, G., and I.N. McCave, Holocene periodicity in North Atlantic climate and deep-ocean flow south of Iceland, *Nature*, 397, 515-517, 1999.
- Bond, G., W. Showers, M. Cheseby, R. Lotti, P. Almasi, P. deMenocal, P. Priore, H. Cullen, I. Hajdas, and G. Bonani, A pervasive millennial-scale cycle in North Atlantic Holocene and glacial climates, *Science*, 278, 1257-1266, 1997.
- Frederichs, T. (1995): Regionale und altersabhängige Variation gesteinsmagnetischer Parameter in marinen Sedimenten der Arktis, *Rep. Polar Res.*, 164, 212p.
- Hass, H.C., R.F. Spielhagen, N. Nørgaard-Pedersen, and H. Juhre, A decadal to centennial-scale record of Holocene climate fluctuations from the Yermak Plateau, Arctic Ocean, EOS, AGU Fall Meeting 1999 abstract volume, in press.
- Nam, S.-I. (1997): Late Quaternary glacial history and paleoceanographic reconstructions along the East Greenland continental margin: Evidence from high-resolution records of stable isotopes and ice-rafted debris, *Rep. Polar Res.*, 241, 157 p.
- Niessen, F., Kleiber, H.P. & Nehrke, G. (1997), Physical properties and core logging. In: Stein, R. & Fahl, K. (eds): Scientific Cruise Report of the Arctic Expedition ARK-XIII/2 of RV "POLARSTERN" in 1997. *Rep. Polar Res.*, 255, 115-120.
- Nowaczyk, N. (1991): Hochauflösende Magnetostratigraphie spätquartärer Sedimente arktischer Meeresgebiete, *Rep. Polar Res.*, 78, 187p.
- Nowaczyk, N.R., Frederichs, T.W., Eisenhauer, A. & Gard, G. (1994): Magnetostratigraphic data from late Quaternary sediments from the Yermak Plateau, Arctic Ocean: evidence for four geomagnetic polarity events within the last 170 Ka of the Brunhes Chron, *Geophys. J. Int.*, 117, 453-471.
- Schubert, C.J., Knies, J., Levitan, M., Musatov, E. & Stein, R. (1997): Lithostratigraphy and sediment characteristics. In: Stein, R. & Fahl, K. (eds): Scientific Cruise Report of the Arctic Expedition ARK-XIII/2 of RV "POLARSTERN" in 1997. *Rep. Polar Res.*, 255, 121-135.
- Spiess, V., Digitale Sedimentechographie- Neue Wege zu einer hochauflösenden Akustostratigraphie, *Berichte aus dem Fachbereich Geowissenschaften der Universität Bremen*, 35, 1-199, 1992.
- Stein, R., and K. Fahl, Scientific cruise report of the Arctic Expedition ARK XIII/2 of RV/ "POLARSTERN" in 1997, *Berichte zur Polarforschung/Reports on Polar Research*, 1-235, 1997.
- Thomson, R. & Oldfield, F. (1986): *Environmental magnetism*. 227 p., London: Allen & Unwin.
- Weber, M.E., Niessen, F., Kuhn, G. & Wiedicke, M. (1997): Calibration and application of marine sedimentary physical properties using a multi-sensor core logger, *Marine Geology*, 136, 151-172.

Appendix 1

- Geophysical tables for
magnetic surveys -

Date	Flight No.	Binary File	Fiducial		Time		Position				ASCII File	
			Start	End	Start	End	Start	End	Start	End		
04.08.1999	1	S9080410.B47	1	451	10:47:44	10:55:15	04.69 W	81.43 N			99080401.dat	
		S9080410.B55	452	455	10:55:15	10:55:20						...
		S9080410.B5F	456	456	10:55:20	10:55:22						...
		S9080410.B5W	457	471	10:55:22	10:55:38						...
		S9080410.B5h	472	474	10:55:38	10:55:42						...
		S9080410.B5y	475	505	10:55:42	10:56:14						...
		S9080410.B56	506	598	10:56:14	10:57:48						...
		S9080410.B57	599	599	10:57:48	10:57:50						...
		S9080410.B5j	600	605	10:57:51	10:57:57						...
		S9080410.B5	606	606	10:57:57	10:57:59						...
	S9080410.B58	607	607	10:57:59	10:58:01			...				
	S9080410.B5Z	608	608	10:58:01	10:58:03			...				
	S9080410.B5k	609	609	10:58:03	10:58:05			...				
	S9080411.B00	610	1033	10:58:05	11:05:05			05.02 W	81.48 N	...		
	S9080411.B20	1	1607	11:20:17	11:47:04	02.99 W	81.47 N	00.46 E	81.28 N	99080402.dat		
	S9080411.B51	1608	2962	11:51:37	12:14:12	00.01 W	81.27 N	02.99 W	81.28 N	99080403.dat		
	2	S9080413.B08	1	1882	13:08:44	13:40:06	03.53 W	81.36 N	06.09 W	81.26 N	99080404.dat	
		S9080413.B44	1883	4575	13:44:30	14:29:22	06.09 W	81.17 N	00.02 E	81.05 N	99080405.dat	
		S9080414.B29	4576	7754	14:29:28	15:22:27	00.03 E	81.05 N	04.10 W	81.30 N	99080406.dat	
	3	S9080416.B16	1	1891	16:16:58	16:48:29	03.32 W	81.39 N	06.06 W	81.49 N	99080407.dat	
S9080416.B48		1892	4475	16:48:29	17:31:34	06.07 W	81.49 N	00.07 E	81.61 N	99080408.dat		
S9080417.B31		4476	6829	17:31:34	18:10:49	00.07 E	81.61 N	03.12 W	81.35 N	99080409.dat		
06.08.1999	4	S9080609.B54	1	2603	09:54:33	10:37:56	00.14 W	81.01 N	06.14 E	80.95 N	99080601.dat	
		S9080610.B39	1	49	10:39:57	10:40:46	06.32 E	80.93 N	06.35 E	80.91 N	99080602.dat	
		S9080610.B45	1	1351	10:45:00	11:07:32	06.14 E	80.90 N	03.31 E	80.90 N	99080603.dat	
		S9080611.B09	1	1420	11:09:04	11:32:44	03.11 E	80.91 N	00.03 W	80.93 N	99080604.dat	
	S9080611.B32	1421	3265	11:32:44	12:03:30	00.04 W	80.93 N	00.68 E	80.87 N	99080605.dat		
	S9080613.B14	1	119	13:14:15	13:16:14	01.47 E	80.81 N	01.69 E	80.81 N	99080606.dat		
09.08.1999	6	S9080913.B38	1	38	13:38:44	13:39:23	02.22 E	81.30 N			99080901.dat	
		S9080913.B39	39	40	13:39:23	13:39:26					...	
		S9080913.B3J	41	41	13:39:26	13:39:28					...	

Date	Flight No.	Binary File	Fiducial		Time		Position				ASCII File
			Start	End	Start	End	Start		End		
	7	S9080913.B40	42	3770	13:40:33	14:42:42			00.06 W	81.61 N	...
		S9080914.B42	3771	6723	14:42:42	15:31:56	00.06 W	81.61 N	06.08 E	81.48 N	99080902.dat
		S9080915.B31	6724	9748	15:31:56	16:22:22	06.08 E	81.48 N	01.89 E	81.29 N	99080903.dat
		S9080917.B10	1	782	17:10:18	17:23:21	01.75 E	81.25 N	00.09 W	81.38 N	99080904.dat
		S9080917.B24	1	2072	17:24:00	17:58:32	00.29 W	81.38 N	05.39 W	81.39 N	99080905.dat
		S9080918.B08	1	333	18:08:12	18:13:45	05.90 W	81.38 N			99080906.dat
		S9080918.B13	334	334	18:13:45	18:13:47			05.24 W	81.39 N	...
	S9080918.B1D	335	1455	18:13:47	18:32:29	05.23 W	81.39 N			99080907.dat	
	S9080918.B32	1456	1462	18:32:29	18:32:37					...	
	S9080918.B3C	1463	1463	18:32:37	18:32:39					...	
	S9080918.B3T	1464	1467	18:32:39	18:32:44					...	
	S9080918.B3e	1468	1470	18:32:44	18:32:48			06.12 W	81.16 N	...	
	S9080918.B3v	1471	4807	18:32:48	19:28:26	06.12 W	81.16 N	00.03 W	81.27 N	99080908.dat	
	S9080919.B29	1	719	19:29:08	19:41:08	00.07 E	81.27 N	01.37 E	81.25 N	99080909.dat	
	8	S9080920.B09	1	2244	20:09:38	20:47:02	01.28 E	81.21 N	06.06 E	81.27 N	99080910.dat
S9080920.B47	2245	5070	20:47:02	21:34:09	06.07 E	81.27 N	01.21 E	81.18 N	99080911.dat		
10.08.1999	9	S9081010.B14	1	1843	10:14:58	10:45:41	05.88 E	81.82 N	00.02 E	81.83 N	99081001.dat
		S9081010.B46	1	1831	10:46:47	11:17:18	00.21 W	81.83 N	06.03 W	81.83 N	99081002.dat
		S9081011.B17	1832	4336	11:17:18	11:59:04	06.03 W	81.83 N	00.02 W	81.72 N	99081003.dat
		S9081011.B59	1	2454	11:59:55	12:40:49	00.13 E	81.72 N	05.96 E	81.72 N	99081004.dat
	10	S9081015.B14	1	3350	15:14:14	16:10:05	02.24 E	80.74 N	06.02 W	80.93 N	99081005.dat
		S9081016.B10	3351	7139	16:10:05	17:13:15	06.06 W	80.93 N	02.32 E	80.60 N	99081006.dat
13.08.1999	11	S9081309.B47	1	3129	09:47:31	10:39:40	15.61 E	81.70 N	13.78 E	83.03 N	99081301.dat
		S9081310.B39	3130	10100	10:39:40	12:35:52	13.78 E	83.04 N	18.20 E	81.93 N	99081302.dat
	12	S9081313.B03	1	2591	13:03:11	13:46:22	18.34 E	81.93 N	18.21 E	83.08 N	99081303.dat
		S9081313.B46	2592	7642	13:46:22	15:10:34	18.21 E	83.08 N	19.17 E	81.55 N	99081304.dat
		S9081315.B10	7643	8870	15:10:34	15:31:03	19.17 E	81.55 N			99081305.dat
		S9081315.B31	8871	8871	15:31:03	15:31:05			19.03 E	81.96 N	...
		S9081315.B3B	8872	9042	15:31:05	15:33:57	19.04 E	81.96 N			99081306.dat
		S9081315.B33	9043	9059	15:33:58	15:34:15			19.42 E	81.94 N	...
	13	S9081316.B25	1	2328	16:25:43	17:04:31	19.51 E	81.93 N	19.33 E	83.08 N	99081307.dat

Date	Flight No.	Binary File	Fiducial		Time		Position				ASCII File	
			Start	End	Start	End	Start		End			
		S9081317.B04	2329	6825	17:04:31	18:19:29	19.32 E	83.08 N	20.08 E	81.54 N	99081308.dat	
		S9081318.B19	6826	9007	18:19:29	18:55:52	20.08 E	81.54 N	19.95 E	81.71 N	99081309.dat	
14.08.1999	14	S9081409.B00	1	1849	09:00:56	09:31:45	19.63 E	80.89 N			99081401.dat	
		S9081409.B31	1850	1851	09:31:45	09:31:47					...	
		S9081409.B3B	1852	1852	09:31:47	09:31:50			20.07 E	81.58 N	...	
		S9081409.B3S	1853	2280	09:31:50	09:38:57	20.06 E	81.58 N	19.64 E	81.49 N	99081402.dat	
		S9081409.B51	1	513	09:51:47	10:00:20	19.53 E	81.25 N	19.66 E	81.10 N	99081403.dat	
		S9081410.B00	514	1699	10:00:20	10:20:07	19.66 E	81.10 N			99081404.dat	
		S9081410.B20	1700	2355	10:20:07	10:31:02			18.76 E	81.38 N	...	
		S9081410.B33	1	758	10:33:45	10:46:24	18.73 E	81.39 N	18.78 E	81.09 N	99081405.dat	
		S9081410.B46	759	1895	10:46:24	11:05:22	18.78 E	81.09 N	18.24 E	81.56 N	99081406.dat	
		S9081411.B05	1896	3601	11:05:22	11:33:47	18.23 E	81.56 N	18.49 E	81.06 N	99081407.dat	
	15	S9081412.B20	1	1822	12:20:04	12:50:27	18.38 E	81.19 N	17.20 E	81.93 N	99081408.dat	
		S9081412.B50	1823	2106	12:50:27	12:55:12	17.19 E	81.93 N	16.51 E	81.94 N	99081409.dat	
		S9081412.B55	2107	4969	12:55:12	13:42:56	16.52 E	81.94 N	16.84 E	83.10 N	99081410.dat	
		S9081413.B42	4970	10000	13:42:56	15:06:48	16.83 E	83.10 N	17.16 E	81.39 N	99081411.dat	
		S9081415.B27	1	3771	15:27:50	16:30:41	17.67 E	81.43 N	17.65 E	83.08 N	99081412.dat	
		S9081416.B30	3772	3775	16:30:41	16:30:46	17.64 E	83.08 N	17.64 E	83.08 N	99081413.dat	
	16	S9081416.B3A	3776	3809	16:30:46	16:31:21	17.64 E	83.08 N	17.52 E	83.09 N	99081414.dat	
		S9081416.B31	3810	8439	16:31:21	17:48:31	17.51 E	83.09 N	16.24 E	81.55 N	99081415.dat	
		15.08.1999	17	S9081509.B28	1	192	09:28:30	09:31:42	11.69 E	81.35 N		99081501.dat
		S9081509.B31		193	193	09:31:42	09:31:44					...
S9081509.B3B		194		195	09:31:44	09:31:47					...	
S9081509.B3S		196		196	09:31:47	09:31:49					...	
S9081509.B3d		197		385	09:31:49	09:34:59			11.63 E	81.36 N	...	
S9081509.B40		1		48	09:40:53	09:41:42	11.61 E	81.33 N			99081502.dat	
S9081509.B42	49	3781		09:42:27	10:44:40			11.77 E	83.03 N	...		
S9081510.B44	3782	9757		10:44:40	12:24:17	11.78 E	83.03 N	12.12 E	81.15 N	99081503.dat		
S9081513.B00	1	2306		13:00:28	13:38:54	12.16 E	81.06 N	13.66 E	81.03 N	99081504.dat		
S9081513.B38	2307	3473		13:38:54	13:58:21	13.66 E	81.03 N	13.72 E	81.51 N	99081505.dat		
S9081513.B58	3474	5331	13:58:21	14:29:21	13.73 E	81.51 N	13.80 E	81.00 N	99081506.dat			

Date	Flight No.	Binary File	Fiducial		Time		Position				ASCII File
			Start	End	Start	End	Start		End		
		S9081514.B29	5332	5501	14:29:21	14:32:12	13.79 E	81.00 N			99081507.dat
		S9081514.B32	5502	5511	14:32:12	14:32:23					...
		S9081514.B3C	5512	5521	14:32:23	14:32:34					...
		S9081514.B3T	5522	5526	14:32:34	14:32:40					...
		S9081514.B3e	5527	5634	14:32:40	14:34:29					...
		S9081514.B34	5635	5890	14:34:29	14:38:44			12.84 E	80.97 N	...
17.08.1999	19	S9081709.B09	1	360	09:09:00	09:15:00	16.29 E	81.49 N	15.21 E	81.50 N	99081701.dat
		S9081709.B20	1	3300	09:20:23	10:15:23	14.36 E	81.51 N	12.74 E	83.03 N	99081702.dat
		S9081710.B15	3301	4740	10:15:23	10:39:22	12.74 E	83.03 N	13.72 E	82.56 N	99081703.dat
		S9081710.B42	1	2958	10:42:57	11:32:15	13.66 E	82.55 N	14.67 E	81.49 N	99081704.dat
		S9081711.B32	2959	2959	11:32:15	11:32:17	14.67 E	81.49 N	14.67 E	81.49 N	99081705.dat
		S9081711.B3C	2960	4309	11:32:17	11:54:48	14.67 E	81.49 N	15.86 E	81.07 N	99081706.dat
		S9081711.B54	4310	5450	11:54:48	12:13:50	15.86 E	81.07 N	17.24 E	81.49 N	99081707.dat
	20	S9081712.B56	1	5039	12:56:31	14:20:30	18.14 E	81.63 N			99081708.dat
		S9081714.B20	5040	5041	14:20:30	14:20:33					...
		S9081714.B2A	5042	5042	14:20:33	14:20:35			14.90 E	83.06 N	...
		S9081714.B2R	5043	12000	14:20:35	16:16:34	14.91 E	83.07 N	19.25 E	81.74 N	99081709.dat
18.08.1999	21	S9081809.B12	1	5472	09:12:49	10:44:01	25.89 E	81.17 N	27.22 E	83.06 N	99081801.dat
		S9081810.B44	5473	9733	10:44:01	11:55:03	27.22 E	83.06 N	26.19 E	81.06 N	99081802.dat
		S9081811.B55	9734	9770	11:55:03	11:55:41	26.18 E	81.06 N	26.13 E	81.05 N	99081803.dat
21.08.1999	22	S9082116.B29	1	455	16:29:03	16:36:39	01.72 E	79.12 N	02.22 E	79.21 N	99082101.dat
		S9082116.B39	1	1267	16:39:36	17:00:43	02.06 E	79.19 N	04.16 E	79.42 N	99082102.dat
		S9082117.B00	1268	1315	17:00:43	17:01:32	04.17 E	79.42 N	04.19 E	79.44 N	99082103.dat
		S9082117.B01	1316	1325	17:01:32	17:01:43	04.19 E	79.44 N	04.18 E	79.44 N	99082104.dat
		S9082117.B0B	1326	1326	17:01:43	17:01:45	04.18 E	79.44 N	04.18 E	79.44 N	99082105.dat
		S9082117.B0S	1327	1327	17:01:45	17:01:47	04.18 E	79.44 N	04.18 E	79.44 N	99082106.dat
		S9082117.B0d	1328	2845	17:01:47	17:27:06	04.18 E	79.44 N	01.89 E	79.27 N	99082107.dat
		S9082117.B27	2846	2847	17:27:06	17:27:09	01.89 E	79.27 N	01.89 E	79.27 N	99082108.dat
		S9082117.B2H	2848	4222	17:27:09	17:50:05	01.90 E	79.27 N	03.23 E	79.21 N	99082109.dat
		S9082117.B50	4223	5304	17:50:05	18:08:08	03.24 E	79.21 N	01.84 E	78.96 N	99082110.dat
		S9082118.B08	5305	7193	18:08:08	18:39:38	01.84 E	78.95 N	01.90 E	78.98 N	99082111.dat

Appendix 2

- Core descriptions -

Geological tables and core descriptions

Legend:

Lithology

-  sand
-  sandy silt
-  sandy clay
-  sandy mud
-  silt
-  mud
-  clay
-  diamicton

-  foraminiferal ooze
-  nannofossil ooze
-  diatomaceous ooze
-  radiolarian ooze
-  volcanic ash
-  chert / porcellanite
-  pebbles, dropstones
-  sediment clasts

Structure

-  bioturbation
-  stratification
-  lamination
-  coarsening upward sequence
-  fining upwards sequence
-  sharp boundary
-  gradational boundary
-  transition zone

PS55/077-4 (GKG)

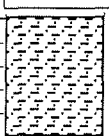
Fram Strait

ARK-XV/2

Recovery: 0.48 m

80°09.40 N 03°51.81 E

Water depth: 1512 m

Lithology	Texture	Color	Description	Age
Surface : Ophiuræ (-7), worm tubes, silty clay				
		5Y 5/2 10YR4/2	5-6 cm: dark yellowish brown, silty clay.	
		5Y 5/2	0-48 cm: light olive gray, silty clay .	

PS55/077-5 (SL)

Fram Strait

ARK XV/2

Recovery: 7.55 m

80°09.0'N, 03°49.0'E

Water depth: 1475 m

	Lithology	Texture Color	Description	Age
0		10YR4/2	0-54 cm: dark grayish brown, silty clay, homogenous, sharp boundary.	
			64 cm: dropstone.	
			54-170 cm: olive gray, silty clay, homogenous; weakly visible black laminae, c. 0.5-1cm thick, every 3-5cm; (single black/grayish zones).	
1		5Y 3/2	from 170 cm: black mottles, black laminae seem to disappear.	
			170-182 cm: olive gray, silty clay, homogenous, slightly lighter.	
		5Y 3/2	182-255 cm: olive gray, silty clay, homogenous; black mottles.	
2		5Y 3/2	255-294 cm: olive gray, silty clay, homogenous; weak black laminae intercalated about 2-3 cm thick, every 1 cm.	
		5Y 3/2	294-316 cm: olive gray, silty clay, homogenous; weak black laminae intercalated (about 2-3 cm thick, c. every 1 cm); black mottles.	
		5Y 3/2	316-347cm: light olive gray, fining upward sequence (turbidite?); sandy-silty clay at the bottom.	
3		5Y 3/2	347-352 cm: yellowish colors, consolidated silty clay, spots, coarser particles ("cottage cheese" structure).	
		5Y 5/2	352-366 cm: olive gray, silty clay, homogenous; weak lamination intercalated (about 2-3 cm thick, every ca. 1 cm).	
		2.5Y 4/2		
		5Y 3/2		
		5Y 5/2	366-380 cm: light olive gray, sandy silt; one or more turbidites (fining upwards).	
4		10Y 4/2	380-397 cm: grayish olive, silty clay.	
		5Y 3/2	383, 387, 389 cm: yellowish "laminae".	
			396-397 cm: darker laminae.	
			397-430 cm: olive gray, silty clay, homogenous	
			430-653 cm: olive gray, silty clay, homogenous; black mottles.	
		5Y 3/2	from 525 and below: occasionally occuring black and reddish layers.	
5				

PS55/077-5 (SL)

Fram Strait

ARK XV/2

Recovery: 7.55 m

80°09.0'N, 03°49.0'E

Water depth: 1475 m

Lithology	Texture	Color	Description	Age	
			430-653 cm: olive gray, silty clay, homogenous; 430-550 cm: black mottles. from 525 and below: occasionally occuring black and reddish layers. 525-527 cm: reddish dark layer. 535, 543, 548 cm: darker irregular layers.		
		5Y 3/2			
		5Y 3/2		595 cm: silty-sandy laver (c. 1 cm). 596-602 cm: olive gray, clayey silt, slightly lighter color. 602-607 cm: olive gray; coarsening upward section. 610-612 cm: bended black layer.	
		5Y 3/2		638 cm: dropstone 643-647 cm: darker (blackish zone). 653-667 cm: olive gray, silty clay, homogenous, black mottles. 667 cm: black and lighter colors, sandy layer (c. 1 cm thick).	
		5Y 3/2		668-693 cm: olive gray, clayey zone, homogenous. 682 cm: black concretion 693-705 cm: olive gray, silty clay, homogenous, bigger black spots.	
		5Y 3/2	705-755 cm: olive gray, silty clay, homogenous, small black spots (mottles).		

PS55/092-4 (GKG)

Fram Strait

ARK-XV/2

Recovery: 0.50 m

80°49.62 N 02°49.98 W

Water depth: 1037 m

Lithology	Texture	Color	Description	Age
Surface : dark yellowish brown silty clay with ophiuarae, worm tubes, holes and foraminifera				
		10YR4/2	0-3 cm: dark yellowish brown silty clay , oxidation layer.	
		5Y 4/1	3-50 cm: olive gray, homogenous silty clay.	

PS55/093-2 (GKG)

Fram Strait

ARK-XV/2

Recovery: 0.48 m

80°56.91 N 02°26.85 E

Water depth: 1089 m

Lithology	Texture	Color	Description	Age
Surface : Ophiuræ, worm tubes, silty clay				
0		10YR4/2	0-7 cm: dark yellowish brown, silty clay.	
		5Y 4/1	7-48cm: olive gray, silty clay.	
1				

PS55/095-2 (GKG)

Fram Strait

ARK-XV/2

Recovery: 0.50 m

81°16.75 N 03°22.98 E

Water depth: 769 m

Lithology	Texture	Color	Description	Age
Surface : light olive gray silty clay, homogenous with some foraminifera, one platy dropstone 5 cm.				
0		10YR 4/2	0-8 cm: dark yellowish brown, silty clay.	
		10YR 3/2	8-14 cm: dark/dusky yellowish brown, silty clay.	
		5B 6/1	14-25 cm: light/medium blueish gray, silty clay.	
		10YR 4/2	25-31 cm: dark yellowish brown, silty clay.	
		5Y 5/1	31-38 cm: light olive/olive gray, silty clay.	
		5YR 4/4	38-39 cm: moderate brown, concretionary crust.	
		N5	39-42 cm: medium gray, silty clay.	
		5YR 4/4	42-45 cm: lamination of moderate brown and medium gray silty clay.	
		N5	45-50 cm: medium gray, silty clay.	
		1		

PS55/096-3 (GKG)

Fram Strait

ARK-XV/2

Recovery: 0.49 m

81°26.25 N 04°02.25 E

Water depth: 769 m

Lithology	Texture	Color	Description	Age
Surface : 5Y 5/2 light olive gray, worm tubes, foraminifera, homogenous silty clay				
0		10YR5/2	0-10 cm: dark/pale yellowish brown, silty clay.	
		10YR3/2	10-17 cm: dark/dusky yellowish brown, silty clay.	
		10YR6/2	17-23 cm: pale yellowish brown, silty clay.	
		N4	23-35 cm: medium dark gray, silty clay .	
		N4 + 5YR 4/3	35-49 cm: medium dark gray/moderate brown, silty clay. "cottage cheese structure" , gray silty clay.	
1				

PS55/097-2 (KAL)

Fram Strait

ARK XV/2

Recovery: 1.97 m

81°15.79'N, 03°13.37'E

Water depth: 799 m

Depth in core (m)	Lithology	Texture	Color	Description	Age
	0			10 YR 3/2	0-25 cm: dark/dusky yellowish brown, sandy clay, silty clay, homogenous.
			N 4	25-59 cm: Med. dark gray, sandy silty clay, homogenous.	
			10 YR 5/2	59-64 cm: pale/dark yellowish brown, sandy clayey silt.	
			10 YR 4/2	64-77 cm: color change from dark yellowish brown (10 YR 4/2) to dark/dusky yellowish brown (10 YR 3/2) to grayish brown (5 YR 3/2).	
			5 YR 3/2		
			10 YR 5/2	64-70 cm: sandy, clayey silt, streaky.	
				70-77 cm: silty fine sand, IRD-rich.	
1			10 YR 5/4	77-95 cm: pale/dark yellowish brown, sandy silty clay, streaky.	
			2.5Y 4/2	95-104 cm: moderate yellowish brown, sandy silty clay.	
			10 YR 4/2	104-105 cm: harder, "cottage cheese structure".	97 cm: dropstone.
			10 YR 2/2	105-117 cm: dark yellowish brown, clayey silt, light & dark brown laminae.	103 cm: black spot. 108 cm: black spot.
				117-120 cm: dusky yellowish brown, clayey silt, transition.	
				142 cm: (clayey) silty dropstone.	
			10 YR 2/2	120-197 cm: dusky yellowish brown, sandy clayey silt.	
				195 cm: gneissic dropstone.	

PS55/097-3 (KAL)

Fram Strait

ARK XV/2

Recovery: 5.45 m

81°15.55 N, 03°00.37 E

Water depth: 860

Depth in core (m)	Lithology	Texture	Color	Description	Age
	0				
0-1			5Y 3/2	0-106 cm: olive gray, silty clay, homogenous.	
1				ca. 93 cm: very thin silty layer.	
1-2			5Y 3/2	106-116 cm: olive gray, silty clay, small olive brown layers with sand. 116-141 cm: greybrown, silty clay. 141-164 cm: greybrown, sandy-silty clay, mottled with black nodules. 164-173 cm: light brown, sandy silty clay.	
2			5Y 2/1	173-184 cm: yellowish brown, silty clay, ferric nodules; "cottage cheese" structure.	
2			5Y 4/2 (188-230cm)	184-188 cm: olive black, sandy silty clay. 188-192 cm: light olive/olive gray, silty clay, homogenous. 192-196 cm: light olive brown (5Y 5/6), silty clay. 196-210 cm: grey, silty clay, homogenous. 205 cm: dropstone. 210-214 cm: yellowish brownish, silty clay, homogenous. 214-215 cm: layer with reddish (oxidation?) colors. 215-230 cm: light olive/olive gray, silty clay, homogenous. 215-222 cm: reddish-brown, several silty-clay layers. 224.5, 226, 228 cm: oxidized silty-clay layer.	
2-3				230-508 cm: olive gray (5Y 3/2), silty clay, homogenous; variations in between (see below). 234 cm: oxidized silty-clay layer. 250, 260 cm: weak black layer 266-280 cm: mottled with black sulfidic spots.	
3				295-302 cm: four hardly visible brownish layers. 309 cm: indistinct, black zones. 319 cm: indistinct, black zones. 329 cm: indistinct, black zones. 336 cm: indistinct, black zones. 346 cm: disturbed black layer.	
3-4			5Y 3/2	360-383 cm: black spots. 379, 382 cm: disturbed black layers.	
4				398 cm: worm tube. 399 cm: brownish layer. 403 cm: brownish layer. 407 cm: brownish layer. 414 cm: brownish layer. 425 cm: weak black layer.	
5				460-500 cm: traces of bioturbation visible, black spots.	

Lithology	Texture	Color	Description	Age
5		5Y 4/2	508-510 cm: transition.	
		5Y 3/2	510-522 cm: light olive/olive gray, silty clay, homogenous. 512-522 cm: light olive/olive gray sandy silt, fining upward. 522-545 cm: olive gray, sandy silt, sandy base; in general coarser than the upper unit.	

PS55/098-2 (GKG)

Fram Strait

ARK-XV/2

Recovery: 0.33 m

81°10.74 N 01°12.29 E

Water depth: 1823 m

Lithology	Texture	Color	Description	Age
Surface : 5Y 5/2 light olive gray, sandy clay, many lifeforms (arthropods, anemones, worm tubes, foraminifers).				
0		10YR 5/2	0-7 cm: dark/pale yellowish brown, sandy clay.	
		5Y 5/1	7-16 cm: light olive/olive gray sandy silty clay.	
		5Y 5/1	16-33 cm: light olive/olive gray sandy clay.	
1				

PS55/100-3 (GKG)

Fram Strait

ARK-XV/2

Recovery: 0.51 m

80°28.87 N 02°56.01 E

Water depth: 1541 m

Lithology	Texture	Color	Description	Age
Surface: very soft, dark yellowish silty clay, many agglutinated foraminifers, ophiuræ.				
0		10YR 4/2	0-5 cm: dark yellowish brown, silty clay, oxidated	
		5Y 5/5	5-51.5 cm: olive gray, silty clay.	
1				

PS55/151-1 (GKG)

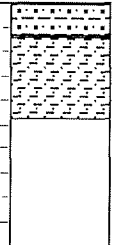
Eastern Yermak Plateau

ARK-XV/2

Recovery: 0.48 m

80°43.43 N 08°02.71 E

Water depth: 962 m

Lithology	Texture	Color	Description	Age
Surface : 5Y 5/2 dark yellowish brown, silty mud, sandy, shell of bivalve				
0  Depth in core (m) 1	10YR4/2		0-13 cm: dark yellowish brown, sandy silty mud.	
	10YR4/2		13-25 cm: dark yellowish brown, silty mud. 25 cm: transition.	
	5YR 4/2		25-34 cm: pale/grayish brown, silty mud.	
	10YR 5/2		34-35 cm: pale/dark yellowish brown, homogenous, silty mud.	
	5YR 4/2		35-39 cm: pale/grayish brown, silty mud.	
	N5		39-48 cm: medium gray, silty mud.	

PS55/151-2 (KAL)

Eastern Yermak Plateau

ARK XV/2

Recovery: 5.15 m

80°43.47'N, 08°01.32'E

Water depth: 971 m

	Lithology	Texture	Color	Description	Age
0			10YR4/2	0-40 cm: dark yellowish brown, silty clay, probably disturbed.	
			10YR5/4	40-45 cm: moderate yellowish brown, silty clay, two horizons.	
			5Y 5/2	45-61 cm: light olive gray, silty clay, dark gray streaks.	
			10YR5/4	61-71 cm: moderate yellowish brown, silty clay.	
1			10YR4/2	71-112 cm: dark yellowish brown, silty clay with sand, black mottles.	
			10YR5/4	112-130 cm: moderate yellowish brown, silty clay with black streaks.	
			10YR5/4	130-137 cm: moderate yellowish brown, silty clay.	
			10Y 5/2	137-229 cm: pale/grayish olive, silty clay.	
2			10Y 5/2	221-222 cm: dark gray, silty clay with sand.	
			5Y 5/6	229-236 cm: light olive brown, silty-clay.	
			10Y 5/2	236-261 cm: pale/grayish olive, silty clay, black mottles.	
			5Y 5/6	261-268 cm: light olive brown, silty-clay, white/light spots.	
			10Y 4/2	268-302 cm: grayish olive, silty clay.	
3			10Y 5/2	302-391 cm: pale/grayish clay. 321-322 cm: oxidized horizon. 331-322 cm: oxidized horizon.	
			10Y 5/2	354 cm: oxidized horizon.	
			10Y 5/2	373 cm: oxidized horizon.	
			10Y 5/2	384-391 cm: oxidized horizon.	
4			10Y 5/2	391-406 cm: pale/grayish olive, silty clay, sulfide spots.	
			5Y 5/6	406-410 cm: light olive brown, silty clay, cottage cheese structure.	
			10Y 5/2	410-506 cm: pale/grayish olive, silty clay.	
			10Y 5/2	453 cm: oxidized horizon.	
			10Y 5/2	461 cm: oxidized horizon.	
			10Y 5/2	473 cm: oxidized horizon.	
5			10Y 5/2	489-492 cm: oxidized horizon.	

Lithology	Texture	Color	Description	Age
5		10Y 5/2	:506-515 cm: pale/grayish olive, silty clay. :Zones with lighter colours (5Y 6/4 - dusky yellow), silty clay.	

PS55/158-1 (GKG)

Fram Strait

ARK-XV/2

Recovery:0.50 m

79°38.05 N 06°00.0 E

Water depth: 1544 m

Lithology	Texture	Color	Description	Age
Surface: dark yellowish brown, agglutin. foraminifers, 2 gastropods, bivalvs, shrimps, black IRD, sandy silt.				
0		10YR4/2	0-7 cm: brown, sandy silty clay. 7-10 cm: gray-brown, silty clay. 10-50 cm: gray-brown, silty clay.	
1				

Depth in core (m)

Appendix 3

- Geological Tables -

Core depth (cm)	Quartz	Feldspar	Mica	Opaque	Terr. Carbonate	Biogen. Carbonate	Clay Minerals	Organic Remains	Amphiboles	Biotite	Pyroxenes	Epidote	Chlorite	Garnet	Titanite	Fe-Mn nodules	Hydroxides Fe	Black ores
0	34.2	7.6	0.1	0	3.3	0.1	16.2	10.3	4.3	4.3	8.5	4.3	4.3	0.4	0	0	0.5	1.6
10	29	9.7	8.6	0	4.3	0.5	22.6	5.4	0.5	2.2	3.2	5.4	3.2	1.2	1	0	2.2	1
20	26.6	15.6	3.1	0	1.6	3.1	17.2	4.7	6.3	1.6	3.1	0.7	4	3.1	1.6	0	7.4	0.3
30	25.8	17.8	0.8	0.2	0.9	6.3	9.4	1.1	6.1	1.8	11.1	4.2	5.1	0.7	0.3	0	6.1	2.3
40	31.6	12.6	2.1	0.1	3.2	0.9	22.1	1.1	3.2	4.2	6.3	4.2	1	1.4	0.1	2.1	2.7	1.1
54	20.7	21.3	1.2	0	10	0	4.1	12.4	1.8	1.8	4.7	1.9	6.5	5.9	4.3	0	0.1	3.3
60	35.8	21.3	0.2	0.3	6.4	0.2	7.3	3.6	3	1	6.7	5.8	3.7	0.3	3	0.3	0.6	0.5
73	26.8	21.9	0.7	0.8	5.1	0	15.8	0.8	2.1	0.5	12.2	7.9	1.6	0.5	0.4	0.3	2.5	0.1
92	25.9	17.4	2.4	0	2.1	2.1	14.2	4.8	1.3	0.8	10	9.1	4.1	0	0	0.5	4.3	1
100	32.6	25.3	0.9	0	4.3	1.2	21.2	0.6	5.6	0	2.6	2.6	1.1	0	1.3	0	0.1	0.6
110	29.6	14.3	0.2	0	2.1	0	19.3	5.3	5.2	0.1	9.2	5.1	3.1	1.2	1.1	0	2.6	1.6
120	25	30	8.3	0.9	5.1	3.2	6.8	4.7	1.7	0.1	8.3	1.6	0.9	0.2	1.7	0	1.4	0.1
128	33.8	29.1	5.1	1.1	2.6	2.1	14.9	1.1	2.1	0	6.1	0.5	0.1	0	0.3	0	0.9	0.2
140	24.6	21.3	0.8	0.2	0.9	0.3	8.1	5.4	2.1	0.1	8.6	3.9	2.4	1.6	0.8	0.1	15.9	2.9
154	23.2	18.9	0	0	5.3	0	23.2	4.2	4.2	7.4	5.3	1.8	2.1	1.1	0.2	0	1	2.1
160	28.7	21.6	0	0	4.8	0	18.5	3.5	3.9	5.6	8.2	1.2	1.2	0.9	0.3	0	0.9	0.7
170	19.4	14.3	0.2	0	2.6	0	15.2	7.9	3.1	2.6	6.3	1.1	1.2	2.9	1.5	5.2	11.3	5.2
186	24.1	9.3	0	0	6.1	0	16.2	5.9	5.1	2.1	5.2	2.9	3.2	3.6	2.6	5	5.6	3.1
200	32.7	8.3	0	0	2.1	0	17.4	8.3	6.9	3.6	4.1	2.1	1.1	1.1	0.9	3.9	5.2	2.3
210	33.4	9.6	0	0.4	0.3	0	12.4	5.1	1.2	0.2	5.4	4.5	0.9	2.4	1.6	6.9	9.8	5.9
220	33.3	16.6	0.1	0.9	2.3	0	10	2.2	2.2	2.1	5.1	2.1	3.6	2.1	2.2	3.1	10	2.1
237	30.2	18.2	0	1.6	2.2	0	9.6	1	2.4	5.3	15.2	5.3	3.1	2.8	0.1	0	3	0
248	30.2	14.6	0	1.3	0.9	0	9.3	2.3	3.1	4.2	14.3	5.9	2.4	1.7	2.6	0.1	4.8	2.3
255	17	14.8	4.5	1.1	1.1	0	28.7	3.4	6.5	4.5	9.1	0.1	2.3	1.1	0	0	2.4	3.4
270	18.3	15.3	3.1	1.3	1.6	0	22.1	0.6	3.9	3.8	16.2	7.3	1.9	2.1	0	0	1.4	1.1
290	18.3	16.2	2.6	1.1	2.6	0	14.2	4.2	2.3	4.5	13.3	5.9	3.1	3.4	0	0	4.6	3.7
310	33.1	13	0.6	2.9	0.6	0	22.6	1.2	4.5	6.1	6.1	2.1	0.9	3.1	0	0	2.1	1.1
329	31.5	16.7	0	2.6	2.3	0	19.3	1.3	2.3	2.1	11.3	3.9	2.6	2.8	0.2	0	0	1.1
350	22.3	14.2	3.1	1.2	5.3	0	14.3	0	3.3	5.6	10.2	3.6	3.8	2.6	0.6	0	8.1	1.8
353	31.4	15.3	0	1.3	2	0	13.2	0.5	2.1	2.1	5.9	2.6	0.6	2.9	2.3	5.1	9.4	3.3
355	35.5	19.6	1.4	0.7	10.9	0	3.6	6.5	2.2	5.7	1.4	0.7	2.9	2.2	0.1	0	3.1	3.5
360	33.2	15.6	0.2	0.5	6.1	0	6.1	6.5	2.6	4.1	4.2	1.2	3.4	2.3	0.1	2.1	8.3	3.5
370	41.2	22.2	0	2.1	3.1	0	5.9	0.6	3.6	3.1	6.8	3.1	4.2	3.1	0.1	0	0	0.9
382	23.1	14.3	0.6	0.1	3.4	0	26.1	0.2	3.9	2.8	11.3	5.6	5.9	1.1	0.2	0	0	1.4
400	20.1	11.3	0.3	0.1	0.3	0	29.6	0.3	4.1	1.2	11.6	6.6	5.9	1.2	1.1	0	3.6	2.7
420	26.3	8.3	0.1	0	0	0	33.9	0	3.1	2.1	12.3	6.3	4.1	1.1	1.1	0	0	1.3
440	26.3	16.9	1.1	0.5	3.9	0	26.1	0.6	2.1	2.9	4.1	2.4	2.2	0.9	3.1	0	3.8	3.1
456	31.5	21.3	2.4	1.1	4.5	0	16.7	3.4	0.2	3.4	4.5	0.3	4.5	2.2	2.2	0	1.1	0.7
477	33.2	21.2	0.2	1.2	0.2	0	12.6	2.1	1.6	3.3	5.6	2.1	2.6	2.4	2.1	0	6.4	3.2
490	44	29.1	0	3.4	0.1	0	11.3	0.3	2.1	1.1	3.6	1.3	0.8	1	0.7	0	1	0.2
510	32.6	22.1	1.1	3.6	0.9	0	16.3	2.9	1.2	1.6	4.6	3.9	2.6	2.1	2.6	0	1.3	0.6
528	26.3	14.3	2.1	3.3	2	0	8.1	1.6	2.6	2.3	5.9	5.1	6.3	2.3	2.6	0.6	10	4.6
543	33.9	21.3	0.9	3.4	3.1	0	19.1	0.3	3.3	3.1	4.9	3.1	2.1	0.9	0.3	0	0.3	0
552	21.9	16.3	4.5	0	1.1	0	30.2	9.4	2.6	0.8	5.9	2.9	1.2	2.1	0.9	0	0	0.2
567	15.6	16.3	2.6	2.6	2.9	0	12.6	5.9	2.6	0.8	5.9	2.6	1.1	2.9	4	3.9	10.9	6.8
570	26.2	21.3	2.1	0.9	3.6	0	13.9	2.1	1.9	2.1	7.1	3.4	2.5	2.7	2.1	1.9	2.6	3.6
571	36.8	22.5	3.9	0	5.6	0	15.9	0.3	0.9	2.1	5.9	2.1	2.1	0.9	0.1	0.3	0.6	0
600	32.1	16.3	6.1	3.5	2.1	0	10.1	0.6	2.6	3.6	6.9	4.1	5.2	1.8	2.9	0	0	2.1
611	24.6	21.1	5.9	2.1	3.4	0	11.2	2.4	1.9	2.1	7.9	5.9	4.7	2.2	2.3	0	1.8	0.5
630	21.6	22.5	4.9	0.9	5.4	0	16.7	1.9	2.8	1.3	7.4	4.2	3.2	1.8	1.7	0	2.2	1.5
645	23.6	16.2	3.5	0	4.2	0	18.1	0.3	3.1	4.2	6.5	2.3	1.1	1.2	2.2	0	6.4	7.1
653	29.2	23.4	3.4	0	5.8	0	5.8	2.9	0.9	4.4	6.9	3.3	5.1	4.4	1.6	0	0	2.9
660	23.6	15.9	3.4	0	5.2	0	14.3	0.6	0.5	2.1	6.7	4.1	4.2	3.6	2.9	0.9	8.2	3.8
668	22.1	17.6	3.1	0	5.6	0	15.9	2.3	2.5	4.5	8.3	5.4	2.3	2.6	2.1	0	2.6	3.1
683	21.3	12.6	5.2	0	2.3	0	22.1	0.3	3.5	2.9	7.3	4.3	4.3	2.2	2.2	0	5.6	3.9
700	18.7	13.2	4.1	0	0.9	0	12.9	2.3	0.9	1	5.4	2.1	2.6	3.2	4.3	3.5	15.1	9.8
720	31.6	21.1	2.1	0	0.9	0	11.3	2.1	2.9	2	4.6	3.6	3.9	3.3	3.3	2.1	2.6	2.6
740	31.2	19.3	1.3	0	2.5	0	12.6	1.2	3.2	4.5	6.1	4.2	3.9	2.6	2.1	0.4	2.6	2.3
755	24.5	26.3	2.3	0	7.8	0	9.1	2.1	0.2	6.9	10.8	2	1.1	2	2.1	0	1.3	1.5

Tab. 9: Bulk and heavy mineralogy of sediments from Core P555/077-55L based on smear-slide estimates (%).

Tab. 10: Bulk and heavy mineralogy of sediments from Core PS55/097-3KAL based on smear-slide estimates (%).

Core depth [cm]	Quartz	Feldspar	Mica	Opaque	Terr. Carbonate	Clay Minerals	Organic Remains	Amphiboles	Biotite	Pyroxenes	Epidote	Chlorite	Garnet	Titanite	Fe-Mn nodules	Hydroxides Fe	Black ores
1	30.5	22.1	1.1	0	7.4	14.7	4.2	0	3.2	7.4	3.2	2.1	1.1	0	0	3	0
50	27	14.3	0.2	0.6	3.2	11.1	9.5	1.6	1.6	12.7	4.8	3.2	1	3.2	0	5.4	0.6
70	40.9	17.6	3.4	0	0.1	15.8	1.3	2.2	0.2	2.1	1.1	2.6	0.3	0.5	3.6	8.3	0
90	36.8	14.2	2.1	0	0.5	13.2	2.3	2.6	0.4	3.1	1.1	3.6	0.4	0.8	4.1	12.3	2.5
110	41.2	18.2	0.9	0.2	2.1	16.4	2	2.1	0.2	3.5	2.6	5.9	0.6	0.1	0.8	3.1	0.1
130	36.5	19.6	2.5	3.1	2.1	7.1	0.6	7.3	4.2	3.1	0.6	4.2	0	0	4.2	4.8	0.1
159	21.4	8.6	0.3	0	0.2	7.1	3.6	2.7	0.6	7.4	0.2	8.7	2.6	5.2	6.8	18.7	5.9
165	33.3	16.2	4.6	0.6	4.5	5.6	2.1	1.6	0.5	11.3	3.1	9.9	1	1.1	0	3.1	1.5
175	38.9	20.8	0.2	0.1	0.9	10.4	3.5	4.7	2.8	1.1	0.3	0.7	0.3	0	0.3	10.4	4.6
180	53.3	19.3	0.1	3.7	0.7	5.2	0	5	3.1	2.2	0.7	1.1	2	0	0.1	3.5	0
185	40.8	12.7	0	1.4	2.8	14.1	1.4	4.2	3.6	0.9	0.1	1.4	1.6	0.2	0.6	12.4	1.8
192	39.6	12.8	0	2.3	1.1	16.1	3.6	6.4	3.2	0.6	0.2	1.1	4.1	1.3	0	4.9	2.7
210	34.9	10.6	0.2	2.4	2.4	21.9	0.8	4.9	3.3	4.9	0.8	5.7	1.6	0.8	0	2.6	2.2
226	29.2	10	0.2	0.8	0.8	10.8	0	2.5	0.8	1.7	0.1	2.3	0.8	1.7	3.6	29.5	5.2
250	33.3	11.1	0.6	4.6	3.3	15.7	5.9	1.3	0.6	7.8	3.3	4.6	0.6	1.3	0	5.1	0.9
270	31.6	9.1	0.5	5.1	2.1	12.9	11.2	0.9	0.3	8.9	2.6	5.4	0.2	1.1	0.4	2.2	5.5
300	31.7	13.5	0.1	3.8	0.6	18.3	0.9	0.9	1.9	7.7	4.8	3.9	0.9	0.3	0.1	8.4	2.2
350	22.9	6.9	0.3	4.2	1.3	16.2	4.6	0.9	1.1	7.9	6.4	4.8	0.2	1.3	3.9	9.6	7.5
395	29.6	11.2	0.6	2.6	4.4	12.1	2.1	2.3	2.2	5.2	2.1	2.6	1.1	0.6	0.2	12.3	8.8
430	26.6	9.4	0.9	5.3	3.3	9.6	3.9	1.2	0.6	12.9	4.2	11.6	1.2	1.6	0.2	3.1	4.4
495	26.3	6.4	2.1	0.5	2.9	12.9	0.6	6.3	2.9	5.2	1.3	3.8	3.1	1.9	0	11.5	12.3
520	29.8	11.2	3.1	0.9	3.6	15.8	0.2	3.1	1.3	8.9	7.3	11.9	0.2	0.2	0	1.1	1.4

Tab. 11: Bulk and heavy mineralogy of sediments from Core PS55/092-5SL based on smear-slide estimates (%).

Minerals/ Depth [cm]	0	22	122	222	322	422	552	cc
Quartz	15	20.7	37.6	40.3	31.6	36.3	37.9	39.5
Feldspar	5.6	11.2	13.5	12.1	17.5	14.4	8.9	13.8
Mica	0.8	0.9	1.2	1.1	1.8	2.3	2.2	4.6
Opaque	0.1	0.4	0.5	0.8	1.6	0.9	1.3	2.3
Terr. Carbonate	2.8	2.8	0.9	1.8	3.2	2.1	2.8	0.5
Clay Minerals	7.1	7.3	10.2	14.8	12.4	7.6	7.3	11.3
Organic Rem.	7.9	6.8	3.1	1.2	2.9	0.8	0.8	0.5
Amphiboles	9.5	9.9	7.6	7.2	9.1	9.3	9.4	5.2
Pyroxenes	7.8	7.3	5.6	5.3	5.4	5.4	6.3	6.8
Epidote	2.9	2.9	2.9	2.1	3.1	2.4	3.8	1.3
Chlorite	4.2	3	2.1	2.4	2.8	1.2	1.6	0.2
Biotite	3.8	3.4	3.1	3.9	4.1	5.8	5.4	6.8
Garnet	3.1	3.1	2.8	2.3	2.3	3.7	3.9	1.4
Hydroxides Fe	13.2	9.8	4.1	2.1	0	3.1	2.8	0.8
Black Ores	9.1	5.8	1.9	0.8	0.5	1.8	2.9	3.8
Titanite	0.2	0.5	0.6	0.9	1.7	1.2	0.9	1.2
Fe-Mn nodules	6.9	4.2	2.3	0.9	0	1.7	1.8	0

Tab. 12: Bulk and heavy mineralogy of sediments from Core PS55/093-1SL based on smear-slide estimates (%).

Minerals/Cores Depth, cm	0	62	162	263	363	467	567
Quartz	25.6	30.2	49.6	37	41.6	44.7	42.5
Feldspar	12.2	12.5	21.9	12.1	22.4	14.4	18.5
Mica	1.6	0.8	1.5	0.9	1.2	3.4	2.8
Opaque	0	0	0.9	3.4	2.1	3.2	0.1
Terr. Carbonate	1.3	1.3	0.8	0.2	0.5	0.8	0.2
Clay Minerals	8.9	17.2	5.4	14.8	10.9	6.8	7.3
Organic Rem.	11.9	10.2	0.9	1.6	1.6	0.5	1.8
Amphiboles	7.6	7.1	5.4	7.3	6.3	6.2	4.1
Pyroxenes	5.7	2.1	2.7	3.6	3.6	4.8	2.7
Epidote	2.8	0.4	0.6	1.6	0.9	1.8	1.1
Chlorite	1.8	0	0	0.5	0.3	1.3	0
Biotite	3.7	5.8	3.8	4.5	3.2	4.6	2.1
Garnet	1.2	3.4	2.6	2.8	1.9	2.8	1.8
Titanite	0.5	0.5	0.6	0.9	0.2	0	0.9
Hydroxides Fe	9.6	5.8	2.1	3.9	1.1	2.3	10.2
Black Ores	3.9	2.7	1.1	4.6	2.1	2.1	1.8
Fe-Mn nodules	1.7	0	0.1	0.3	0.1	0.3	2.1

Tab. 13: Bulk and heavy mineralogy of sediments from Core PS55/095-3SL based on smear-slide estimates (%).

Minerals/Cores Depth, cm	0	61	161	261	362	462	562
Quartz	36.2	32.2	22.6	36	40.7	43.5	29.3
Feldspar	17.8	12.5	7.9	13.3	17.6	12.3	12.7
Mica	0.8	0.8	0.6	1.3	0.6	0.9	2.3
Opaque	0	0.9	1.2	0.9	0.1	0.6	0.9
Terr. Carbonate	2.4	2.8	0.9	0.6	0.4	0.8	0.3
Clay Minerals	13.8	13.9	12.3	11.8	7.9	7.3	13.1
Organic Rem.	6.8	5.7	0.9	0	0	0.5	0.9
Amphiboles	6.6	7.3	6.3	7.6	7.8	7.3	7.3
Pyroxenes	4.2	4.2	8.1	7.1	7.8	8.9	7.8
Epidote	2.1	3.1	4.4	5.4	3.4	3.8	3.7
Chlorite	0.8	1.9	2.1	2.7	2.6	2.8	2.1
Biotite	4.1	4.6	4.8	7.6	4.9	4.2	8.2
Garnet	2.1	2.6	3.6	2.9	2.1	2.6	1.9
Titanite	0.2	1.2	5.3	0.2	0.3	0.5	0.2
Hydroxides Fe	1.4	3.9	10.7	0.5	0.7	0.8	3.8
Black Ores	0.6	1.8	5.4	1.8	3.1	3.2	4.3
Fe-Mn nodules	0.1	0.6	2.9	0.3	0	0	1.2

Tab. 14: Bulk and heavy mineralogy of sediments from Core PS55/096-2SL based on smear-slide estimates (%).

Minerals/ Depth [cm]	0	69	159	259	359	459	559
Quartz	26.3	28.3	20.4	29.9	25.5	30.3	29.8
Feldspar	25.6	26.5	13.9	26.4	21	28.3	28
Mica	0.8	0.9	0.9	1.6	0.7	0.6	0.5
Opaque	1.1	1.2	0.1	0.8	1.6	0.9	1.9
Terr. Carbonate	0.5	0.2	1.2	1.1	2.9	1.2	1.1
Clay Minerals	14.6	10.1	23.9	13.1	18.9	8.9	11
Organic Rem.	2.3	6.8	0.8	0.8	0	0	0
Amphiboles	5.8	5.4	5.6	5.3	5.8	5.2	5.3
Pyroxenes	5.6	6	5.8	4.6	5.9	5.6	5.5
Epidote	4.8	3.2	3.3	3.2	4.8	2.6	1.6
Chlorite	0.9	1.2	1.1	0.8	1.9	1.9	1.1
Biotite	2.6	4.3	3.6	3.6	2.1	2.6	1.3
Garnet	2.3	2.9	2.4	1.2	0.9	0.8	1.9
Titanite	0.3	0.6	0.8	0.9	0.4	1.2	1.1
Hydroxides Fe	3.2	1.2	8.9	4.2	5.2	5.6	4.6
Black Ores	2.8	0.9	4.2	1.8	2.3	4.3	5.3
Fe-Mn nodules	0.5	0.3	3.1	0.7	0.1	0	0

Tab. 15: Bulk and heavy mineralogy of sediments from Core PS55/098-3SL based on smear-slide estimates (%).

Minerals/ Depth [cm]	0	12	113	215	316	416	516
Quartz	21.3	23.8	29.4	28.6	29.5	33.9	22.1
Feldspar	5.6	11.2	13.5	9.2	17.5	8.4	5.4
Mica	0.9	0.1	1.3	0.3	0.8	0.6	0.1
Opaque	2.1	0.9	1.1	2.4	3.9	4.2	3.4
Terr. Carbonate	0.2	1.1	0.9	0.6	0.3	0.2	0.6
Clay Minerals	13.2	19.6	21	22.4	14.9	13.6	23.1
Organic Rem.	9.3	2.6	1.8	0.6	0.5	0.5	0.3
Amphiboles	6.2	10.4	9.1	9.3	6.9	6.2	6.2
Pyroxenes	5.2	3.6	4.6	4	5.3	6.3	9.9
Epidote	1.8	1.3	1.1	1.2	2.3	2.6	2.3
Chlorite	1.6	2.1	1.1	0.6	0.2	1.1	1.2
Biotite	8.3	8.2	7.4	8.3	6.2	8.1	7.2
Garnet	3.1	3.1	2.4	1.1	3.3	2.4	0.9
Hydroxides Fe	13.8	6.2	2.1	3.8	2.9	3.2	7.9
Black Ores	2.8	4.1	1.3	6.7	3.8	6.8	4.8
Titanite	4.6	1.7	1.9	0.9	1.7	1.9	4.6

Tab. 16: Bulk and heavy mineralogy of sediments from Core PS55/100-2SL based on smear-slide estimates (%).

Minerals/ Depth [cm]	41	136	235	324	423	523
Quartz	25.6	30.2	23	33.2	30.1	30.2
Feldspar	13.9	26.2	21.3	28	26.5	29.3
Mica	1.5	1.9	1.1	0.9	1.4	2
Opaque	1.8	2.6	1.1	2.1	2.6	2.8
Terr. Carbonate	2.3	1.2	1.6	0.9	1.2	0.9
Clay Minerals	11.8	7.1	12.6	8.6	7.6	8
Organic Rem.	10.2	1.1	0.8	0.5	0	0
Amphiboles	5.6	4.2	4	5.6	6.3	5.6
Pyroxenes	7.6	8.3	7.3	7.1	7.9	6.2
Epidote	3.1	3.2	3.7	3.1	2.6	3.8
Chlorite	0.9	1.3	1.6	1.1	1.3	2.3
Biotite	2.3	3.2	2.9	0.9	3.6	2.9
Garnet	2.3	2.6	2.2	1.1	2.2	3.1
Titanite	0.9	1.3	0.8	0.9	0.3	0.9
Hydroxides Fe	5.8	3.2	7.9	3.8	3.6	1.1
Black Ores	4.1	1.8	5.3	1.9	2.8	0.9
Fe-Mn nodules	0.3	0.6	2.8	0.3	0	0

Participating Institutions
 ARK-XV/2

Address Participants

Germany

AWI	Alfred-Wegener-Institut für Polar-und Meeresforschung 27515 Bremerhaven	12
DWD	Deutscher Wetterdienst Geschäftsfeld Seeschifffahrt Bordwetterdienst Bernhard-Nocht-Str. 76 20359 Hamburg	2
GEOMAR	Forschungszentrum für marine Geowissenschaften der Christian-Albrechts-Universität Wischhofstraße 1 - 3 24148 Kiel	2
HSW	Helikopter Service Wasserthal GmbH Kätnerweg 43 22393 Hamburg	4
IGM	Institut für Geophysik der Westfälischen Wilhelms-Universität Corrensstr. 24 48149 Münster	2
MPIM	Max-Planck-Institut f. Chemie Abt. Geochemie Postfach 30 60 55020 Mainz	1

Denmark

GEUS	Geological Survey of Denmark and Greenland Thoravej 8 DK-2400 Copenhagen NV	1
------	---	---

Great Britain

IES	Institute of Geography and Earth Sciences University of Wales, Aberystwyth Aberystwyth Ceredigion SY23 3DB	1
-----	---	---

Participating Institutions

ARK-XV/2

Address

Participants

Poland/Polen

PAS	Institute of Geophysics Polish Academy of Sciences KS Janusza 64 01-452 Warsaw	2
-----	---	---

Russia/Rußland	Murmansk Marine Biological Institute Russian Academy of Sciences 17, Vladimirska street Murmansk, 183019	1
----------------	---	---

Cruise Participants

ARK-XV/2

Name		Institute
Böhm,	Joachim	HSW
Brauner,	Ralf	DWD
Czuba,	Wojciech	PAS
Didié,	Claudia	GEOMAR
Dzewas,	Jessica	AWI
Ehrhardt,	Axel	AWI
Forwick,	Matthias	AWI
Gierlichs,	Anette	AWI
Gussone,	Nikolaus	GEOMAR
Hass,	Christian	AWI
Hellebrand,	Eric	MPIM
Hillebrandt,	Marc-Oliver	HSW
Hohmann,	Constanze	AWI
Jokat,	Wilfried (Fahrtleiter)	AWI
Köhler,	Herbert	DWD
Kühn,	Daniela	IGM
Kukina,	Natalia	MMBI
Lahrmann,	Uwe	HSW
Lange,	Gert	Freier Journalist
Lauer,	Britta	Fotografin (?)
Lensch,	Norbert	AWI
Martens,	Hartmut	AWI
Meyer,	Sandra	AWI
Netzer,	Jennifer	GEOMAR
Nicolaus,	Marcel	IGM
Olesen,	Ole	GEUS
Schewe,	Ingo	AWI
Schmidt-Aursch,	Mechita	AWI
Sroda,	Piotr	PAS
Stangeew,	Elena	GEOMAR
Whittington,	Robert	IES
Wildeboer Schut,	Etienne	AWI
Zepick,	Burkhard	HSW

Ship's Crew

ARK-XV/2

Rank	Name
Master	Keil, Jürgen
1. Offc.	Grundmann, Uwe
1. Offc.	Rodewald, Martin
Ch.Eng.	Schulz, Volker
2. Offc.	Peine, Lutz
2. Offc.	Thieme, Wolfgang
Doctor	Zavrakidis, Nikolaos
R. Offc.	Hecht, Andreas
2. Eng.	Delff, Wolfgang
2. Eng.	Folta, Henryk
2. Engl.	Simon, Wolfgang
Electron.	Piskorzynski, Andreas
Electron.	Fröb, Martin
Electron.	Baier, Ulrich
Electron.	Bretfeld, Holger
Electr.	Holtz, Hartmut
Boatsw.	Loidl, Reiner
Carpenter	Neisner, Winfried
A.B.	Bäcker, Andreas
A.B.	Hagemann, Manfred
A.B.	Schmidt, Uwe
A.B.	Winkler, Michael
A.B.	Moser, Siegfried
A.B.	Bindernagel, Kurt
A.B.	Bohne, Jens
A.B.	Hartwig, Andreas
Storek.	Beth, Detlef
Mot-man	Arias Iglesias, Enr.
Mot-man	Giermann, Frank
Mot-man	Fritz, Günter
Mot-man	Krösche, Eckard
Mot-man	Dinse, Horst
Cook	Silinski, Frank
Cooksmate	Tupy, Mario
Cooksmate	Fischer, Matthias
1. Stwdess	Dinse, Petra
Stwdess/KS	Wöckener, Martina
2. Stwdess	Streit, Christina
2. Stwdess	Schmidt, Maria
2. Stwdess	Silinski, Carmen
2. Steward	Huang, Wu-Mei
2. Steward	Wu, Chi Lung
Laundrym.	Yu, Kwok Yuen

Folgende Hefte der Reihe „Berichte zur Polarforschung“ sind bisher erschienen:

- **Sonderheft Nr. 1/1981** – „Die Antarktis und ihr Lebensraum“
Eine Einführung für Besucher – Herausgegeben im Auftrag von SCAR
- **Heft Nr. 1/1982** – „Die Filchner-Schelfeis-Expedition 1980/81“
zusammengestellt von Heinz Kohnen
- **Heft Nr. 2/1982** – „Deutsche Antarktis-Expedition 1980/81 mit FS ‚Meteor‘“
First International BIOMASS Experiment (FIBEX) – Liste der Zooplankton- und Mikronektonnetzfüge
zusammengestellt von Norbert Klages
- **Heft Nr. 3/1982** – „Digitale und analoge Krill-Echolot-Rohdatenerfassung an Bord des Forschungsschiffes ‚Meteor‘“ (im Rahmen von FIBEX 1980/81, Fahrtabschnitt ANT III), von Bodo Morgenstern
- **Heft Nr. 4/1982** – „Filchner-Schelfeis-Expedition 1980/81“
Liste der Planktonfänge und Lichtstärkemessungen
zusammengestellt von Gerd Hubold und H. Eberhard Drescher
- **Heft Nr. 5/1982** – „Joint Biological Expedition on RRS ‚John Biscoe‘, February 1982“
by G. Hempel and R. B. Heywood
- **Heft Nr. 6/1982** – „Antarktis-Expedition 1981/82 (Unternehmen ‚Eiswarte‘)“
zusammengestellt von Gode Gravenhorst
- **Heft Nr. 7/1982** – „Marin-Biologisches Begleitprogramm zur Standorterkundung 1979/80 mit MS ‚Polarisirkel‘ (Pre-Site Survey)“ – Stationslisten der Mikronekton- und Zooplanktonfänge sowie der Bodenfischerei
zusammengestellt von R. Schneppenheim
- **Heft Nr. 8/1983** – „The Post-Fibex Data Interpretation Workshop“
by D. L. Cram and J.-C. Freytag with the collaboration of J. W. Schmidt, M. Mall, R. Kresse, T. Schwinghammer
- **Heft Nr. 9/1983** – „Distribution of some groups of zooplankton in the inner Weddell Sea in summer 1979/80“
by I. Hempel, G. Hubold, B. Kaczmaruk, R. Keller, R. Weigmann-Haass
- **Heft Nr. 10/1983** – „Fluor im antarktischen Ökosystem“ – DFG-Symposium November 1982
zusammengestellt von Dieter Adelung
- **Heft Nr. 11/1983** – „Joint Biological Expedition on RRS ‚John Biscoe‘, February 1982 (II)“
Data of micronekton and zooplankton hauls, by Uwe Piatkowski
- **Heft Nr. 12/1983** – „Das biologische Programm der ANTARKTIS-I-Expedition 1983 mit FS ‚Polarstern‘“
Stationslisten der Plankton-, Benthos- und Grundsleppnetzfüge und Liste der Probennahme an Robben und Vögeln, von H. E. Drescher, G. Hubold, U. Piatkowski, J. Plötz und J. Voß
- **Heft Nr. 13/1983** – „Die Antarktis-Expedition von MS ‚Polarbjörn‘ 1982/83“ (Sommerkampagne zur Atka-Bucht und zu den Kraul-Bergen), zusammengestellt von Heinz Kohnen
- **Sonderheft Nr. 2/1983** – „Die erste Antarktis-Expedition von FS ‚Polarstern‘ (Kapstadt, 20. Januar 1983 – Rio de Janeiro, 25. März 1983)“, Bericht des Fahrtleiters Prof. Dr. Gotthilf Hempel
- **Sonderheft Nr. 3/1983** – „Sicherheit und Überleben bei Polarexpeditionen“
zusammengestellt von Heinz Kohnen
- **Heft Nr. 14/1983** – „Die erste Antarktis-Expedition (ANTARKTIS I) von FS ‚Polarstern‘ 1982/83“
herausgegeben von Gotthilf Hempel
- **Sonderheft Nr. 4/1983** – „On the Biology of Krill *Euphausia superba*“ – Proceedings of the Seminar and Report of the Krill Ecology Group, Bremerhaven 12. - 16. May 1983, edited by S. B. Schnack
- **Heft Nr. 15/1983** – „German Antarctic Expedition 1980/81 with FRV ‚Walther Herwig‘ and RV ‚Meteor‘“ –
First International BIOMASS Experiment (FIBEX) – Data of micronekton and zooplankton hauls
by Uwe Piatkowski and Norbert Klages
- **Sonderheft Nr. 5/1984** – „The observatories of the Georg von Neumayer Station“, by Ernst Augstein
- **Heft Nr. 16/1984** – „FIBEX cruise zooplankton data“
by U. Piatkowski, I. Hempel and S. Rakusa-Suszczewski
- **Heft Nr. 17/1984** – Fahrtbericht (cruise report) der ‚Polarstern‘-Reise ARKTIS I, 1983“
von E. Augstein, G. Hempel und J. Thiede
- **Heft Nr. 18/1984** – „Die Expedition ANTARKTIS II mit FS ‚Polarstern‘ 1983/84“,
Bericht von den Fahrtabschnitten 1, 2 und 3, herausgegeben von D. Fütterer
- **Heft Nr. 19/1984** – „Die Expedition ANTARKTIS II mit FS ‚Polarstern‘ 1983/84“,
Bericht vom Fahrtabschnitt 4, Punta Arenas-Kapstadt (Ant-II/4), herausgegeben von H. Kohnen
- **Heft Nr. 20/1984** – „Die Expedition ARKTIS II des FS ‚Polarstern‘ 1984, mit Beiträgen des FS ‚Valdivia‘
und des Forschungsflugzeuges ‚Falcon 20‘ zum Marginal Ice Zone Experiment 1984 (MIZEX)“
von E. Augstein, G. Hempel, J. Schwarz, J. Thiede und W. Weigel
- **Heft Nr. 21/1985** – „Euphausiid larvae in plankton from the vicinity of the Antarctic Peninsula,
February 1982“ by Sigrid Marschall and Elke Mizdalski
- **Heft Nr. 22/1985** – „Maps of the geographical distribution of macrozooplankton in the Atlantic sector of
the Southern Ocean“ by Uwe Piatkowski
- **Heft Nr. 23/1985** – „Untersuchungen zur Funktionsmorphologie und Nahrungsaufnahme der Larven
des Antarktischen Krills *Euphausia superba* Dana“ von Hans-Peter Marschall

- Heft Nr. 24/1985** – „Untersuchungen zum Periglazial auf der König-Georg-Insel Südshetlandinseln/ Antarktika. Deutsche physiogeographische Forschungen in der Antarktis. – Bericht über die Kampagne 1983/84“ von Dietrich Barsch, Wolf-Dieter Blümel, Wolfgang Flügel, Roland Mäusbacher, Gerhard Stäblein, Wolfgang Zick
- * **Heft Nr. 25/1985** – „Die Expedition ANTARKTIS III mit FS ‚Polarstern‘ 1984/1985“ herausgegeben von Gotthilf Hempel.
 - * **Heft Nr. 26/1985** – “The Southern Ocean”; A survey of oceanographic and marine meteorological research work by Hellmer et al.
 - * **Heft Nr. 27/1986** – „Spätpleistozäne Sedimentationsprozesse am antarktischen Kontinentalhang vor Kapp Norvegia, östliche Weddell-See“ von Hannes Grobe
 - Heft Nr. 28/1986** – „Die Expedition ARKTIS III mit ‚Polarstern‘ 1985 mit Beiträgen der Fahrtteilnehmer, herausgegeben von Rainer Gersonde
 - * **Heft Nr. 29/1986** – „5 Jahre Schwerpunktprogramm ‚Antarktisforschung‘ der Deutschen Forschungsgemeinschaft.“ Rückblick und Ausblick. Zusammenge stellt von Gotthilf Hempel, Sprecher des Schwerpunktprogramms
 - Heft Nr. 30/1986** – “The Meteorological Data of the Georg-von-Neumayer-Station for 1981 and 1982“ by Marianne Gube and Friedrich Obleitner
 - * **Heft Nr. 31/1986** – „Zur Biologie der Jugendstadien der Notothenioidei (Pisces) an der Antarktischen Halbinsel“ von A. Kellermann
 - * **Heft Nr. 32/1986** – „Die Expedition ANTARKTIS IV mit FS ‚Polarstern‘ 1985/86“ mit Beiträgen der Fahrtteilnehmer, herausgegeben von Dieter Fütterer
 - Heft Nr. 33/1987** – „Die Expedition ANTARKTIS-IV mit FS ‚Polarstern‘ 1985/86 – Bericht zu den Fahrtabschnitten ANT-IV/3-4“ von Dieter Karl Fütterer
 - Heft Nr. 34/1987** – „Zoogeographische Untersuchungen und Gemeinschaftsanalysen an antarktischen Makroplankton“ von U. Piatkowski
 - Heft Nr. 35/1987** – „Zur Verbreitung des Meso- und Makrozooplanktons in Oberflächenwasser der Weddell See (Antarktis)“ von E. Boysen-Ennen
 - Heft Nr. 36/1987** – „Zur Nahrungs- und Bewegungsphysiologie von *Salpa thompsoni* und *Salpa fusiformis*“ von M. Reinke
 - Heft-Nr. 37/1987** – “The Eastern Weddell Sea Drifting Buoy Data Set of the Winter Weddell Sea Project (WWSP)” 1986 by Heinrich Hoerber und Marianne Gube-Lenhardt.
 - Heft Nr. 38/1987** – “The Meteorological Data of the Georg von Neumayer Station for 1983 and 1984“ by M. Gube-Lenhardt
 - Heft Nr. 39/1987** – „Die Winter-Expedition mit FS ‚Polarstern‘ in die Antarktis (ANT V/1-3)“ herausgegeben von Sigrid Schnack-Schiel
 - Heft Nr. 40/1987** – “Weather and Synoptic Situation during Winter Weddell Sea Project 1986 (ANT V/2) July 16 - September 10, 1986“ by Werner Rabe
 - Heft Nr. 41/1988** – „Zur Verbreitung und Ökologie der Seegurken im Weddellmeer (Antarktis)“ von Julian Gutt
 - Heft Nr. 42/1988** – “The zooplankton community in the deep bathyal and abyssal zones of the eastern North Atlantic“ by Werner Beckmann
 - * **Heft Nr. 43/1988** – “Scientific cruise report of Arctic Expedition ARK IV/3“ Wissenschaftlicher Fahrtbericht der Arktis-Expedition ARK IV/3, compiled by Jörn Thiede
 - * **Heft Nr. 44/1988** – “Data Report for FV ‘Polarstern‘ Cruise ARK IV/1, 1987 to the Arctic and Polar Fronts“ by Hans-Jürgen Hirche
 - Heft Nr. 45/1988** – „Zoogeographie und Gemeinschaftsanalyse des Makrozoobenthos des Weddellmeeres (Antarktis)“ von Joachim Voß
 - Heft Nr. 46/1988** – “Meteorological and Oceanographic Data of the Winter-Weddell-Sea Project 1986 (ANT V/3)“ by Eberhard Fahrbach
 - Heft Nr. 47/1988** – „Verteilung und Herkunft glazial-mariner Gerölle am Antarktischen Kontinentalrand des östlichen Weddellmeeres“ von Wolfgang Oskierski
 - Heft Nr. 48/1988** – „Variationen des Erdmagnetfeldes an der GvN-Station“ von Arnold Brodscholl
 - * **Heft Nr. 49/1988** – „Zur Bedeutung der Lipide im antarktischen Zooplankton“ von Wilhelm Hagen
 - * **Heft Nr. 50/1988** – „Die gezeitenbedingte Dynamik des Ekström-Schelfeises, Antarktis“ von Wolfgang Kobarg
 - Heft Nr. 51/1988** – „Ökomorphologie nototheniider Fische aus dem Weddellmeer, Antarktis“ von Werner Ekau
 - Heft Nr. 52/1988** – „Zusammensetzung der Bodenfauna in der westlichen Fram-Straße“ von Dieter Piepenburg
 - * **Heft Nr. 53/1988** – „Untersuchungen zur Ökologie des Phytoplanktons im südöstlichen Weddellmeer (Antarktis) im Jan./Febr. 1985“ von Eva-Maria Nöthig
 - Heft Nr. 54/1988** – „Die Fischfauna des östlichen und südlichen Weddellmeeres: geographische Verbreitung, Nahrung und trophische Stellung der Fischarten“ von Wiebke Schwarzbach
 - Heft Nr. 55/1988** – “Weight and length data of zooplankton in the Weddell Sea in austral spring 1986 (Ant. V/3)“ by Elke Mizdalski
 - Heft Nr. 56/1989** – “Scientific cruise report of Arctic expeditions ARK IV/1, 2 & 3“ by G. Krause, J. Meinke und J. Thiede

- Heft Nr. 57/1989** – „Die Expedition ANTARKTIS V mit FS ‚Polarstern‘ 1986/87“
Bericht von den Fahrtabschnitten ANT V/4-5 von H. Müller und H. Oerter
- * **Heft Nr. 58/1989** – „Die Expedition ANTARKTIS VI mit FS ‚Polarstern‘ 1987/88“
von D. K. Fütterer
- Heft Nr. 59/1989** – „Die Expedition ARKTIS V/1a, 1b und 2 mit FS ‚Polarstern‘ 1988“
von M. Spindler
- Heft Nr. 60/1989** – „Ein zweidimensionales Modell zur thermohalinen Zirkulation unter dem Schelfeis“
von H. H. Hellmer
- Heft Nr. 61/1989** – „Die Vulkanite im westlichen und mittleren Neuschwabenland, Vestfjella und Ahlmannryggen, Antarktika“ von M. Peters
- * **Heft Nr. 62/1989** – „The Expedition ANTARKTIS VII/1 and 2 (EPOS I) of RV ‚Polarstern‘
in 1988/89“, by I. Hempel
- Heft Nr. 63/1989** – „Die Eisalgenflora des Weddellmeeres (Antarktis): Artenzusammensetzung und Biomasse
sowie Ökophysiologie ausgewählter Arten“ von Annette Bartsch
- Heft Nr. 64/1989** – „Meteorological Data of the G.-v.-Neumayer-Station (Antarctica)“ by L. Helmes
- Heft Nr. 65/1989** – „Expedition Antarktis VII/3 in 1988/89“ by I. Hempel, P. H. Schalk, V. Smetacek
- Heft Nr. 66/1989** – „Geomorphologisch-glaziologische Detailkartierung
des arid-hochpolaren Borgmassivet, Neuschwabenland, Antarktika“ von Karsten Brunk
- Heft Nr. 67/1990** – „Identification key and catalogue of larval Antarctic fishes“,
edited by Adolf Kellermann
- Heft Nr. 68/1990** – „The Expedition Antarktis VII/4 (Epos leg 3) and VII/5 of RV ‚Polarstern‘ in 1989“,
edited by W. Arntz, W. Ernst, I. Hempel
- Heft Nr. 69/1990** – „Abhängigkeiten elastischer und rheologischer Eigenschaften des Meereises vom
Eisgefüge“, von Harald Hellmann
- * **Heft Nr. 70/1990** – „Die beschalten benthischen Mollusken (Gastropoda und Bivalvia) des
Weddellmeeres, Antarktis“, von Stefan Hain
- Heft Nr. 71/1990** – „Sedimentologie und Paläomagnetik an Sedimenten der Maudkuppe (Nordöstliches
Weddellmeer)“, von Dieter Cordes
- Heft Nr. 72/1990** – „Distribution and abundance of planktonic copepods (Crustacea) in the Weddell Sea
in summer 1980/81“, by F. Kurbjewit and S. Ali-Khan
- Heft Nr. 73/1990** – „Zur Frühdiagenese von organischem Kohlenstoff und Opal in Sedimenten des südlichen
und östlichen Weddellmeeres“, von M. Schlüter
- Heft Nr. 74/1990** – „Expeditionen ANTARKTIS-VIII/3 und VIII/4 mit FS ‚Polarstern‘ 1989“
von Rainer Gersonde und Gotthilf Hempel
- Heft Nr. 75/1991** – „Quartäre Sedimentationsprozesse am Kontinentalhang des Süd-Orkey-Plateaus im
nordwestlichen Weddellmeer (Antarktis)“, von Sigrun Grünig
- Heft Nr. 76/1990** – „Ergebnisse der faunistischen Arbeiten im Benthal von King George Island
(Südshetlandinseln, Antarktis)“, von Martin Rauschert
- Heft Nr. 77/1990** – „Verteilung von Mikroplankton-Organismen nordwestlich der Antarktischen Halbinsel
unter dem Einfluß sich ändernder Umweltbedingungen im Herbst“, von Heinz Klöser
- Heft Nr. 78/1991** – „Hochauflösende Magnetostratigraphie spätquartärer Sedimente arktischer
Meeresgebiete“, von Norbert R. Nowaczyk
- Heft Nr. 79/1991** – „Ökophysiologische Untersuchungen zur Salinitäts- und Temperaturtoleranz
antarktischer Grünalgen unter besonderer Berücksichtigung des β -Dimethylsulfoniumpropionat
(DMSP) - Stoffwechsels“, von Ulf Karsten
- Heft Nr. 80/1991** – „Die Expedition ARKTIS VII/1 mit FS ‚Polarstern‘ 1990“,
herausgegeben von Jörn Thiede und Gotthilf Hempel
- Heft Nr. 81/1991** – „Paläoglaziologie und Paläozeanographie im Spätquartär am Kontinentalrand des
südlichen Weddellmeeres, Antarktis“, von Martin Melles
- Heft Nr. 82/1991** – „Quantifizierung von Meeresereigenschaften: Automatische Bildanalyse von
Dünnschnitten und Parametrisierung von Chlorophyll- und Salzgehaltsverteilungen“, von Hajo Eicken.
- Heft Nr. 83/1991** – „Das Fließen von Schelfeisen - numerische Simulationen
mit der Methode der finiten Differenzen“, von Jürgen Determann
- Heft Nr. 84/1991** – „Die Expedition ANTARKTIS-VIII/1-2, 1989 mit der Winter Weddell Gyre Study
der Forschungsschiffe ‚Polarstern‘ und ‚Akademik Fedorov““, von Ernst Augstein,
Nikolai Bagriantsev und Hans Werner Schenke
- Heft Nr. 85/1991** – „Zur Entstehung von Unterwassereis und das Wachstum und die Energiebilanz
des Meereises in der Atka Bucht, Antarktis“, von Josef Kipfstuhl
- * **Heft Nr. 86/1991** – „Die Expedition ANTARKTIS-VIII mit FS ‚Polarstern‘ 1989/90. Bericht vom
Fahrtabschnitt ANT-VIII/5“, von Heinz Müller und Hans Oerter
- Heft Nr. 87/1991** – „Scientific cruise reports of Arctic expeditions ARK VI/1-4 of RV ‚Polarstern‘
in 1989“, edited by G. Krause, J. Meincke & H. J. Schwarz
- Heft Nr. 88/1991** – „Zur Lebensgeschichte dominanter Copepodenarten (*Calanus finmarchicus*,
C. glacialis, *C. hyperboreus*, *Metridia longa*) in der Framstraße“, von Sabine Diel

- Heft Nr. 89/1991** – „Detaillierte seismische Untersuchungen am östlichen Kontinentalrand des Weddell-Meereres vor Kapp Norvegia, Antarktis“, von Norbert E. Kaul
- Heft Nr. 90/1991** – „Die Expedition ANTARKTIS-VIII mit FS ‚Polarstern‘ 1989/90. Bericht von den Fahrtabschnitten ANT-VIII/6-7“, herausgegeben von Dieter Karl Fütterer und Otto Schrems
- Heft Nr. 91/1991** – „Blood physiology and ecological consequences in Weddell Sea fishes (Antarctica)“, by Andreas Kunzmann
- Heft Nr. 92/1991** – „Zur sommerlichen Verteilung des Mesozooplanktons im Nansen-Becken, Nordpolarmeer“, von Nicolai Mumm
- Heft Nr. 93/1991** – „Die Expedition ARKTIS VII mit FS ‚Polarstern‘, 1990. Bericht vom Fahrtabschnitt ARK VII/2“, herausgegeben von Gunther Krause
- Heft Nr. 94/1991** – „Die Entwicklung des Phytoplanktons im östlichen Weddellmeer (Antarktis) beim Übergang vom Spätwinter zum Frühjahr“, von Renate Scharek
- Heft Nr. 95/1991** – „Radioisotopenstratigraphie, Sedimentologie und Geochemie jungquartärer Sedimente des östlichen Arktischen Ozeans“, von Horst Bohrmann
- Heft Nr. 96/1991** – „Holozäne Sedimentationsentwicklung im Scoresby Sund, Ost-Grönland“, von Peter Marienfeld
- Heft Nr. 97/1991** – „Strukturelle Entwicklung und Abkühlungsgeschichte von Heimefrontfjella (Westliches Dronning Maud Land/Antarktika)“, von Joachim Jacobs
- Heft Nr. 98/1991** – „Zur Besiedlungsgeschichte des antarktischen Schelfes am Beispiel der Isopoda (Crustacea, Malacostraca)“, von Angelika Brandt
- * **Heft Nr. 99/1992** – „The Antarctic ice sheet and environmental change: a three-dimensional modelling study“, by Philippe Huybrechts
 - * **Heft Nr. 100/1992** – „Die Expeditionen ANTARKTIS IX/1-4 des Forschungsschiffes ‚Polarstern‘ 1990/91“ herausgegeben von Ulrich Bathmann, Meinhard Schulz-Baldes, Eberhard Fahrbach, Victor Smetacek und Hans-Wolfgang Hubberten
 - Heft Nr. 101/1992** – „Wechselbeziehungen zwischen Schwermetallkonzentrationen (Cd, Cu, Pb, Zn) im Meerwasser und in Zooplanktonorganismen (Copepoda) der Arktis und des Atlantiks“, von Christa Pohl
 - Heft Nr. 102/1992** – „Physiologie und Ultrastruktur der antarktischen Grünalge *Prasiola crispa* ssp. *antarctica* unter osmotischem Streß und Austrocknung“, von Andreas Jacob
 - * **Heft Nr. 103/1992** – „Zur Ökologie der Fische im Weddellmeer“, von Gerd Hubold
 - Heft Nr. 104/1992** – „Mehrkanalige adaptive Filter für die Unterdrückung von multiplen Reflexionen in Verbindung mit der freien Oberfläche in marinen Seismogrammen“, von Andreas Rosenberger
 - Heft Nr. 105/1992** – „Radiation and Eddy Flux Experiment 1991 (REFLEX I)“, von Jörg Hartmann, Christoph Kottmeier und Christian Wamser
 - Heft Nr. 106/1992** – „Ostracoden im Epipelagial vor der Antarktischen Halbinsel - ein Beitrag zur Systematik sowie zur Verbreitung und Populationsstruktur unter Berücksichtigung der Saisonalität“, von Rüdiger Kock
 - * **Heft Nr. 107/1992** – „ARCTIC '91: Die Expedition ARK-VIII/3 mit FS ‚Polarstern‘ 1991“, von Dieter K. Fütterer
 - Heft Nr. 108/1992** – „Dehnungsbeben an einer Störungszone im Ekström-Schelfeis nördlich der Georg-von-Neumayer-Station, Antarktis. – Eine Untersuchung mit seismologischen und geodätischen Methoden“, von Uwe Nixdorf.
 - * **Heft Nr. 109/1992** – „Spätquartäre Sedimentation am Kontinentalrand des südöstlichen Weddellmeeres, Antarktis“, von Michael Weber.
 - * **Heft Nr. 110/1992** – „Sedimentfazies und Bodenwasserstrom am Kontinentalhang des norwestlichen Weddellmeeres“, von Isa Brehme.
 - Heft Nr. 111/1992** – „Die Lebensbedingungen in den Solekanälchen des antarktischen Meereises“, von Jürgen Weissenberger.
 - Heft Nr. 112/1992** – „Zur Taxonomie von rezenten benthischen Foraminiferen aus dem Nansen Becken, Arktischer Ozean“, von Jutta Wollenburg.
 - Heft Nr. 113/1992** – „Die Expedition ARKTIS VIII/1 mit FS ‚Polarstern‘ 1991“, herausgegeben von Gerhard Kattner.
 - * **Heft Nr. 114/1992** – „Die Gründungsphase deutscher Polarforschung, 1865 - 1875“, von Reinhard A. Krause.
 - Heft Nr. 115/1992** – „Scientific Cruise Report of the 1991 Arctic Expedition ARK VIII/2 of RV ‚Polarstern‘ (EPOS II)“, by Eike Racher.
 - Heft Nr. 116/1992** – „The Meteorological Data of the Georg-von-Neumayer-Station (Antarctica) for 1988, 1989, 1990 and 1991“, by Gert König-Langlo.
 - Heft Nr. 117/1992** – „Petrogenese des metamorphen Grundgebirges der zentralen Heimefrontfjella (westliches Dronning Maud Land / Antarktis)“, von Peter Schulze.
 - Heft Nr. 118/1993** – „Die mafischen Gänge der Shackleton Range / Antarktika: Petrographie, Geochemie, Isotopengeochemie und Paläomagnetik“, von Rüdiger Hotten.
 - * **Heft Nr. 119/1993** – „Gefrierschutz bei Fischen der Polarmeere“, von Andreas P. A. Wöhrmann.
 - * **Heft Nr. 120/1993** – „East Siberian Arctic Region Expedition '92: The Laptev Sea - its Significance for Arctic Sea-Ice Formation and Transpolar Sediment Flux“, by D. Dethleff, D. Nürnberg, E. Reimnitz, M. Saarso and Y. P. Sacchenko. – „Expedition to Novaja Zemlja and Franz Josef Land with RV ‚Dalnie Zelentsy‘“, by D. Nürnberg and E. Groth.

- * **Heft Nr. 121/1993** – „Die Expedition ANTARKTIS X/3 mit FS ‚Polarstern‘ 1992“, herausgegeben von Michael Spindler, Gerhard Dieckmann und David Thomas
- Heft Nr. 122/1993** – „Die Beschreibung der Korngestalt mit Hilfe der Fourier-Analyse: Parametrisierung der morphologischen Eigenschaften von Sedimentpartikeln“, von Michael Diepenbroek.
- * **Heft Nr. 123/1993** – „Zerstörungsfreie hochauflösende Dichteuntersuchungen mariner Sedimente“, von Sebastian Gerland.
- Heft Nr. 124/1993** – „Umsatz und Verteilung von Lipiden in arktischen marinen Organismen unter besonderer Berücksichtigung unterer trophischer Stufen“, von Martin Graeve.
- Heft Nr. 125/1993** – „Ökologie und Respiration ausgewählter arktischer Bodenfischarten“, von Christian F. von Dorrien.
- Heft Nr. 126/1993** – „Quantitative Bestimmung von Paläoumweltparametern des Antarktischen Oberflächenwassers im Spätquartier anhand von Transferfunktionen mit Diatomeen“, von Ulrich Zielinski
- * **Heft Nr. 127/1993** – „Sedimenttransport durch das arktische Meereis: Die rezente lithogene und biogene Materialfracht“, von Ingo Wollenburg.
- Heft Nr. 128/1993** – „Cruise ANTARKTIS X/3 of RV ‚Polarstern‘: CTD-Report“, von Marek Zwierz.
- Heft Nr. 129/1993** – „Reproduktion und Lebenszyklen dominanter Copepodenarten aus dem Weddellmeer, Antarktis“, von Frank Kurbjeweit
- Heft Nr. 130/1993** – „Untersuchungen zu Temperaturregime und Massenhaushalt des Filchner-Ronne-Schelfeises, Antarktis, unter besonderer Berücksichtigung von Anfrier- und Abschmelzprozessen“, von Klaus Grosfeld
- Heft Nr. 131/1993** – „Die Expedition ANTARKTIS X/5 mit FS ‚Polarstern‘ 1992“, herausgegeben von Rainer Gersonde
- Heft Nr. 132/1993** – „Bildung und Abgabe kurzketziger halogenierter Kohlenwasserstoffe durch Makroalgen der Polarregionen“, von Frank Laturnus
- Heft Nr. 133/1994** – „Radiation and Eddy Flux Experiment 1993 (REFLEX II)“, by Christoph Kottmeier, Jörg Hartmann, Christian Wamser, Axel Bochert, Christof Lüpkes, Dietmar Freese and Wolfgang Cohrs
- * **Heft Nr. 134/1994** – „The Expedition ARKTIS-IX/1“, edited by Hajo Eicken and Jens Meincke
- Heft Nr. 135/1994** – „Die Expeditionen ANTARKTIS X/6-8“, herausgegeben von Ulrich Bathmann, Victor Smetacek, Hein de Baar, Eberhard Fahrbach und Gunter Krause
- Heft Nr. 136/1994** – „Untersuchungen zur Ernährungsökologie von Kaiserpinguinen (*Aptenodytes forsteri*) und Königspinguinen (*Aptenodytes patagonicus*)“, von Klemens Pütz
- * **Heft Nr. 137/1994** – „Die känozoische Vereisungsgeschichte der Antarktis“, von Werner U. Ehrmann
- Heft Nr. 138/1994** – „Untersuchungen stratosphärischer Aerosole vulkanischen Ursprungs und polarer stratosphärischer Wolken mit einem Mehrwellenlängen-Lidar auf Spitzbergen (79° N, 12° E)“, von Georg Beyerle
- Heft Nr. 139/1994** – „Charakterisierung der Isopodenfauna (Crustacea, Malacostraca) des Scotia-Bogens aus biogeographischer Sicht: Ein multivariater Ansatz“, von Holger Winkler.
- Heft Nr. 140/1994** – „Die Expedition ANTARKTIS X/4 mit FS ‚Polarstern‘ 1992“, herausgegeben von Peter Lemke
- Heft Nr. 141/1994** – „Satellitaltimetrie über Eis – Anwendung des GEOSAT-Altimeters über dem Ekströmisen, Antarktis“, von Clemens Heidland
- Heft Nr. 142/1994** – „The 1993 Northeast Water Expedition. Scientific cruise report of RV ‚Polarstern‘ Arctic cruises ARK IX/2 and 3, USCG ‚Polar Bear‘ cruise NEWP and the NEWLand expedition“, edited by Hans-Jürgen Hirche and Gerhard Kattner
- Heft Nr. 143/1994** – „Detaillierte refraktionsseismische Untersuchungen im inneren Scoresby Sund Ost-Grönland“, von Notker Fechner
- Heft Nr. 144/1994** – „Russian-German Cooperation in the Siberian Shelf Seas: Geo-System Laptev Sea“, edited by Heidmarie Kassens, Hans-Wolfgang Hubberten, Sergey M. Pryamikov and Rüdiger Stein
- * **Heft Nr. 145/1994** – „The 1993 Northeast Water Expedition. Data Report of RV ‚Polarstern‘ Arctic Cruises IX/2 and 3“, edited by Gerhard Kattner and Hans-Jürgen Hirche.
- Heft Nr. 146/1994** – „Radiation Measurements at the German Antarctic Station Neumayer 1982 - 1992“, by Torsten Schmidt and Gerd König-Langlo.
- Heft Nr. 147/1994** – „Krustenstrukturen und Verlauf des Kontinentalrandes im Weddell-See / Antarktis“, von Christian Hübscher.
- * **Heft Nr. 148/1994** – „The expeditions NORILSK/TAYMYR 1993 and BUNGER OASIS 1993/94 of the AWI Research Unit Potsdam“, edited by Martin Melles.
- ** **Heft Nr. 149/1994** – „Die Expedition ARCTIC '93. Der Fahrtabschnitt ARK-IX/4 mit FS ‚Polarstern‘ 1993“, herausgegeben von Dieter K. Fütterer.
- Heft Nr. 150/1994** – „Der Energiebedarf der Pygoscelis-Pinguine: eine Synopse“, von Boris M. Culik.
- Heft Nr. 151/1994** – „Russian-German Cooperation: The Transdrift I Expedition to the Laptev Sea“, edited by Heidmarie Kassens and Valeriy Y. Karpiy.
- Heft Nr. 152/1994** – „Die Expedition ANTARKTIS-X mit FS ‚Polarstern‘ 1992. Bericht von den Fahrtabschnitten / ANT-X / 1a und 2“, herausgegeben von Heinz Miller.
- Heft Nr. 153/1994** – „Aminosäuren und Huminstoffe im Stickstoffkreislauf polarer Meere“, von Ulrike Hubberten.
- Heft Nr. 154/1994** – „Regional and seasonal variability in the vertical distribution of mesozooplankton in the Greenland Sea“, by Claudio Richter.

- Heft Nr. 155/1995 – „Benthos in polaren Gewässern“, herausgegeben von Christian Wiencke und Wolf Arntz.
- Heft Nr. 156/1995 – „An adjoint model for the determination of the mean oceanic circulation, air-sea fluxes and mixing coefficients“, by Reiner Schlitzer.
- Heft Nr. 157/1995 – „Biochemische Untersuchungen zum Lipidstoffwechsel antarktischer Copepoden“, von Kirsten Fahl.
- Heft Nr. 158/1995 – „Die Deutsche Polarforschung seit der Jahrhundertwende und der Einfluß Erich von Drygalskis“, von Cornelia Lüdecke.
 - * Heft Nr. 159/1995 – „The distribution of $\delta^{18}\text{O}$ in the Arctic Ocean: Implications for the freshwater balance of the halocline and the sources of deep and bottom waters“, by Dorothea Bauch.
 - * Heft Nr. 160/1995 – „Rekonstruktion der spätquartären Tiefenwasserzirkulation und Produktivität im östlichen Südatlantik anhand von benthischen Foraminiferenvergesellschaftungen“, von Gerhard Schmiedl.
 - Heft Nr. 161/1995 – „Der Einfluß von Salinität und Lichtintensität auf die Osmolytkonzentrationen, die Zellvolumina und die Wachstumsraten der antarktischen Eisdiatomeen *Chaetoceros sp.* und *Navicula sp.* unter besonderer Berücksichtigung der Aminosäure Prolin“, von Jürgen Nothnagel.
 - Heft Nr. 162/1995 – „Meereistransportiertes lithogenes Feinmaterial in spätquartären Tiefseesedimenten des zentralen östlichen Arktischen Ozeans und der Framstraße“, von Thomas Letzig.
 - Heft Nr. 163/1995 – „Die Expedition ANTARKTIS-XI/2 mit FS ‚Polarstern‘ 1993/94“, herausgegeben von Rainer Gersonde.
 - Heft Nr. 164/1995 – „Regionale und altersabhängige Variation gesteinsmagnetischer Parameter in marinen Sedimenten der Arktis“, von Thomas Frederichs.
 - Heft Nr. 165/1995 – „Vorkommen, Verteilung und Umsatz biogener organischer Spurenstoffe: Sterole in antarktischen Gewässern“, von Georg Hanke.
 - Heft Nr. 166/1995 – „Vergleichende Untersuchungen eines optimierten dynamisch-thermodynamischen Meereismodells mit Beobachtungen im Weddellmeer“, von Holger Fischer.
 - * Heft Nr. 167/1995 – „Rekonstruktionen von Paläo-Umweltparametern anhand von stabilen Isotopen und Faunen-Vergesellschaftungen planktischer Foraminiferen im Südatlantik“, von Hans-Stefan Niebler
 - Heft Nr. 168/1995 – „Die Expedition ANTARKTIS XII mit FS ‚Polarstern‘ 1993/94. Bericht von den Fahrtabschnitten ANT XII/1 und 2“, herausgegeben von Gerhard Kattner und Dieter Karl Fütterer
 - Heft Nr. 169/1995 – „Medizinische Untersuchung zur Circadianrhythmik und zum Verhalten bei Überwinterern auf einer antarktischen Forschungsstation“, von Hans Wortmann
 - Heft-Nr. 170/1995 – DFG-Kolloquium: Terrestrische Geowissenschaften – Geologie und Geophysik der Antarktis.
 - Heft Nr. 171/1995 – „Strukturentwicklung und Petrogenese des metamorphen Grundgebirges der nördlichen Heimfrontjella (westliches Dronning Maud Land/Antarktika)“, von Wilfried Bauer.
 - Heft Nr. 172/1995 – „Die Struktur der Erdkruste im Bereich des Scoresby Sund, Ostgrönland: Ergebnisse refraktionsseismischer und gravimetrischer Untersuchungen“, von Holger Mandler.
 - Heft Nr. 173/1995 – „Paläozoische Akkretion am paläopazifischen Kontinentalrand der Antarktis in Nordvictorialand – P-T-D-Geschichte und Deformationsmechanismen im Bowers Terrane“, von Stefan Matzer.
 - Heft Nr. 174/1995 – „The Expedition ARKTIS-X/2 of RV ‚Polarstern‘ in 1994“, edited by Hans-W. Hubberten
 - Heft Nr. 175/1995 – „Russian-German Cooperation: The Expedition TAYMYR 1994“, edited by Christine Siebert and Gmitry Bolshiyarov.
 - Heft Nr. 176/1995 – „Russian-German Cooperation: Laptev Sea System“, edited by Heidemarie Kassens, Dieter Piepenburg, Jörn Thiede, Leonid Timokhov, Hans-Wolfgang Hubberten and Sergey M. Priamikov.
 - Heft Nr. 177/1995 – „Organischer Kohlenstoff in spätquartären Sedimenten des Arktischen Ozeans: Terrigener Eintrag und marine Produktivität“, von Carsten J. Schubert
 - Heft Nr. 178/1995 – „Cruise ANTARKTIS XII/4 of RV ‚Polarstern‘ in 1995: CTD-Report“, by Jüri Sildam.
 - Heft Nr. 179/1995 – „Benthische Foraminiferenfaunen als Wassermassen-, Produktions- und Eisdriftanzeiger im Arktischen Ozean“, von Jutta Wollenburg.
 - Heft Nr. 180/1995 – „Biogenopal und biogenes Barium als Indikatoren für spätquartäre Produktivitätsänderungen am antarktischen Kontinentalhang, atlantischer Sektor“, von Wolfgang J. Bonn.
 - Heft Nr. 181/1995 – „Die Expedition ARKTIS X/1 des Forschungsschiffes ‚Polarstern‘ 1994“, herausgegeben von Eberhard Fahrbach.
 - Heft Nr. 182/1995 – „Laptev Sea System: Expeditions in 1994“, edited by Heidemarie Kassens.
 - Heft Nr. 183/1996 – „Interpretation digitaler Parasound Echolotaufzeichnungen im östlichen Arktischen Ozean auf der Grundlage physikalischer Sedimenteigenschaften“, von Uwe Bergmann.
 - Heft Nr. 184/1996 – „Distribution and dynamics of inorganic nitrogen compounds in the troposphere of continental, coastal, marine and Arctic areas“, by Maria Dolores Andrés Hernández.
 - Heft Nr. 185/1996 – „Verbreitung und Lebensweise der Aphroditen und Polynoiden (Polychaeta) im östlichen Weddellmeer und im Lazarevmeer (Antarktis)“, von Michael Stiller.
 - Heft Nr. 186/1996 – „Reconstruction of Late Quaternary environmental conditions applying the natural radionuclides ^{230}Th , ^{10}Be , ^{231}Pa and ^{238}U : A study of deep-sea sediments from the eastern sector of the Antarctic Circumpolar Current System“, by Martin Frank.
 - Heft Nr. 187/1996 – „The Meteorological Data of the Neumayer Station (Antarctica) for 1992, 1993 and 1994“, by Gert König-Langlo and Andreas Herber.
 - Heft Nr. 188/1996 – „Die Expedition ANTARKTIS-XI/3 mit FS ‚Polarstern‘ 1994“, herausgegeben von Heinz Miller und Hannes Grobe.
 - Heft Nr. 189/1996 – „Die Expedition ARKTIS-VII/3 mit FS ‚Polarstern‘ 1990“, herausgegeben von Heinz Miller und Hannes Grobe

- Heft Nr. 190/1996** – "Cruise report of the Joint Chilean-German-Italian Magellan 'Victor Hensen' Campaign in 1994", edited by Wolf Arntz and Matthias Gorny.
- Heft Nr. 191/1996** – „Leitfähigkeits- und Dichtemessung an Eisbohrkernen“, von Frank Wilhelms.
- Heft Nr. 192/1996** – „Photosynthese-Charakteristika und Lebensstrategie antarktischer Makroalgen“, von Gabriele Weykam.
- Heft Nr. 193/1996** – „Heterogene Reaktionen von N_2O_5 und HBr und ihr Einfluß auf den Ozonabbau in der polaren Stratosphäre“, von Sabine Seisel.
- Heft Nr. 194/1996** – „Ökologie und Populationsdynamik antarktischer Ophiuroiden (Echinodermata)“, von Corinna Dahm.
- Heft Nr. 195/1996** – „Die planktische Foraminifere *Neogloboquadrina pachyderma* (Ehrenberg) im Weddellmeer, Antarktis“, von Doris Berberich.
- Heft Nr. 196/1996** – „Untersuchungen zum Beitrag chemischer und dynamischer Prozesse zur Variabilität des stratosphärischen Ozons über der Arktis“, von Birgit Heese.
- Heft Nr. 197/1996** – "The Expedition ARKTIS-XI/2 of 'Polarstern' in 1995", edited by Gunther Krause.
- Heft Nr. 198/1996** – „Geodynamik des Westantarktischen Riftsystems basierend auf Apatit-Spaltspuranalysen“, von Frank Lisler.
- Heft Nr. 199/1996** – "The 1993 Northeast Water Expedition. Data Report on CTD Measurements of RV 'Polarstern' Cruises ARKTIS IX/2 and 3", by Gerion Budéus and Wolfgang Schneider.
- Heft Nr. 200/1996** – "Stability of the Thermohaline Circulation in analytical and numerical models", by Gerrit Lohmann.
- Heft Nr. 201/1996** – „Trophische Beziehungen zwischen Makroalgen und Herbivoren in der Potter Cove (King George-Insel, Antarktis)“, von Katrin Iken.
- Heft Nr. 202/1996** – „Zur Verbreitung und Respiration ökologisch wichtiger Bodentiere in den Gewässern um Svalbard (Arktis)“, von Michael K. Schmid.
- Heft Nr. 203/1996** – „Dynamik, Rauigkeit und Alter des Meereises in der Arktis – Numerische Untersuchungen mit einem großskaligen Modell“, von Markus Harder.
- Heft Nr. 204/1996** – „Zur Parametrisierung der stabilen atmosphärischen Grenzschicht über einem antarktischen Schelfeis“, von Dörthe Handorf.
- Heft Nr. 205/1996** – "Textures and fabrics in the GRIP ice core, in relation to climate history and ice deformation", by Thorsteinn Thorsteinsson.
- Heft Nr. 206/1996** – „Der Ozean als Teil des gekoppelten Klimasystems: Versuch der Rekonstruktion der glazialen Zirkulation mit verschiedenen komplexen Atmosphärenkomponenten“, von Kerstin Fieg.
- Heft Nr. 207/1996** – „Lebensstrategien dominanter antarktischer Oithonidae (Cyclopoida, Copepoda) und Oncaeiidae (Poecilostomatoida, Copepoda) im Bellingshausenmeer“, von Cornelia Metz.
- Heft Nr. 208/1996** – „Atmosphäreinfluß bei der Fernerkundung von Meereis mit passiven Mikrowellenradiometern“, von Christoph Oelke.
- Heft Nr. 209/1996** – „Klassifikation von Radarsatellitendaten zur Meereisererkennung mit Hilfe von Line-Scanner-Messungen“, von Axel Bochert.
- Heft Nr. 210/1996** – „Die mit ausgewählten Schwämmen (Hexactinellida und Demospongiae) aus dem Weddellmeer, Antarktis, vergesellschaftete Fauna“, von Kathrin Kunzmann.
- Heft Nr. 211/1996** – "Russian-German Cooperation: The Expedition TAYMYR 1995 and the Expedition KOLYMA 1995", by Dima Yu. Bolshiyarov and Hans-W. Hubberten.
- Heft Nr. 212/1996** – "Surface-sediment composition and sedimentary processes in the central Arctic Ocean and along the Eurasian Continental Margin", by Ruediger Stein, Gennadij I. Ivanov, Michael A. Levitan, and Kirsten Fahl.
- Heft Nr. 213/1996** – „Gonadenentwicklung und Eiproduktion dreier *Calanus*-Arten (Copepoda): Freilandbeobachtungen, Histologie und Experimente“, von Barbara Niehoff.
- Heft Nr. 214/1996** – „Numerische Modellierung der Übergangszone zwischen Eisschild und Eisschelf“, von Christoph Mayer.
- Heft Nr. 215/1996** – „Arbeiten der AWI-Forschungsstelle Potsdam in Antarktika, 1994/95“, herausgegeben von Ulrich Wand.
- Heft Nr. 216/1996** – „Rekonstruktion quartärer Klimaänderungen im atlantischen Sektor des Südpolarmeeres anhand von Radiolarien“, von Uta Brathauer.
- Heft Nr. 217/1996** – „Adaptive Semi-Lagrange-Finite-Elemente-Methode zur Lösung der Flachwassergleichungen: Implementierung und Parallelisierung“, von Jörn Behrens.
- Heft Nr. 218/1997** – "Radiation and Eddy Flux Experiment 1995 (REFLEX III)", by Jörg Hartmann, Axel Bochert, Dietmar Freese, Christoph Kottmeier, Dagmar Nagel and Andreas Reuter.
- Heft Nr. 219/1997** – „Die Expedition ANTARKTIS-XII mit FS 'Polarstern' 1995. Bericht vom Fahrtabschnitt ANT-XII/3, herausgegeben von Wilfried Jokat und Hans Oerter.
- Heft Nr. 220/1997** – „Ein Beitrag zum Schwerfeld im Bereich des Weddellmeeres, Antarktis. Nutzung von Altimetermessungen des GEOSAT und ERS-1“, von Tilo Schöne.
- Heft Nr. 221/1997** – „Die Expeditionen ANTARKTIS-XIII/1-2 des Forschungsschiffes 'Polarstern' 1995/96“, herausgegeben von Ulrich Bathmann, Mike Lukas und Victor Smetacek.
- Heft Nr. 222/1997** – "Tectonic Structures and Glaciomarine Sedimentation in the South-Eastern Weddell Sea from Seismic Reflection Data", by László Oszkó.

- Heft Nr. 223/1997** – „Bestimmung der Meereisdicke mit seismischen und elektromagnetisch-induktiven Verfahren“, von Christian Haas.
- Heft Nr. 224/1997** – „Troposphärische Ozonvariationen in Polarregionen“, von Silke Wessel.
- Heft Nr. 225/1997** – „Biologische und ökologische Untersuchungen zur kryopelagischen Amphipodenfauna des arktischen Meereises“, von Michael Poltermann.
- Heft Nr. 226/1997** – “Scientific Cruise Report of the Arctic Expedition ARK-XI/1 of RV 'Polarstern' in 1995“, edited by Eike Rachor.
- Heft Nr. 227/1997** – „Der Einfluß kompatibler Substanzen und Kryoprotektoren auf die Enzyme Malatdehydrogenase (MDH) und Glucose-6-phosphat-Dehydrogenase (G6P-DH) aus *Acrosiphonia arcta* (Chlorophyta) der Arktis“, von Katharina Kück.
- Heft Nr. 228/1997** – „Die Verbreitung epibenthischer Mollusken im chilenischen Beagle-Kanal“, von Katrin Linse.
- Heft Nr. 229/1997** – „Das Mesozooplankton im Laptevmeer und östlichen Nansen-Becken - Verteilung und Gemeinschaftsstrukturen im Spätsommer“, von Hinrich Hanssen.
- Heft Nr. 230/1997** – „Modell eines adaptierbaren, rechnergestützten, wissenschaftlichen Arbeitsplatzes am Alfred-Wegener-Institut für Polar- und Meeresforschung“, von Lutz-Peter Kurdelski
- Heft Nr. 231/1997** – „Zur Ökologie arktischer und antarktischer Fische: Aktivität, Sinnesleistungen und Verhalten“, von Christopher Zimmermann
- Heft Nr. 232/1997** – „Persistente chlororganische Verbindungen in hochantarktischen Fischen“, von Stephan Zimmermann
- Heft Nr. 233/1997** – „Zur Ökologie des Dimethylsulfoniumpropionat (DMSP)-Gehaltes temperierter und polarer Phytoplanktongemeinschaften im Vergleich mit Laborkulturen der Coccolithophoride *Emiliania huxleyi* und der antarktischen Diatomee *Nitzschia lecointeri*“, von Doris Meyerdierks.
- Heft Nr. 234/1997** – „Die Expedition ARCTIC '96 des FS ‚Polarstern‘ (ARK XIII) mit der Arctic Climate System Study (ACSYS)“, von Ernst Augstein und den Fahrtteilnehmern.
- Heft Nr. 235/1997** – „Polonium-210 und Blei-210 im Südpolarmeer: Natürliche Tracer für biologische und hydrographische Prozesse im Oberflächenwasser des Antarktischen Zirkumpolarstroms und des Weddellmeeres“, von Jana Friedrich
- Heft Nr. 236/1997** – “Determination of atmospheric trace gas amounts and corresponding natural isotopic ratios by means of ground-based FTIR spectroscopy in the high Arctic“, by Arndt Meier.
- Heft Nr. 237/1997** – “Russian-German Cooperation: The Expedition TAYMYR/SEVERNAYA ZEMLYA 1996“, edited by Martin Melles, Birgit Hagedorn and Dmitri Yu. Bolshiyarov
- Heft Nr. 238/1997** – “Life strategy and ecophysiology of Antarctic macroalgae“, by Iván M. Gómez.
- Heft Nr. 239/1997** – „Die Expedition ANTARKTIS XIII/4-5 des Forschungsschiffes ‚Polarstern‘ 1996“, herausgegeben von Eberhard Fahrbach und Dieter Gerdes.
- Heft Nr. 240/1997** – „Untersuchungen zur Chrom-Speziation in Meerwasser, Meereis und Schnee aus ausgewählten Gebieten der Arktis“, von Heide Giese.
- Heft Nr. 241/1997** – “Late Quaternary glacial history and paleoceanographic reconstructions along the East Greenland continental margin: Evidence from high-resolution records of stable isotopes and ice-rafted debris“, by Seung-II Nam.
- Heft Nr. 242/1997** – “Thermal, hydrological and geochemical dynamics of the active layer at a continuous permafrost site, Taymyr Peninsula, Siberia“, by Julia Boike.
- Heft Nr. 243/1997** – „Zur Paläoozeanographie hoher Breiten: Stellvertreterdaten aus Foraminiferen“, von Andreas Mackensen.
- Heft Nr. 244/1997** – “The Geophysical Observatory at Neumayer Station, Antarctica, Geomagnetic and seismological observations in 1995 and 1996“, by Alfons Eckstaller, Thomas Schmidt, Viola Graw, Christian Müller and Johannes Rogenhagen.
- Heft Nr. 245/1997** – „Temperaturbedarf und Biogeographie mariner Makroalgen - Anpassung mariner Makroalgen an tiefe Temperaturen, von Bettina Bischoff-Bäsmann.
- Heft Nr. 246/1997** – „Ökologische Untersuchungen zur Fauna des arktischen Meereises“, von Christine Friedrich.
- Heft Nr. 247/1997** – „Entstehung und Modifizierung von marinen gelösten organischen Substanzen“, von Berit Kirchoff.
- Heft Nr. 248/1997** – “Laptev Sea System: Expeditions in 1995“, edited by Heidemarie Kassens.
- Heft Nr. 249/1997** – “The Expedition ANTARKTIS XIII/3 (EASIZ I) of RV 'Polarstern' to the eastern Weddell Sea in 1996“, edited by Wolf Arntz and Julian Gutt.
- Heft Nr. 250/1997** – „Vergleichende Untersuchungen zur Ökologie und Biodiversität des Mega-Epibenthos der Arktis und Antarktis“, von Andreas Starmans.
- Heft Nr. 251/1997** – „Zeitliche und räumliche Verteilung von Mineralvergesellschaftungen in spätquartären Sedimenten des Arktischen Ozeans und ihre Nützlichkeit als Klimaindikatoren während der Glazial/Interglazial-Wechsel“, von Christoph Vogt.
- Heft Nr. 252/1997** – „Solitäre Ascidien in der Potter Cove (King George Island, Antarktis). Ihre ökologische Bedeutung und Populationsdynamik“, von Stephan Kühne.
- Heft Nr. 253/1997** – “Distribution and role of microprotozoa in the Southern Ocean“, by Christine Klaas.
- Heft Nr. 254/1997** – „Die spätquartäre Klima- und Umweltgeschichte der Bunge-Oase, Ostantarktis“, von Thomas Kulbe

- Heft Nr. 255/1997** – "Scientific Cruise Report of the Arctic Expedition ARK-XIII/2 of RV 'Polarstern' in 1997", edited by Ruediger Stein and Kirsten Fahl.
- Heft Nr. 256/1998** – „Das Radionuklid Tritium im Ozean: Meßverfahren und Verteilung von Tritium im Südatlantik und im Weddellmeer“, von Jürgen Süttenfuß.
- Heft Nr. 257/1998** – „Untersuchungen der Saisonalität von atmosphärischem Dimethylsulfid in der Arktis und Antarktis“, von Christoph Kleefeld.
- Heft Nr. 258/1998** – „Bellingshausen- und Amundsenmeer: Entwicklung eines Sedimentationsmodells“, von Frank-Oliver Nitsche.
- Heft Nr. 259/1998** – "The Expedition ANTARKTIS-XIV/4 of RV 'Polarstern' in 1997", by Dieter K. Fütterer.
- * **Heft Nr. 260/1998** – „Die Diatomeen der Laptevsee (Arktischer Ozean): Taxonomie und biogeographische Verbreitung“, von Holger Cremer
- Heft Nr. 261/1998** – „Die Krustenstruktur und Sedimentdecke des Eurasischen Beckens, Arktischer Ozean: Resultate aus seismischen und gravimetrischen Untersuchungen“, von Estella Weigelt.
- Heft Nr. 262/1998** – "The Expedition ARKTIS-XIII/3 of RV 'Polarstern' in 1997", by Gunther Krause.
- Heft Nr. 263/1998** – „Thermo-tektonische Entwicklung von Oates Land und der Shackleton Range (Antarktis) basierend auf Spaltspuranalysen“, von Thorsten Schäfer.
- Heft Nr. 264/1998** – „Messungen der stratosphärischen Spurengase ClO, HCl, O₃, N₂O, H₂O und OH mittels flugzeuggetragener Submillimeterwellen-Radiometrie“, von Joachim Urban.
- Heft Nr. 265/1998** – „Untersuchungen zu Massenhaushalt und Dynamik des Ronne Ice Shelves, Antarktis“, von Astrid Lambrecht.
- Heft Nr. 266/1998** – "Scientific Cruise Report of the Kara Sea Expedition of RV 'Akademic Boris Petrov' in 1997", edited by Jens Matthiessen and Oleg Stepanets.
- Heft Nr. 267/1998** – „Die Expedition ANTARKTIS-XIV mit FS ‚Polarstern‘ 1997. Bericht vom Fahrtabschnitt ANT-XIV/3“, herausgegeben von Wilfried Jokat und Hans Oerter.
- Heft Nr. 268/1998** – „Numerische Modellierung der Wechselwirkung zwischen Atmosphäre und Meereis in der arktischen Eisrandzone“, von Gerit Birnbaum.
- Heft Nr. 269/1998** – "Katabatic wind and Boundary Layer Front Experiment around Greenland (KABEG '97)", by Günther Heinemann.
- Heft Nr. 270/1998** – "Architecture and evolution of the continental crust of East Greenland from integrated geophysical studies", by Vera Schindwein.
- Heft Nr. 271/1998** – "Winter Expedition to the Southwestern Kara Sea - Investigations on Formation and Transport of Turbid Sea-Ice", by Dirk Dethleff, Per Loewe, Dominik Weiel, Hartmut Nies, Gesa Kuhlmann, Christian Bahe and Gennady Tarasov.
- Heft Nr. 272/1998** – „FTIR-Emissionsspektroskopische Untersuchungen der arktischen Atmosphäre“, von Edo Becker.
- Heft Nr. 273/1998** – „Sedimentation und Tektonik im Gebiet des Agulhas Rückens und des Agulhas Plateaus („SETA-RAP“)“, von Gabriele Uenzelmann-Neben.
- Heft Nr. 274/1998** – "The Expedition ANTARKTIS XIV/2", by Gerhard Kattner.
- Heft Nr. 275/1998** – „Die Auswirkung der 'NorthEastWater'-Polynya auf die Sedimentation von NO-Grönland und Untersuchungen zur Paläo-Ozeanographie seit dem Mittelweichsel“, von Hanne Notholt.
- Heft Nr. 276/1998** – „Interpretation und Analyse von Potentialfelddaten im Weddellmeer, Antarktis: der Zerfall des Superkontinents Gondwana“, von Michael Studinger.
- Heft Nr. 277/1998** – „Koordiniertes Programm Antarktisforschung“. Berichtskolloquium im Rahmen des Koordinierten Programms „Antarktisforschung mit vergleichenden Untersuchungen in arktischen Eisgebieten“, herausgegeben von Hubert Miller.
- Heft Nr. 278/1998** – „Messung stratosphärischer Spurengase über Ny-Ålesund, Spitzbergen, mit Hilfe eines bodengebundenen Mikrowellen-Radiometers“, von Uwe Raffalski.
- Heft Nr. 279/1998** – "Arctic Paleo-River Discharge (APARD). A New Research Programme of the Arctic Ocean Science Board (AOSB)", edited by Ruediger Stein.
- Heft Nr. 280/1998** – „Fernerkundungs- und GIS-Studien in Nordostgrönland“ von Friedrich Jung-Rothenhäusler.
- Heft Nr. 281/1998** – „Rekonstruktion der Oberflächenwassermassen der östlichen Laptevsee im Holozän anhand von aquatischen Palynomorphen“, von Martina Kunz-Pirring.
- Heft Nr. 282/1998** – "Scavenging of ²³¹Pa and ²³⁰Th in the South Atlantic: Implications for the use of the ²³¹Pa/²³⁰Th ratio as a paleoproductivity proxy", by Hans-Jürgen Walter.
- Heft Nr. 283/1998** – „Sedimente im arktischen Meereis - Eintrag, Charakterisierung und Quantifizierung“, von Frank Lindemann.
- Heft Nr. 284/1998** – „Langzeitanalyse der antarktischen Meereisbedeckung aus passiven Mikrowellendaten“, von Christian H. Thomas.
- Heft Nr. 285/1998** – „Mechanismen und Grenzen der Temperaturanpassung beim Pierwurm *Arenicola marina* (L.)“, von Angela Sommer.
- Heft Nr. 286/1998** – „Energieumsätze benthischer Filtrierer der Potter Cove (King George Island, Antarktis)“, von Jens Kowalke.
- Heft Nr. 287/1998** – "Scientific Cooperation in the Russian Arctic: Research from the Barents Sea up to the Laptev Sea", edited by Eike Rachor.

- Heft Nr. 288/1998** – „Alfred Wegener. Kommentiertes Verzeichnis der schriftlichen Dokumente seines Lebens und Wirkens“, von Ulrich Wutzke.
- Heft Nr. 289/1998** – „Retrieval of Atmospheric Water Vapor Content in Polar Regions Using Spaceborne Microwave Radiometry“, by Jungang Miao.
- Heft Nr. 290/1998** – „Strukturelle Entwicklung und Petrogenese des nördlichen Kristallingürtels der Shackleton Range, Antarktis: Proterozoische und Ross-orogene Krustendynamik am Rand des Ostantarktischen Kratons“, von Axel Brommer.
- Heft Nr. 291/1998** – „Dynamik des arktischen Meeres - Validierung verschiedener Rheologieansätze für die Anwendung in Klimamodellen“, von Martin Kreyscher.
- Heft Nr. 292/1998** – „Anthropogene organische Spurenstoffe im Arktischen Ozean, Untersuchungen chlorierter Biphenyle und Pestizide in der Laptevsee, technische und methodische Entwicklungen zur Probenahme in der Arktis und zur Spurenstoffanalyse“, von Sven Utschakowski.
- Heft Nr. 293/1998** – „Rekonstruktion der spätquartären Klima- und Umweltgeschichte der Schirmacher Oase und des Wohlthat Massivs (Ostantarktika)“, von Markus Julius Schwab.
- Heft Nr. 294/1998** – „Besiedlungsmuster der benthischen Makrofauna auf dem ostgrönländischen Kontinentalhang“, von Klaus Schnack.
- Heft Nr. 295/1998** – „Gehäuseuntersuchungen an planktischen Foraminiferen hoher Breiten: Hinweise auf Umweltveränderungen während der letzten 140.000 Jahre“, von Harald Hommers.
- Heft Nr. 296/1998** – „Scientific Cruise Report of the Arctic Expedition ARK-XIII/1 of RV 'Polarstern' in 1997“, edited by Michael Spindler, Wilhelm Hagen and Dorothea Stübing.
- Heft Nr. 297/1998** – „Radiometrische Messungen im arktischen Ozean - Vergleich von Theorie und Experiment“, von Klaus-Peter Johnsen.
- Heft Nr. 298/1998** – „Patterns and Controls of CO₂ Fluxes in Wet Tundra Types of the Taimyr Peninsula, Siberia - the Contribution of Soils and Mosses“, by Martin Sommerkorn.
- Heft Nr. 299/1998** – „The Potter Cove coastal ecosystem, Antarctica. Synopsis of research performed within the frame of the Argentinean-German Cooperation at the Dallmann Laboratory and Jubany Station (King George Island, Antarctica, 1991 - 1997)“, by Christian Wiencke, Gustavo Ferreyra, Wolf Arntz & Carlos Rinaldi.
- Heft Nr. 300/1999** – „The Kara Sea Expedition of RV 'Akademik Boris Petrov' 1997: First Results of a Joint Russian-German Pilot Study“, edited by Jens Matthiessen, Oleg V. Stepanets, Ruediger Stein, Dieter K. Fütterer, and Eric M. Galimov.
- Heft Nr. 301/1999** – „The Expedition ANTARKTIS XV/3 (EASIZ II)“, edited by Wolf E. Arntz and Julian Gutt.
- Heft Nr. 302/1999** – „Sterole im herbstlichen Weddellmeer (Antarktis): Großräumige Verteilung, Vorkommen und Umsatz“, von Anneke Mühlebach.
- Heft Nr. 303/1999** – „Polare stratosphärische Wolken: Lidar-Beobachtungen, Charakterisierung von Entstehung und Entwicklung“, von Jens Biele.
- Heft Nr. 304/1999** – „Spätquartäre Paläoumweltbedingungen am nördlichen Kontinentalrand der Barents- und Kara-See. Eine Multi-Parameter-Analyse“, von Jochen Knies.
- Heft Nr. 305/1999** – „Arctic Radiation and Turbulence Interaction Study (ARTIST)“, by Jörg Hartmann, Frank Albers, Stefania Argentini, Axel Bochert, Ubaldo Bonafé, Wolfgang Cohrs, Alessandro Conidi, Dietmar Freese, Teodoro Georgiadis, Alessandro Ippoliti, Lars Kaleschke, Christof Lüpkes, Uwe Malxner, Giangiuseppe Mastrantonio, Fabrizio Ravegnani, Andreas Reuter, Giuliano Trivellone and Angelo Viola.
- Heft Nr. 306/1999** – „German-Russian Cooperation: Biogeographic and biostratigraphic investigations on selected sediment cores from the Eurasian continental margin and marginal seas to analyze the Late Quaternary climatic variability“, edited by Robert R. Spielhagen, Max S. Barash, Gennady I. Ivanov, and Jörn Thiede.
- Heft Nr. 307/1999** – „Struktur und Kohlenstoffbedarf des Makrobenthos am Kontinentalhang Ostgrönlands“, von Dan Seiler.
- Heft Nr. 308/1999** – „ARCTIC '98: The Expedition ARK-XIV/1a of RV 'Polarstern' in 1998“, edited by Wilfried Jokat.
- Heft Nr. 309/1999** – „Variabilität der arktischen Ozonschicht: Analyse und Interpretation bodengebundener Millimeterwellenmessungen“, von Björn-Martin Sinnhuber.
- Heft Nr. 310/1999** – „Rekonstruktion von Meereisdrift und terrigenem Sedimenteintrag im Spätquartär: Schwermineralassoziationen in Sedimenten des Laptev-See-Kontinentalrandes und des zentralen Arktischen Ozeans“, von Marion Behrends.
- Heft Nr. 311/1999** – „Parameterisierung atmosphärischer Grenzschichtprozesse in einem regionalen Klimamodell der Arktis“, von Christoph Abegg.
- Heft Nr. 312/1999** – „Solare und terrestrische Strahlungswechselwirkung zwischen arktischen Eisflächen und Wolken“, von Dietmar Freese.
- Heft Nr. 313/1999** – „Snow accumulation on Ekströmsen, Antarctica“, by Elisabeth Schlosser, Hans Oerter and Wolfgang Graf.
- Heft Nr. 314/1999** – „Die Expedition ANTARKTIS XV/4 des Forschungsschiffes ‚Polarstern‘ 1998“, herausgegeben von Eberhard Fahrbach.
- Heft Nr. 315/1999** – „Expeditions in Siberia in 1998“, edited by Volker Rachold.
- Heft Nr. 316/1999** – „Die postglaziale Sedimentationsgeschichte der Laptevsee: schwermineralogische und sedimentpetrographische Untersuchungen“, von Bernhard Peregovich.
- Heft-Nr. 317/1999** – „Adaption an niedrige Temperaturen: Lipide in Eisdiatomeen“, von Heidi Lehmal.
- Heft-Nr. 318/1999** – „Effiziente parallele Lösungsverfahren für elliptische partielle Differentialgleichungen in der numerischen Ozeanmodellierung“, von Natalja Rakowsky.

- Heft-Nr. 319/1999** – “The Ecology of Arctic Deep-Sea Copepods (Euchaetidae and Aetideidae). Aspects of their Distribution, Trophodynamics and Effect on the Carbon Flux”, by Holger Auel.
- Heft-Nr. 320/1999** – “Modellstudien zur arktischen stratosphärischen Chemie im Vergleich mit Meßdaten”, von Veronika Eyring.
- Heft-Nr. 321/1999** – “Analyse der optischen Eigenschaften des arktischen Aerosols”, von Dagmar Nagel.
- Heft-Nr. 322/1999** – “Messungen des arktischen stratosphärischen Ozons: Vergleich der Ozonmessungen in Ny-Ålesund, Spitzbergen, 1997 und 1998”, von Jens Langer.
- Heft-Nr. 323/1999** – “Untersuchung struktureller Elemente des südöstlichen Weddellmeeres / Antarktis auf der Basis mariner Potentialfelddaten”, von Uwe F. Meyer.
- Heft-Nr. 324/1999** – “Geochemische Verwitterungstrends eines basaltischen Ausgangsgesteins nach dem spätpleistozänen Gletscherrückzug auf der Taimyrhalbinsel (Zentralsibirien) - Rekonstruktion an einer sedimentären Abfolge des Lama Sees”, von Stefanie K. Harwart.
- Heft-Nr. 325/1999** – “Untersuchungen zur Hydrologie des arktischen Meereises - Konsequenzen für den kleinskaligen Stofftransport”, von Johannes Freitag.
- Heft-Nr. 326/1999** – “Die Expedition ANTARKTIS XIV/2 des Forschungsschiffes 'Polarstern' 1998”, herausgegeben von Eberhard Fahrbach.
- Heft-Nr. 327/1999** – “Gemeinschaftsanalytische Untersuchungen der Harpacticoidenfauna der Magellanregion, sowie erste similaritätsanalytische Vergleiche mit Assoziationen aus der Antarktis”, von Kai Horst George.
- Heft-Nr. 328/1999** – “Rekonstruktion der Paläo-Umweltbedingungen am Laptev-See-Kontinentalrand während der beiden letzten Glazial/Interglazial-Zyklen anhand sedimentologischer und mineralogischer Untersuchungen”, von Claudia Müller.
- Heft-Nr. 329/1999** – “Räumliche und zeitliche Variationen atmosphärischer Spurengase aus bodengebundenen Messungen mit Hilfe eines Michelson interferometers”, von Justus Notholt.
- Heft-Nr. 330/1999** – “The 1998 Danish-German Excursion to Disko Island, West Greenland”, edited by Angelika Brandt, Helge A. Thomsen, Henning Heide-Jørgensen, Reinhard M. Kristensen and Hilke Ruhberg.
- Heft-Nr. 331/1999** – “Poseidon” Cruise No. 243 (Reykjavik - Greenland - Reykjavik, 24 August - 11 September 1998): Climate change and the Viking-age fjord environment of the Eastern Settlement, sw Greenland”, by Gerd Hoffmann, Antoon Kuijpers, and Jörn Thiede.
- Heft-Nr. 332/1999** – “Modeling of marine biogeochemical cycles with an emphasis on vertical particle fluxes”, by Regina Usbeck.
- Heft-Nr. 333/1999** – “Die Tanaidaceenfauna des Beagle-Kanals und ihre Beziehungen zur Fauna des antarktischen Festlandssockels”, von Anja Schmidt.
- Heft-Nr. 334/1999** – “D-Aminosäuren als Tracer für biogeochemische Prozesse im Fluß-Schelf-Ozean-System der Arktis”, von Hans Peter Fitznar.
- Heft-Nr. 335/1999** – “Ökophysiologische Ursachen der limitierten Verbreitung reptanter decapoder Krebse in der Antarktis”, von Markus Frederich.
- Heft-Nr. 336/1999** – “Ergebnisse der Untersuchung des grönländischen Inlandeises mit dem elektromagnetischen Reflexionsverfahren in der Umgebung von NGRIP”, von Fidan Göktaş.
- Heft-Nr. 337/1999** – “Paleozoic and mesozoic tectono-thermal history of central Dronning Maud Land, East Antarctica, - evidence from fission-track thermochronology”, by Stefanie Meier.
- Heft-Nr. 338/1999** – “Probleme hoher Stoffwechselraten bei Cephalopoden aus verschiedenen geographischen Breiten”, von Susanne Zielinski.
- Heft-Nr. 339/1999** – “The Expedition ARKTIS XV/1”, edited by Gunther Krause.
- Heft-Nr. 340/1999** – “Microbial Properties and Habitats of Permafrost Soils on Taimyr Peninsula, Central Siberia”, by Nicolé Schmidt.
- Heft-Nr. 341/1999** – “Photoacclimation of phytoplankton in different biogeochemical provinces of the Southern Ocean and its significance for estimating primary production”, by Astrid Bracher.
- Heft-Nr. 342/1999** – “Modern and Late Quaternary Depositional Environment of the St. Anna Trough Area, Northern Kara Sea”, edited by Ruediger Stein, Kirsten Fahl, Gennadij I. Ivanov, Michael A. Levitan, and Gennady Tarasov.
- Heft-Nr. 343/1999** – “ESF-IMPACT Workshop/Oceanic impacts: mechanisms and environmental perturbations, 15-17 April 1999 in Bremerhaven”, edited by Rainer Gersonde and Alexander Deutsch.
- Heft-Nr. 344/1999** – “Die Klimageschichte der hohen nördlichen Breiten seit dem mittleren Miozän: Hinweise aus sedimentologischen- und mineralogischen Analysen (ODP Leg 151, zentrale Framstraße)”, von Amelie Winkler.
- Heft-Nr. 345/1999** – “Kurzfristige Klimaschwankungen im Scotiameer und Ergebnisse zur Kalbungsgeschichte der Antarktis während der letzten 200000 Jahre”, von Annette Hofmann.
- Heft-Nr. 346/2000** – “Glazialmarine Sedimentationsentwicklung am westantarktischen Kontinentalrand im Amundsen- und Bellingshausenmeer - Hinweise auf Paläoumweltveränderungen während der quartären Klimazyklen”, von Claus-Dieter Hillenbrand.
- Heft-Nr. 347/2000** – “Zur Ökologie des Phytoplanktons im arktischen Laptevmeer - ein jahreszeitlicher Vergleich”, von Kirsten Tuschling.
- Heft-Nr. 348/2000** – “Untersuchungen zum Fettstoffwechsel des Südlichen See-Elefanten (*Mirounga leonina* L.) in der Antarktis”, von Sven Ramdohr.
- Heft-Nr. 349/2000** – “Licht- und Temperatureinfluß auf den enzymatischen Oxidationsschutz der antarktischen Eisdiatomee *Entomoneis kufferathii Manguin*”, von Raimund Schriek.

- Heft-Nr. 350/2000** – “Die Expedition ARKTIS XV/3 des Forschungsschiffes ‘Polarstern’ 1999”, herausgegeben von Ursula Schauer.
- Heft-Nr. 351/2000** – “Dissolution kinetics of biogenic silica in marine environments”, by Dirk Rickert.
- Heft-Nr. 352/2000** – “Geometrie und Kinematik des tertiären Deckenbaus im West Spitzbergen Falten- und Überschiebungsgürtel, Brøggerhalvøya, Svalbard”, von Kerstin Saalmann.
- Heft-Nr. 353/2000** – “Zur Ökologie der Benthos-Foraminiferen der Potter Cove (King George Island, Antarktis)”, von Michaela Mayer.
- Heft-Nr. 354/2000** – “Expeditions in Siberia in 1999”, edited by Volker Rachold.
- Heft-Nr. 355/2000** – “Temperaturrekonstruktion im Tropischen Atlantik für das Letzte Glaziale Maximum: CLIMAP neu betrachtet”, von Carsten Porthun.
- Heft-Nr. 356/2000** – “Niederfrequente Variabilität großräumiger atmosphärischer Zirkulationsstrukturen in spektralen Modellen niedriger Ordnung”, von Antje Weisheimer.
- Heft-Nr. 357/2000** – “Late Quaternary paleoclimatic reconstructions along the Eurasian continental margin”, by Hans Peter Kleiber.
- Heft-Nr. 358/2000** – “Holocene environmental history of East Greenland - evidence from lake sediments”, by Bernd Wagner.
- Heft-Nr. 359/2000** – “Scientific Cooperation in the Russian Arctic: Ecology of the White Sea with Emphasis on its Deep Basin”, edited by Eike Rachor.
- Heft-Nr. 360/2000** – “Scientific Cruise Report of the Joint Russian-German Kara-Sea Expedition of RV ‘Akademik Boris Petrov’ in 1999”, edited by Ruediger Stein and Oleg Stepanets.
- Heft-Nr. 361/2000** – “Planktic foraminifer ecology and stable isotope geochemistry in the Arctic Ocean: implications from water column and sediment surface studies for quantitative reconstructions of oceanic parameters.”, by Renate Volkmann.
- Heft-Nr. 362/2000** – “Eisbohrkernuntersuchungen zur räumlichen und zeitlichen Variabilität von Temperatur und Niederschlagsrate im Spätholozän in Nordgrönland”, von Matthias Schwager.
- Heft-Nr. 363/2000** – “Benthische Peracarida (Crustacea, Malacostraca) des arktischen Mellemfjordes, West-Grönland”, von Anne-Nina Lörz.
- Heft-Nr. 364/2000** – “Die Expeditionen ANTARKTIS XVI/3-4 des Forschungsschiffes ‘Polarstern’ 1999”, herausgegeben von Ulrich Bathmann, Victor Smetacek und Manfred Reinke.
- Heft-Nr. 365/2000** – “Organic carbon in Late Quaternary sediments: Responses to paleoenvironmental changes in the Laptev and Kara seas (Arctic Ocean)”, by Bettina Boucsein.
- Heft-Nr. 366/2000** – “Flugzeuggestützte Topographie- und Schweremessung: Meßsystem und Anwendung auf die Region Framstraße, Spitsbergen und Nordostgrönland”, von Tobias Boebel.
- Heft-Nr. 367/2000** – “Messung dielektrischer Eigenschaften polarer Eiskerne”, von Frank Wilhelms.
- Heft-Nr. 368/2000** – “The Expedition ARKTIS-XV/2 of RV ‘Polarstern’ in 1999”, edited by Wilfried Jokat.

* vergriffen / out of print.

** nur noch beim Autor / only from the author.